

AD-A062 442

ARIZONA UNIV TUCSON ENGINEERING EXPERIMENT STATION
CONVECTIVE HEAT TRANSFER FOR SHIP PROPULSION.(U)

F/6 20/13

APR 78 A W SERKSNIS, D M MCELIGOT, M F TAYLOR N00014-75-C-0694
1248-6 NL

UNCLASSIFIED

1 OF 2
AD
A062442



AD A062442

DDC FILE COPY

LEVEL

12

Fourth Annual Summary Report

Contract No. N00014-75-C-0694

Contract Authority NR-097-395

CONVECTIVE HEAT TRANSFER FOR SHIP PROPULSION

Prepared for

Office of Naval Research

Code 473

Arlington, Virginia

Prepared by

A. W. Serksnis

D. M. McEligot

M. F. Taylor

1 APRIL 1978

DDC
RECEIVED
DEC 18 1978
D



DISTRIBUTION STATEMENT A

Approved for public release;
Distribution Unlimited

ENGINEERING EXPERIMENT STATION
COLLEGE OF ENGINEERING
THE UNIVERSITY OF ARIZONA
TUCSON, ARIZONA

78 12 11 129

ACCESSION NO.	
DTIC	White Section <input checked="" type="checkbox"/>
DDC	Dist Section <input type="checkbox"/>
UNANNOUNCED <input type="checkbox"/>	
JUSTIFICATION	
BY	
DISTRIBUTION/AVAILABILITY CODES	
Dist.	AVAIL. and/or SPECIAL
A	

LEVEL II

12

Fourth Annual Summary Report

CONVECTIVE HEAT TRANSFER FOR SHIP PROPULSION

By

A. W. Serksnis, D. M. McEligot and M. F. Taylor
Aerospace and Mechanical Engineering Department
University of Arizona
Tucson, Arizona 85721

Research Sponsored by

Office of Naval Research
ONR Contract Number N00014-75-C-0694
ONR Contract Authority NR-097-395

1 April 1978

DDC
RECEIVED
DEC 18 1978
D

Approved for public release; distribution unlimited. Reproduction in whole or in part is permitted for any purpose of the United States Government.

78 12 11 019

Unclassified

SECURITY CLASSIFICATION OF THIS PAGE (When Data Entered)

REPORT DOCUMENTATION PAGE		READ INSTRUCTIONS BEFORE COMPLETING FORM
1. REPORT NUMBER 1248-6	2. GOVT ACCESSION NO.	3. RECIPIENT'S CATALOG NUMBER
4. TITLE (and Subtitle) Convective Heat Transfer For Ship Propulsion, (Fourth Annual Summary Report)		5. TYPE OF REPORT & PERIOD COVERED Annual Summary Report, No. 4, 1 April 1977 - 31 Mar. 1978
7. AUTHOR(s) A. W. Serksnis, D. M. McEligot and M. F. Taylor		8. CONTRACT OR GRANT NUMBER(s) N00014-75-C-0694
9. PERFORMING ORGANIZATION NAME AND ADDRESS Engineering Experiment Station University of Arizona Tucson, Arizona 85721		10. PROGRAM ELEMENT, PROJECT, TASK AREA & WORK UNIT NUMBERS NR 097-395
11. CONTROLLING OFFICE NAME AND ADDRESS Office of Naval Research Code 473 Arlington, Virginia 22217		12. REPORT DATE 1 April 1978
14. MONITORING AGENCY NAME & ADDRESS (if different from Controlling Office) Office of Naval Research, Resident Representative Room 421, Space Sciences Building University of Arizona Tucson, Arizona 85721		13. NUMBER OF PAGES 134
		15. SECURITY CLASS. (of this report) Unclassified
16. DISTRIBUTION STATEMENT (of this Report) Unlimited		15a. DECLASSIFICATION/DOWNGRADING SCHEDULE
<div style="border: 1px solid black; padding: 5px; display: inline-block;"> DISTRIBUTION STATEMENT A Approved for public release; Distribution Unlimited </div> <div style="margin-left: 20px;">12 135 p.</div>		
17. DISTRIBUTION STATEMENT (of the abstract entered in Block 20, if different from Report) Unlimited <div style="border: 1px solid black; padding: 5px; display: inline-block; margin-left: 20px;"> DISTRIBUTION STATEMENT A Approved for public release; Distribution Unlimited </div>		
18. SUPPLEMENTARY NOTES		
19. KEY WORDS (Continue on reverse side if necessary and identify by block number)		
<div style="display: flex; justify-content: space-between;"> <div>Heat Transfer Turbulent Flow Tubes Boundary Layers</div> <div>Forced Convection Turbulence Structure Gas Turbine Systems</div> <div>Heat Exchangers Noble Gases Gas Mixtures</div> </div> <p style="text-align: center;">APPROXIMATELY EQUAL TO</p>		
20. ABSTRACT (Continue on reverse side if necessary and identify by block number)		
To correspond to conditions expected in components in shipboard propulsion systems, numerical analyses and experiments were conducted for forced convective heat transfer to gases and gas mixtures flowing in ducts. Measurements with a hydrogen-carbon dioxide mixture confirmed the trends of the numerical predictions for turbulent flow in circular tubes; the wall turbulent Prandtl number was determined for Pr = 1/3. The possibility of interaction between carbon dioxide and hydrogen and consideration of dissociating gases are treated briefly in appendices.		

DD FORM 1 JAN 73 1473 EDITION OF 1 NOV 65 IS OBSOLETE

Unclassified

SECURITY CLASSIFICATION OF THIS PAGE (When Data Entered)

033 868

78 12 11 129

ABSTRACT

The results of a numerical and experimental study of convective heat transfer for turbulent flow of hydrogen-carbon dioxide mixtures in smooth, electrically heated, vertical circular tubes are presented. Mixtures with molal masses of approximately 14.5 g/gmole were used; this value corresponds to a molecular Prandtl number of about 1/3. Inlet Reynolds numbers were about 34,000 and 85,000, maximum wall temperatures reached 810°K, and maximum wall-to-bulk temperature ratios were about two. Existing experimental correlations, developed using gases with Prandtl number of the order 0.7, were found to overpredict the observed Nusselt numbers by as much as fifteen percent.

For predictions of heat transfer to wall-bounded turbulent flows, a key to the success of many engineering analyses is the appropriate choice of turbulent Prandtl number, $Pr_t = \epsilon_m/\epsilon_h$. In the experiments reported here, data were extrapolated versus temperature ratio to deduce Nusselt numbers corresponding to the constant property idealization. These results were then compared to numerical predictions at the same inlet Reynolds numbers and molecular Prandtl number, in order to deduce the effective value to $Pr_{t,wall}$ which dominates the thermal resistance. This value was then hypothesized to apply for conditions where the fluid properties vary substantially. Numerical predictions, accounting for property variation, were then compared to the data obtained at the highest heating rates of the investigation to examine the validity of this hypothesis. While earlier studies with air and with helium-argon mixtures ($0.42 < Pr < 0.71$) showed a potential trend of $Pr_{t,wall}$ increasing as Pr is reduced, the present work

does not extend it. For the hydrogen-carbon dioxide mixtures, Reynolds' analogy ($Pr_{t,wall} = 1$) was found suitable for the wall region, for both constant property conditions and the highest heating rates measured.

TABLE OF CONTENTS

	Page
ABSTRACT	iv
LIST OF FIGURES	vi
LIST OF TABLES	viii
NOMENCLATURE	ix
INTRODUCTION	1
GAS PROPERTIES	9
EXPERIMENTAL APPARATUS	20
EXPERIMENTAL RESULTS	22
Friction Results	22
Heat Transfer Results	29
DETERMINATION OF TURBULENT PRANDTL NUMBER	38
Numerical Analysis	38
Prediction with Constant Properties	39
Prediction with Gas Property Variation	45
CONCLUSIONS	49
APPENDICES	
A. MIXTURE PROPERTIES	52
B. EXPERIMENT	53
Apparatus	53
Procedure	58
Heat Loss Calibration	60
Measurement of Test Section Resistance	68
Mass Flow Rate Determination	72
Thermocouple Conduction Error	78
A Note on Safety	83
C. UNCERTAINTY ANALYSIS	84
D. HYDROGEN-CARBON DIOXIDE EXPERIMENTAL DATA	94

APPENDICES (CONTD.)

E. POSSIBILITY OF INTERACTION BETWEEN CARBON DIOXIDE AND HYDROGEN by Professor H. C. Perkins, Jr.....	103
F. CONSIDERATION OF DISSOCIATING GASES by Professor H. C. Perkins, Jr.....	110
REFERENCES.....	117

LIST OF FIGURES

Figure	Page
1. Existing correlations for heat transfer for fully developed turbulent flow in circular tubes	2
2. Local turbulent heat transfer data for air and helium-argon mixture compared to existing correlation for effect of gas property variation	4
3. Molecular Prandtl number of H_2 - CO_2 mixtures at 1 atmosphere	11
4. Comparison of measured adiabatic friction factors to Drew, Koo and McAdams correlation	23
5. Pressure tap location	25
6. Comparison of average friction factors to variable properties correlation of Taylor [1967]	27
7. Technique for determining constant property Nusselt number	30
8. Comparison of Nu_{cp} to empirical correlation of Pickett [1976] for fully developed conditions	34
9. Comparison of local bulk Nusselt numbers to equation 25 for H_2 - CO_2 mixtures	37
10. Determination of Pr_{tw} for constant properties data	41
11. Numerical predictions compared to data for runs at highest heating rates.	47
B1. Schematic diagram of experimental apparatus	54
B2. Diagram of test section	55
B3. Detail of draft shield	56
B4. Energy flows from element of test section	61
B5. Detail of test section upper electrode	63
B6. Axial wall and bulk temperature profiles	64

LIST OF FIGURES (cont.)

Figure	Page
B7. Heat loss calibration profiles	67
B8. Circuit for measurement of test section resistance	69
B9. Variation of test section resistance with respect to temperature	71

LIST OF TABLES

Table	Page
1. Range of variables in the present experiment	5
2. Summary of experimental runs	6-8
3. Summary of Matheson laboratory reports of gas analyses	12
4. Compressibility factors for hydrogen and carbon dioxide	14
5. Values of exponents for temperature variation	18
6. Ratio of NU_{CP}/NU_{DB} for experimental conditions	32
7. Variation of turbulent Prandtl number with respect to molecular Prandtl number	43
B1. Thermocouple heat loss constants	66
B2. Determination of flow meter inside diameter	76
B3. Thermocouple conduction error subroutine	79-82
C1. Uncertainties of measured values	86-87
C2. Change of calculated mass flow for a change in variable	89
C3. Percentage uncertainties in the measured mass flow rate	90
C4. Percentage uncertainties in the measured bulk Nusselt number	92

NOMENCLATURE

a,b,d	exponents used to account for temperature variation of properties;
A	flow area of tube;
c	velocity of sound;
c_p	specific heat at constant pressure;
c_v	specific heat at constant volume;
D	inside diameter;
fn()	function of;
g	acceleration due to gravity
g_c	dimensional conversion factor;
G	average mass flux, \dot{m}/A ;
h	heat transfer coefficient;
i	specific enthalpy;
k	thermal conductivity;
λ	mixing length;
\dot{m}	mass flow rate;
\bar{M}	molal mass;
P,p	pressure;
q''	heat flux;
r	radius;
R	gas constant for a particular gas;
R	universal gas constant;
T	temperature;
V	bulk velocity of gas;
x	axial distance from start of heating;
y	radial distance from wall.

Greek Symbols

α	coefficient of thermal expansion;
$\epsilon/\kappa, \sigma$	force constants in Lennard-Jones potential;
ϵ_H	eddy diffusivity for heat
ϵ_M	eddy diffusivity for momentum;
γ	ratio of specific heats, c_p/c_v ;
κ	empirical constant in van Driest mixing length model, 0.4;
μ	absolute viscosity;
ν	kinematic viscosity;
ρ	density;
σ	standard deviation;
τ	shear stress;
χ	mole fraction.

Non-dimensional Parameters

f	friction factor, $2g_c \rho \tau_w / G^2$;
Gr	Grashof number based on wall heat flux, $g D^4 q_w'' / (\nu^2 \mu c_p T)_i$;
Nu	Nusselt number, hD/K ;
\bar{p}	pressure drop, $\rho_i g_c (p_i - p) / G^2$;
Pr	Prandtl number, $c_p \mu / k$; Pr_t , turbulent Prandtl number, ϵ_M / ϵ_H ;
q^+	heat flux parameter, $q_w'' / (G c_{p,i} T_i)$;
Re	Reynolds number, GD/μ ;
y^+	wall distance parameter, $y) g_c \tau_w \rho)^{1/2} / \nu$;
y_l^+	empirical constant in vanDriest mixing length model, 26.

Subscripts

av	lengthwise average;
b	evaluated at bulk temperature;
$cond$	heat conduction;

CP	constant property condition;
cs	cross sectional area;
DB	Dittus-Boelter;
DKM	Drew, Koo and McAdams;
exp	experiment;
fr	frictional;
gen	heat generation;
i	inlet condition;
Max	maximum;
mom	momentum;
ref	reference;
t	turbulent;
VD	van Driest;
w	wall;
∞	environment condition.

INTRODUCTION

The closed cycle gas turbine system, or closed Brayton cycle, has been found to be an efficient, compact and versatile system for propulsion and power plant applications as shown by Mock [1970] and Bammert, Rurik, and Griepentrog [1974]. The gas entering the compressor is not restricted to air at atmospheric conditions. The entire cycle can be pressurized to reduce the size of components and alternate gases can be employed to avoid contamination and corrosion problems. In addition to being chemically inert, several of the noble gases have higher molecular weights than air. Based on thermodynamic studies, Bammert and Klein [1974] concluded that considerable savings in the cost of a gas turbine cycle could be obtained by mixing a heavier gas with helium.

Recent work at the University of Arizona by Pickett, Taylor, and McEligot [1977] with binary gas mixtures that are being considered for closed Brayton cycle application, has revealed that the Dittus-Boelter relation [McAdams, 1954]

$$Nu_{DB} = \frac{hD}{k} = 0.021 Re^{0.8} Pr^{0.4} \quad (1)$$

thought to be generally valid for gaseous turbulent flow in ducts over the range $0.5 < Pr < 1.0$, seriously overpredicts Nusselt numbers for fluids with Prandtl numbers in the range of 0.4 to 0.5. Fig. 1 shows existing correlations between Nusselt number and Prandtl number for fully developed conditions at a constant Reynolds number of 100,000. As shown, the helium-argon

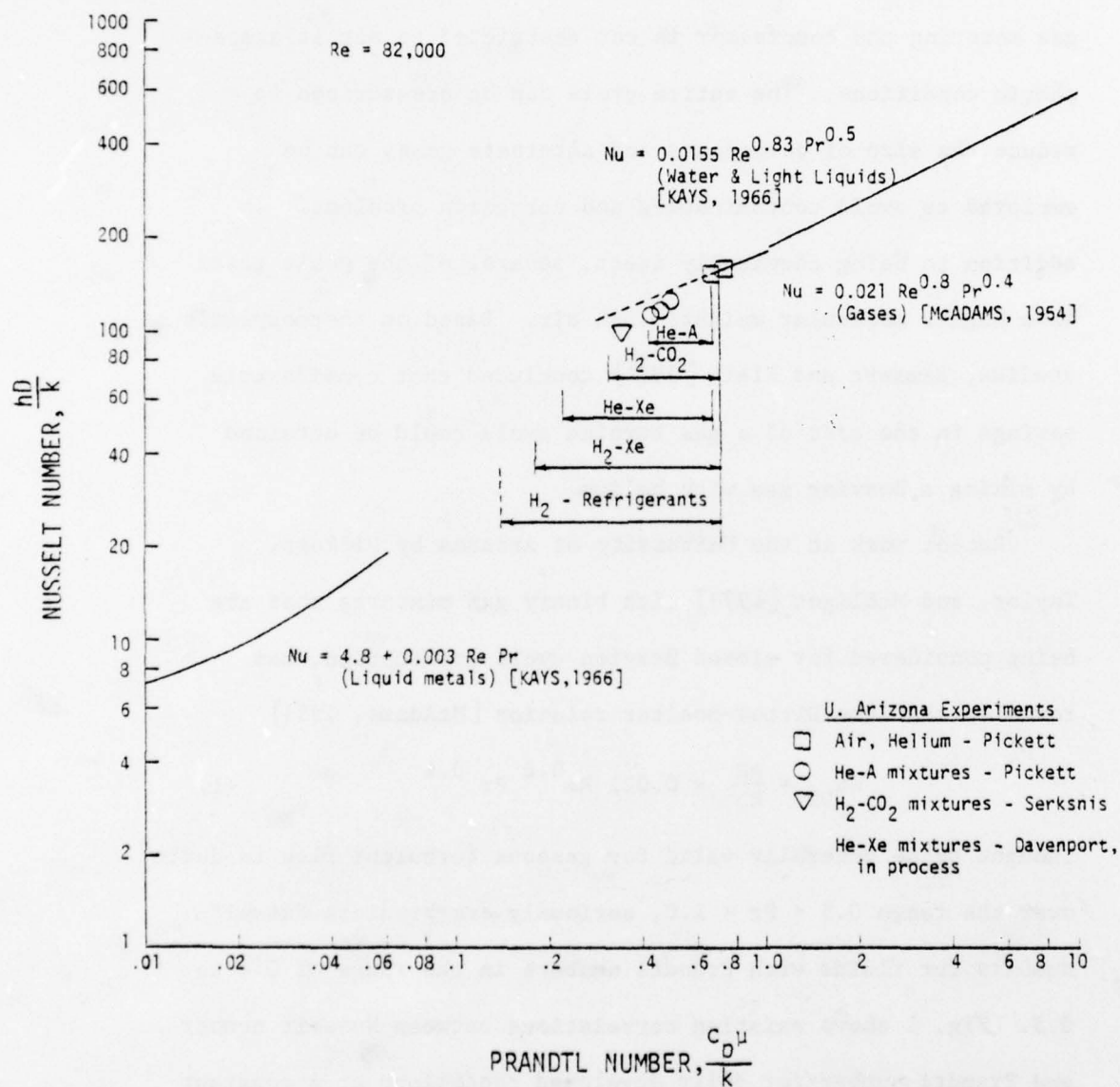


FIGURE 1. EXISTING CORRELATIONS FOR HEAT TRANSFER FOR FULLY DEVELOPED TURBULENT FLOW IN CIRCULAR TUBES

(Prandtl number approximately 0.42) experiments show a deviation from equation (1).

Fig. 2 shows a normalized plot of local turbulent heat transfer data for air and a helium-argon mixture compared to an existing correlation developed by Taylor [1970] for the effects of property variation and entrance effects. For the present study an investigation of the effect of a further lowering of Prandtl number was undertaken. It is expected that the correlation will overpredict the heat transfer coefficient more seriously for mixtures with even lower Prandtl numbers.

The purpose of this research was to determine, for turbulent flow in tubes, the heat and momentum transfer characteristics of hydrogen-carbon dioxide mixtures. Mixtures of H_2 - CO_2 were chosen due to their low Prandtl number and low cost. Tables 1 and 2 summarize the range of data obtained. The ultimate goal of this present research area at the University of Arizona is to predict the heat and momentum transfer characteristics of gas mixtures with Prandtl numbers in the range of about 0.2 to 0.7. These mixtures provide excellent working fluids for proposed closed Brayton cycles. The molecular weight can be varied to take advantage of the higher density component to reduce the size of the compressor and turbine and of the higher thermal conductivity of the lighter component to reduce the size of the heat exchangers.

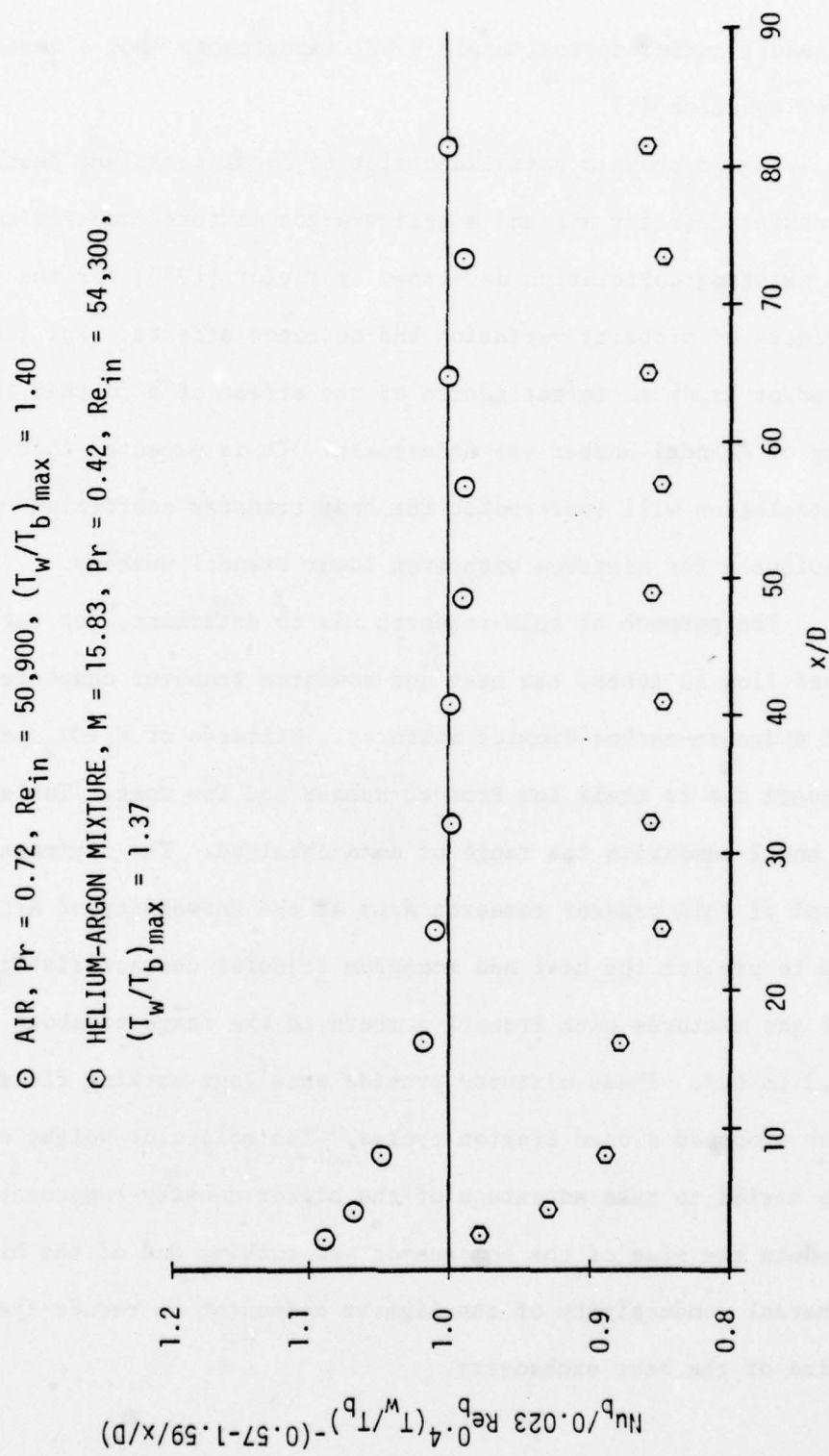


FIGURE 2. LOCAL TURBULENT HEAT TRANSFER DATA FOR AIR AND A HELIUM-ARGON MIXTURE COMPARED TO EXISTING CORRELATION FOR EFFECT OF GAS PROPERTY VARIATION. [PICKETT, 1976]

Table 1

Range of Variables in the Present Experiment

Gas	Air	Helium	H ₂ -CO ₂
	10	11	14
Experimental Runs	(2 adiabatic)	(3 adiabatic)	(6 adiabatic)
Molecular weight	28.97	4.003	14.50
Inlet bulk Reynolds number	28,000-91,900	8900-29,200	33,900-91,900
Exit bulk Reynolds number	18,500-81,000	5800-26,400	19,800-72,900
Inlet bulk Prandtl number	0.72	0.67	0.34
Exit bulk Prandtl number	0.68	0.67	0.39
Maximum T_w/T_b	2.01	1.89	1.85
Maximum T_w (°K)	834	818	824
Maximum q^+	0.0033	0.0035	0.0041
Maximum Gr_i/Re_i^2	6.26×10^{-3}	3.51×10^{-4}	2.16×10^{-3}
Maximum Mach number	0.13	0.12	0.13
x/D for local bulk Nusselt numbers	0.2-59.4	0.2-59.4	0.2-59.4

Table 2

Summary of Experimental Runs

Run	Date	Gas	\dot{m} (#m/hr)	Re_i	T_i (°F)	T_w/T_b MAX	q^+ MAX	P_1 (psia)	P_2 (psia)	f_{exp}	$Mach_i$
201A			21.48	32,140	73.4	ADIABATIC		30.5	30.1	0.00576	0.12
202H			20.61	30,890	72.8	1.20	0.00062	30.7	30.2	0.00634	0.11
203H			19.91	29,834	72.8	1.45	0.00152	31.0	30.4	0.00646	0.11
204H			19.34	28,956	73.2	1.72	0.00243	31.2	30.5	0.00678	0.10
205H	4-17-77	AIR	18.75	28,048	73.7	2.01	0.00334	31.4	30.6	0.00712	0.10
206H			52.94	79,160	74.1	2.01	0.00269	84.9	83.2	0.00522	0.10
207H			54.53	81,552	74.1	1.75	0.00200	84.0	82.5	0.00512	0.11
208H			56.73	84,863	74.1	1.48	0.00124	83.1	81.7	0.00495	0.11
209H			59.34	88,794	74.1	1.21	0.00054	81.9	80.8	0.00466	0.12
210A			61.50	91,930	74.0	ADIABATIC		81.0	80.0	0.00466	0.13
211A	4-27-77		6.72	9267	79.9	ADIABATIC		28.3	27.8	0.00815	0.10
212H	4-27-77		6.71	9235	82.0	1.15	0.00068	29.2	28.7	0.00843	0.10
213H	4-27-77		6.63	9125	81.9	1.37	0.00165	30.5	29.8	0.00926	0.09
214H	4-27-77		6.78	9347	80.5	1.59	0.00259	32.3	31.5	0.00965	0.09
215H	4-27-77		6.43	8854	81.3	1.80	0.00353	31.7	30.8	0.00988	0.08
216A	4-27-77	HELIUM	7.92	10,930	79.5	ADIABATIC		32.1	31.6	0.00763	0.10
217A	4-29-77		21.29	29,180	84.5	ADIABATIC		79.0	77.8	0.00613	0.11
218H	4-29-77		20.95	28,929	80.0	1.17	0.00057	80.9	79.6	0.00625	0.11
219H	4-29-77		20.38	28,693	65.8	1.44	0.00147	83.1	81.5	0.00650	0.10
220H	4-29-77		19.62	27,410	71.1	1.66	0.00234	85.6	83.8	0.00680	0.09
221H	4-29-77		18.68	25,936	75.4	1.89	0.00310	85.3	83.3	0.00721	0.09

Table 2 (cont.)

Summary of Experimental Runs

Run	Date	Gas	\dot{m} (#m/hr)	Re_i	T_i (°F)	T_w/T_b MAX	q^+ MAX	P_1 (psia)	P_2 (psia)	f_{exp}	$Mach_i$
223A	5-11-77	H ₂ -CO ₂	46.58	91,820	58.0	ADIABATIC		85.9	84.9	0.00449	0.13
224A	5-11-77		24.37	47,920	59.5	ADIABATIC		46.6	46.0	0.00513	0.12
225A	5-12-77		17.77	34,560	66.2	ADIABATIC		45.1	44.7	0.00578	0.09
226	5-12-77		17.51	34,253	63.6	1.18	0.00082	46.0	45.5	0.00601	0.09
227	5-12-77		17.46	34,239	62.1	1.39	0.00188	47.4	46.8	0.00618	0.09
228	5-12-77		17.41	34,143	62.0	1.62	0.00294	48.5	47.7	0.00642	0.08
229	5-12-77		17.32	33,940	62.4	1.85	0.00414	49.7	48.8	0.00658	0.08
230A	5-12-77		18.34	35,890	62.5	ADIABATIC		46.9	46.5	0.00568	0.09
231	5-18-77		42.64	83,260	65.1	1.43	0.00157	90.0	88.5	0.00485	0.11
232	5-18-77		42.17	82,574	63.5	1.20	0.00071	85.1	83.9	0.00485	0.12
233A	5-27-77		46.34	91,820	54.9	ADIABATIC		85.8	84.8	0.00459	0.13
234	5-27-77		44.15	87,712	54.7	1.69	0.00250	98.0	96.2	0.00484	0.10
235	5-27-77		43.83	87,065	54.7	1.85	0.00312	100.6	98.6	0.00491	0.10
236A	5-27-77		46.36	91,880	54.8	ADIABATIC		86.5	85.5	0.00456	0.12

The Headings and Their Definitions Used in Table 2

<u>Heading</u>	<u>Definition</u>
Run	Experiment run number
Date	Date on which experimental run was made
Gas	Gas used in the experiment
\dot{m}	Gas flow rate
Re_i	Inlet Reynolds number
T_i	Inlet mixer temperature
$[T_w/T_b]_{MAX}$	Maximum wall-to-bulk temperature ratio
q^+_{MAX}	Maximum heat flux
p_1	Static pressure at inlet pressure tap
p_2	Static pressure at outlet pressure tap
f_{exp}	Experimental friction factor
$Mach_i$	Inlet Mach number

GAS PROPERTIES

The properties needed for this study were the compressibility, viscosity, thermal conductivity, specific heat, enthalpy, speed of sound, and gas constant. The gases used in the experiment were air, helium and a binary mixture of hydrogen and carbon dioxide. Table 1 includes a list of the gases with their molecular weights and Prandtl numbers. Bulk temperatures of the gases ranged from 285K to 560K (55F to 550F) and pressures ranged from 2 to 7 atmospheres (30 to 100 PSIA).

The properties of air from the Tables of the Thermal Properties of Gases [Hilsenrath et al., 1955] were used in this investigation. The air was obtained from a large storage tank that was replenished by a compressor.

The helium properties were calculated using the ideal gas and constant specific heat assumptions. The compressibility of helium was considered to have a constant value of one. This assumption is reasonable for the range of pressures and temperatures used in this experiment. The viscosity and thermal conductivity of the helium were calculated using the Lennard-Jones (6-12) potential in the Chapman-Enskog kinetic theory [Hirschfelder, Curtiss, and Bird, 1964]. The force constants, ϵ/κ and σ , suggested by DiPippo and Kestin [1969] were used to predict viscosity and thermal conductivity. The calculated properties of helium used in this investigation are listed by Pickett [1976]. The helium was bought in high pressure bottles

and certified to have a purity of 99.995 percent minimum.

Hydrogen-carbon dioxide was chosen for this experiment to investigate the effect of a lowering of Prandtl number on heat transfer and friction results. As viscosity and thermal conductivity of this mixture are not simple functions of the composition, the Prandtl number varies with molecular weight and temperature as shown by Figure 3 using calculated values of specific heat, viscosity, and thermal conductivity. For the experiments, a molecular weight of 14.50 was chosen to correspond to the minimum Prandtl number of 0.34. The mixture was of "Certified Standard" grade bought from Matheson Gas Products in high pressure bottles. Throughout the present study, the composition of the mixture is considered homogeneous and constant. Matheson supplied laboratory reports of gas analyses. Table 3 shows a summary of the analyses on the mixtures used. Matheson accuracy certification on the resulting molecular weights is approximately ± 0.07 g/g mole.

A method to check the accuracy of the molecular weight of the mixture was undertaken. As shown in Appendix B, the inside diameter of the tubular flowmeter can be calibrated by an adiabatic friction measurement (equation B8) if an accepted friction correlation (equation B11) is assumed. This was accomplished by using a known mass flow rate and a known gas molecular weight (molecular weight of air = 28.97 g/g mole). Now, with the inside diameter of the tubular flowmeter determined, it can be used in series with a positive displacement

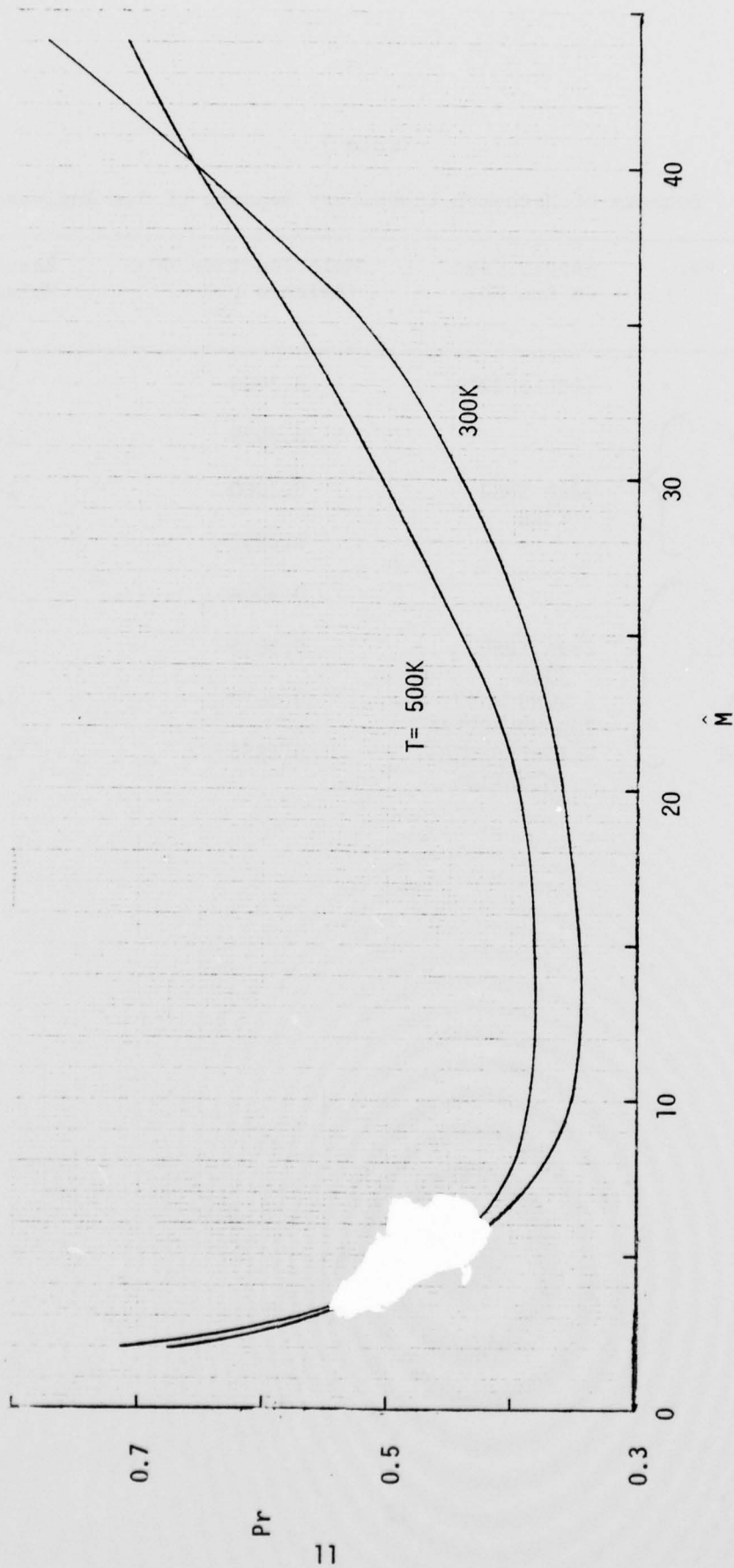


FIGURE 3. MOLECULAR PRANDTL NUMBER OF H_2-CO_2 MIXTURES AT 1 ATMOSPHERE.

Table 3

Summary of Matheson Laboratory Reports of Gas Analyses

Cylinder No.	Supply Used on Run No.	Mole Fraction CO ₂ (Balance H ₂)	Resulting Molecular Weight (g/g mole)
5010	223A & 224A	0.3006	14.64
77446	225A THRU 232H	0.3029	14.74
34388 T		0.3000	14.61
38087		0.2851	13.99
55120 T	233A THRU 236A & RUNS MADE FOR MOLECULAR WEIGHT DETER- MINATION	0.3044	14.80
AA-12112		0.3015	14.68
38938		0.2975	14.51
6984-T		0.2855	14.01

flowmeter (PDFM) to determine the molecular weight of the gas mixture by solving the same equations. The molecular weight at the conditions closest to the experimental runs was determined to be 14.66 g/g mole. With an experimental uncertainty of 0.3 percent for the inside diameter of the flowmeter and the experimental uncertainty in mass flow rate of 0.5 percent, the resulting uncertainty in molecular weight is ± 0.25 g/g mole. Since Matheson's molecular weight was within the uncertainty of the molecular weight determination experiment, Matheson's average molecular weight of 14.50 was accepted to calculate the mixture properties.

The properties of the H_2 - CO_2 mixture were determined in the following manner. The gas constant is calculated from the universal gas constant [Reynolds and Perkins, 1970] as

$$R = R/\hat{M} \quad (2)$$

where $R = 8.317$ J/g mole K (1545.33 ft lbf/lb mole R). As shown by Hilsenrath et al. [1955], neither hydrogen nor carbon dioxide behave as perfect gases, particularly at higher pressures. Table 4 shows the compressibility factor taken from that reference for hydrogen and carbon dioxide. The values of temperature and pressure represent the extreme bulk conditions of this study. To determine the compressibility and density of the mixture, it was assumed to be an ideal solution as defined by Van Wylen and Sonntag [1973], i.e., it was assumed to obey Amagat's rule of additive volumes. The compressibility was

Table 4

Compressibility Factors for Hydrogen and Carbon Dioxide

GAS	TEMPERATURE (°K)	ABSOLUTE PRESSURE (MN/m ²)	Z
H ₂	280	0.1 (1 atm)	1.0006
	580	0.1	1.0003
	280	0.7 (7 atm)	1.0042
	580	0.7	1.0024
CO ₂	280	0.1	0.99372
	580	0.1	0.99968
	280	0.7	0.9550
	580	0.7	0.99783

calculated from the data on the individual components presented in Hilsenrath et al. [1955] as

$$Z_{H_2-CO_2} = x_{H_2} Z_{H_2} + x_{CO_2} Z_{CO_2} \quad (3)$$

where the compressibility of the component is measured at the pressure and temperature of the mixture, and x is the mole fraction of the component. For the concentration, pressures and temperatures of the present investigation, the deviation from a perfect gas was less than one percent, but it was included in the data reduction and the numerical predictions.

The specific heat at constant pressure for carbon dioxide varies by about five percent from one atmosphere to the maximum pressure used in this experiment. To calculate c_p , the mixture was again assumed to be an ideal solution and, consequently, that its enthalpy of mixing was zero. This assumption leads to

$$c_{p_{H_2CO_2}} = x_{H_2} c_{p_{H_2}} + x_{CO_2} c_{p_{CO_2}} \quad (4)$$

which was applied with c_p for the individual components determined by interpolation to the mixture pressure in the tables of NBS 564. Mixture specific enthalpy was then calculated by trapezoidal integration of c_p as a function of temperature.

The relationship between specific heats, R , and Z can be found by the relationship [Liepmann and Roshko, 1957],

$$c_p - c_v = R \frac{\left[Z + T \frac{\partial Z}{\partial T} \right]^2}{Z - p \frac{\partial Z}{\partial p}} \quad (5)$$

The speed of sound can be found by the relationship [McEligot, 1963],

$$c = \sqrt{g_c \gamma Z^2 RT} \quad (6)$$

However, in this experiment, the ideal gas approximations were applied to estimate the specific heat ratio and speed of sound in calculating the Mach number by using the relationships

$$c_p - c_v = R \quad (7)$$

$$\gamma = c_p / c_v \quad (8)$$

$$c = \sqrt{g_c \gamma RT} \quad (9)$$

Viscosity and thermal conductivity of the H_2 - CO_2 mixture are taken from Thermophysical Properties of Matter [Touloukian and Ho, 1970]. This reference uses a graphical smoothing of experimental data. Viscosity and thermal conductivity values were linearly interpolated between values given in 0.05 increments of CO_2 mole fraction (from 0.0 to 1.00). Viscosity values at these increments were given at 300K, 400K, 500K, and 550K. Thermal conductivity values at these increments were given at 258K, 273K, 293K, 296K, 298K, 353K, 393K, 433K, and 473K. The mole fraction of CO_2 used in this experiment was 0.30.

The properties were inserted in tabular form in the numerical programs that reduced the experimental friction and heat transfer measurements. In the numerical analysis used to predict heat transfer results, the properties were inserted in equation form. The ideal gas law was used modified by the compressibility factor for real gases.

For all of the gases in this experiment, viscosity and thermal conductivity were assumed to be independent of pressure. The variation of viscosity, thermal conductivity, and specific heat with temperature was accounted for with the following relationships:

$$\mu / \mu_{\text{ref}} = (T / T_{\text{ref}})^a \quad (10)$$

$$k / k_{\text{ref}} = (T / T_{\text{ref}})^b \quad (11)$$

$$c_p / c_{p_{\text{ref}}} = (T / T_{\text{ref}})^d \quad (12)$$

The values for the above exponents are summarized in Table 5 for the $\text{H}_2\text{-CO}_2$ mixture and air. As shown, the viscosity and thermal conductivity of air and the $\text{H}_2\text{-CO}_2$ mixture vary with temperature in approximately the same manner.

Compressibility of the $\text{H}_2\text{-CO}_2$ mixture was represented as a negative exponential function of temperature at the two pressure levels of the experiment for the range $504\text{R} < T < 1530\text{R}$ as:

$$Z = 1.0005 - 0.0053 \exp[-0.00652(T-504)] \quad (13)$$

at pressures of 0.33 MN/m^2 (48 PSIA)

$$Z = 1.0012 - 0.0106 \exp[-0.00652(T-504)] \quad (14)$$

at pressures of 0.64 MN/m^2 (93 PSIA)

Table 5

Values of Exponents for Temperature Variation

GAS	MOLECULAR WEIGHT (g/g mole)	EXPONENT		
		a (Viscosity)	b (Thermal conductivity)	d (Specific heat)
AIR [Bankston and McEligot, 1970]	28.97	0.67	0.805	0.095
H ₂ -CO ₂	14.50	0.79	0.722	0.132

The values used in this study for the properties of the H_2 - CO_2 mixture are listed in Appendix A. At a later date, a computer program for the calculation of the thermodynamic and transport properties of the mixture by Svehla and McBride [1973] may be used for comparison to the properties calculated in this study. However, the program assumes ideal gases or ideal solutions and may not be valid for some of the present data.

EXPERIMENTAL APPARATUS

The experimental apparatus, arrangement, and procedure was similar to that used by Perkins, Schade, and McEligot [1973] and more recently by Pickett [1976]. The test section is a circular tube of INCONEL 600. The tube had an inside diameter of 0.588 cm (0.231 in) and a wall thickness of 0.028 cm (0.011 in). The test section consisted of a vertical heated section 60 diameters in length preceded by an unheated section 60 diameters in length. The unheated section ensured that the velocity profile approached fully developed flow at the inlet of the heated section. For attachment of a. c. power cables, stainless steel electrodes were brazed at the upper and lower ends of the heated section. Two pressure taps were used. One was located 55 diameters above the lower electrode and the other 5 diameters below the lower electrode. Eighteen 0.013 cm (0.005 in) diameter premium grade chromel-alumel thermocouples were spot welded to the heated section of the tube using the parallel junction suggested by Moen [1960].

In addition to the power supply used by Perkins, Schade, and McEligot [1973], an a. c. Lincoln welder (Model TM-500/500) was used in order to reach the high temperatures at the larger Reynolds numbers used in this experiment. To measure flow rates, a calibrated tubular flowmeter that utilizes a correlation between friction factor and Reynolds number was used. This flowmeter measured mass flow rate to within one percent in the range

of this experiment. A detailed discussion of the flowmeter and its flow rate measurement is included in Appendix B. Bourdon tube gages were used to measure static pressure and a MKS Baratron capacitance type differential pressure meter was used to measure pressure drop.

A vacuum external environment was not used in this experiment. The test section was completely enclosed with a draft shield that restricted the convective air currents and helped stabilize the heat loss from the tube to the environment.

The thermocouple conduction error discussed by Hess [1965] was included in the data reduction and is discussed in Appendix B. The heat loss from the tube to the environment was determined using the method described by Campbell and Perkins [1968].

To reduce the heat transfer data, the same computer program that was used by Perkins, Schade, and McEligot [1973] was employed in this study, but was modified for use with a circular tube. The basics of this computer program are described by McEligot [1963].

Table 1 summarizes the range of variables covered in this investigation. A more detailed discussion of the experiment is contained in Appendix B. A list of the experimental data is contained as Appendix D. Table 2 provides a summary of the experimental run conditions. As shown in Table 2, experiments with air and helium were also performed. These provide a check on the apparatus being able to substantiate previous experimental studies and serve as a basis of comparison in the present experiment.

EXPERIMENTAL RESULTS

Friction Results

Adiabatic friction factors were measured during adiabatic experimental runs. These were compared to other investigators' results, and were also used as a check of the pressure, mixture molecular weight, and flow rate measurements. The method described by Shapiro [1953] was used to calculate the adiabatic friction factors in the test section. The mass flow rate was determined by the calibrated tubular flowmeter as described in Appendix B.

The measured friction factors were compared to the experimental correlation of Drew, Koo and McAdams [1932],

$$f_{DKM} = 0.0014 + 0.125 RE_b^{-0.32} \quad (15)$$

This correlation was developed for turbulent flow in tubes, and was used because of its simplicity and close agreement with the Karman-Nikuradse relation. Fig. 4 shows the measured friction factor divided by that calculated from equation (15) plotted as a function of Reynolds number. Air and helium data points are included for comparison. All of the adiabatic friction factors are within ± 5.0 percent of equation (15).

Since only two pressure taps were used, local friction factors could not be determined for experiments with heat addition. Average friction factors were determined in the manner of Humble, Lowdermilk, and Desmon [1951]. This method calculates the average friction factor from the frictional pressure drop,

○ H₂-CO₂
 □ AIR
 △ HELIUM

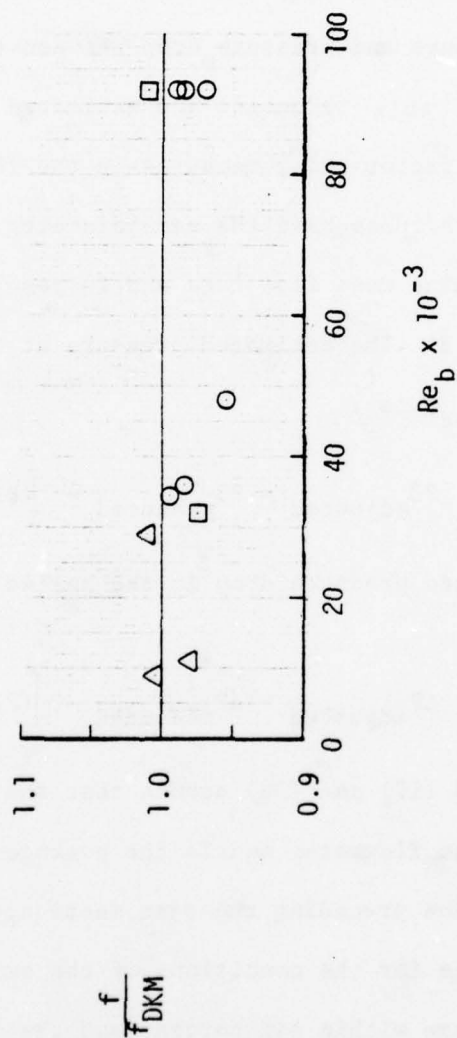


FIGURE 4. COMPARISON OF MEASURED ADIABATIC FRICTION FACTORS TO DREW, KOO AND McADAMS CORRELATION

$$\Delta P_{fr} = [P_1 - P_2] - \frac{G^2 R}{g_c} \left(\frac{T_{b2}}{P_2} - \frac{T_{b1}}{P_1} \right) \quad (16)$$

The pressure taps were located in the test section as shown in Fig. 5. As shown, the upstream pressure tap is just outside of the heated portion of the test section. To account for the upstream pressure tap not being located in the heated region, the pressure and pressure drop between taps were reduced. The amount of this reduction was estimated from the adiabatic friction factor being measured in the flowmeter of the apparatus since both tubes have the same diameter. The flowmeter is used to determine mass flow rate and is described in detail in Appendix B. The estimated pressure at the start of heating, $P3_{adjusted}$, is :

$$P3_{adjusted} = P3_{measured} - \left[(P1 - P2) \frac{2.8}{58.4} \right] \quad (17)$$

The reduced pressure drop in the heated test section, $\Delta P_{adjusted}$, is:

$$\Delta P_{adjusted} = \Delta P_{measured} - \left[(P1 - P2) \frac{2.8}{58.4} \right] \quad (18)$$

Equations (17) and (18) assume that the average density of the gas in the flowmeter equals the average density of the gas in the portion preceding the test section. This assumption is reasonable for the conditions of the experiment since the pressure is the same within six percent and the correction is small compared to the overall pressure drop, $P3 - P4$. The average friction factors were compared to an experimental correlation

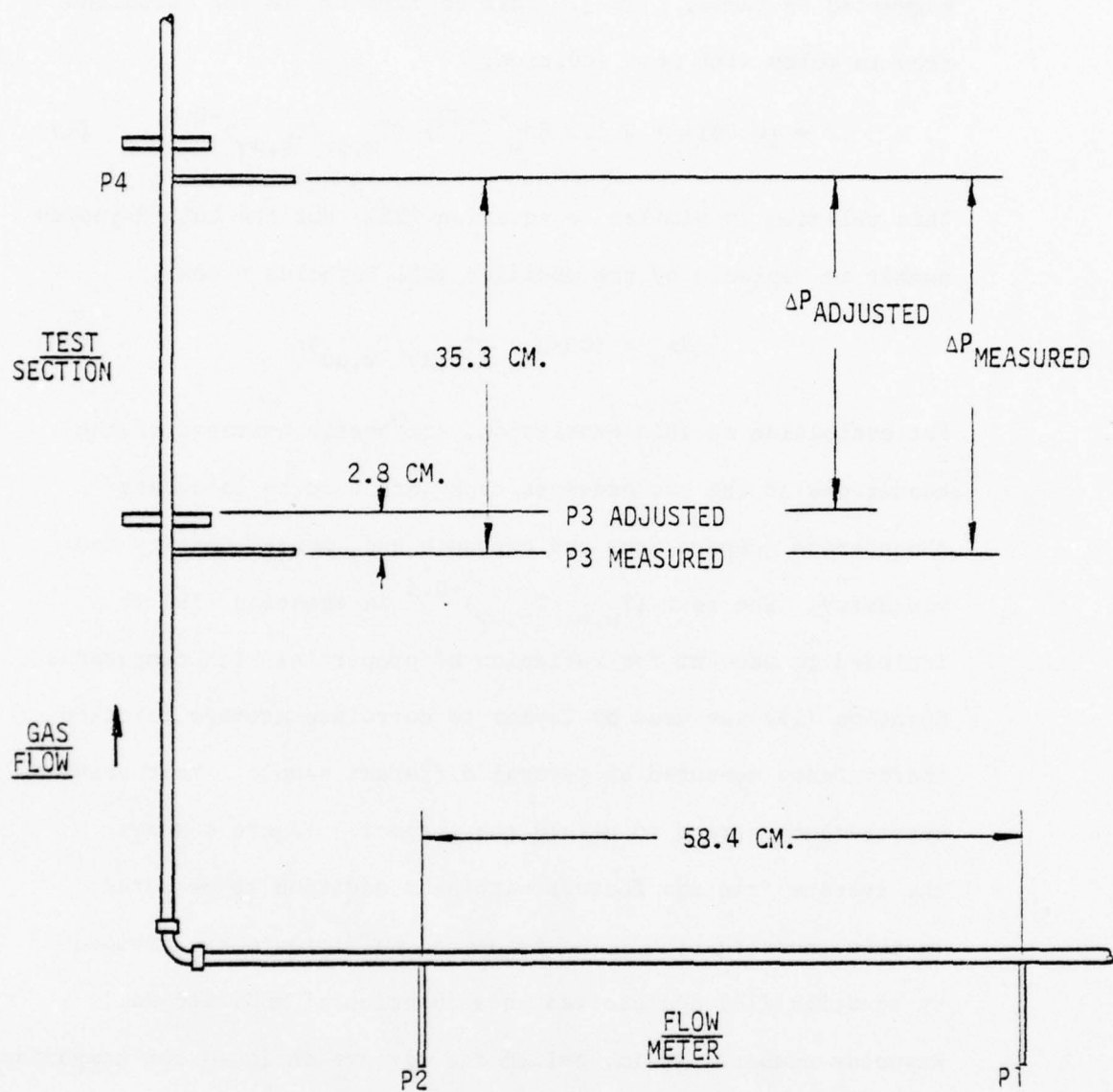


FIGURE 5. PRESSURE TAP LOCATION

suggested by Taylor [1967]. This correlation is for turbulent flow in tubes with heat addition.

$$f = (0.0014 + 0.125 \text{Re}_w^{-0.32}) (T_{w,av}/T_{b,av})^{-0.5} \quad (19)$$

This relation is similar to equation (15), but the bulk Reynolds number is replaced by the modified wall Reynolds number,

$$\text{Re}_w = (GD/\mu_w) (T_{b,av}/T_{w,av}) \quad (20)$$

For evaluation of this expression, arithmetic averages of the conditions at the two pressure taps were used to calculate the average temperatures and pressure and, hence, density and viscosity. The term $(T_{w,av}/T_{b,av})^{-0.5}$ in equation (19) is included to account for variation of properties with temperature. Equation (19) was used by Taylor to correlate average friction coefficients measured by several different people. Most previous measurements agreed to within ten percent. Figure 6 shows the average friction factors with heat addition as measured in this investigation. The friction coefficients are divided by equation (19) and plotted as a function of modified wall Reynolds number. Again, helium and air are included for comparison.

Fig. 6 shows eight experimental data points for each gas. The eight points are the result of two groups of four runs; one group at a higher Reynolds number, one group at a lower Reynolds number. A common flow rate was set approximately for all heating rates in a single group. As the result of an increase in heating rate and average temperatures, the modified

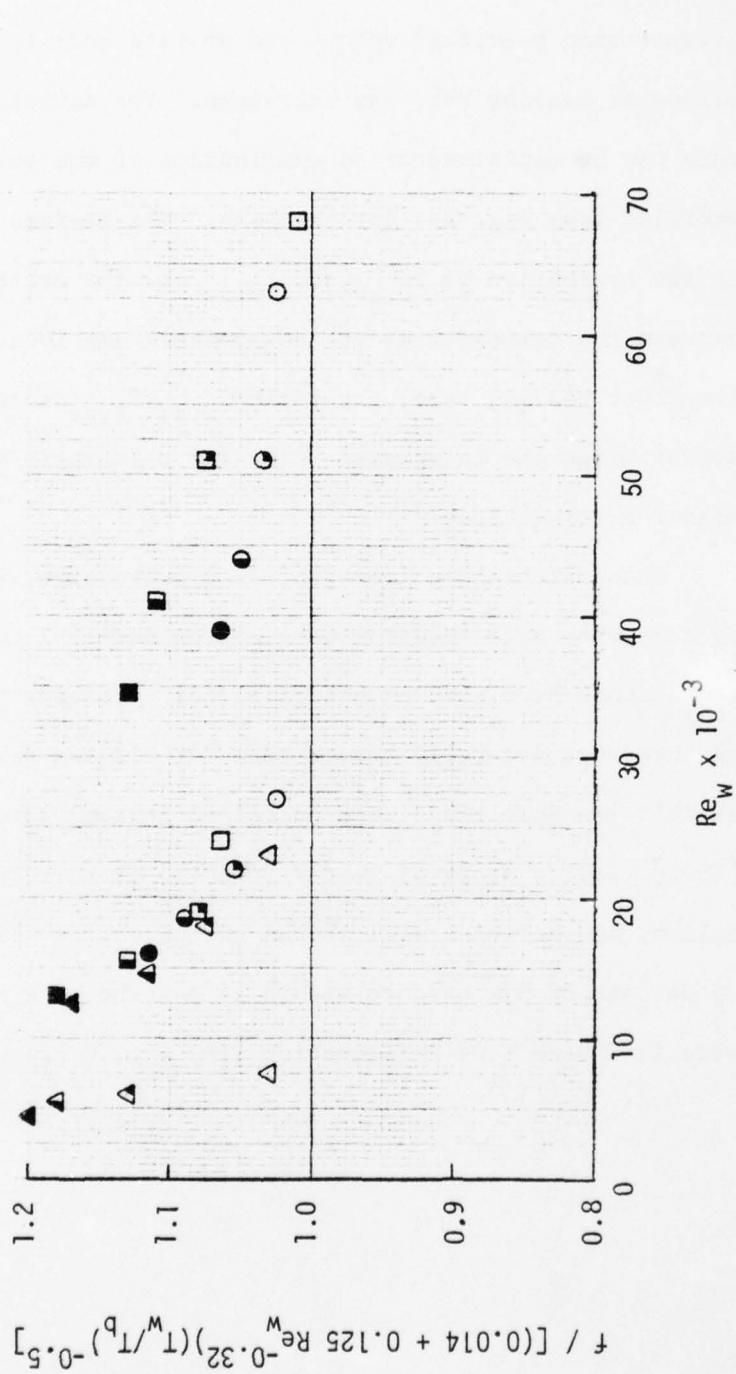


FIGURE 6. COMPARISON OF AVERAGE FRICTION FACTORS TO VARIABLE PROPERTIES CORRELATION OF TAYLOR [1967].

wall Reynolds number was reduced.

As shown on Fig. 6, the experimental results were all greater than predicted values and deviate more from predicted values as heating rate was increased. The deviation with heating rate can be explained by an examination of the temperature profiles (see Fig. B6, for example). The average temperatures in the evaluation of $T_{b,av}$ and $T_{w,av}$ are the arithmetic average between the temperatures at the pressure tap locations. At the lower heating rate, the ratio $T_{w,av}/T_{b,av}$ more closely approximates the integrated value for this ratio than at the higher heating rates.

Thus, within the limits of this evaluation, the friction factors with heat addition were approximately 2 to 20 percent above those predicted by equation (19). Results for the H_2-CO_2 mixture were generally better than for air and helium but still exhibit the same trend with increased heating rate. Pickett's [1976] similar study of heated friction factors (with air, helium, and helium-argon) showed that equation (19) predicted 84 percent of his data to within ± 4 percent, but most of the data were in a band $1.04 > f/\text{equation (19)} > 1.00$, i.e., again high.

Heat Transfer Results

To determine the effects of the lower hydrogen-carbon dioxide Prandtl number on the heat transfer results, the variation of properties with temperature and the entrance effects were minimized. The entrance effects were minimized by considering only the results at which approximately fully developed conditions existed ($x/D > 20$). An extension of the method described by Malina and Sparrow [1964] was used to approach the constant properties idealization.

For the method described by Malina and Sparrow, a fixed inlet Reynolds number is maintained while the wall-to-bulk temperature difference is varied. At a particular axial location, the ratio of experimentally determined bulk Nusselt number to a Dittus-Boelter type correlation is plotted as a function of wall-to-bulk temperature ratio. Extrapolation to a wall-to-bulk temperature ratio of one gives a value that can be interpreted as the constant property Nusselt number, Nu_{cp} . Since the ratio of bulk Nusselt number to a Dittus-Boelter type correlation only partially eliminates any effects caused by small deviations of the Reynolds number, these deviations should be kept as small as possible.

The procedure described in the previous paragraph is demonstrated in Fig. 7 for a H_2 - CO_2 mixture with a molecular weight of 14.5, inlet Reynolds number of approximately 85,000, and inlet Prandtl number of 0.34. Extrapolations for five different

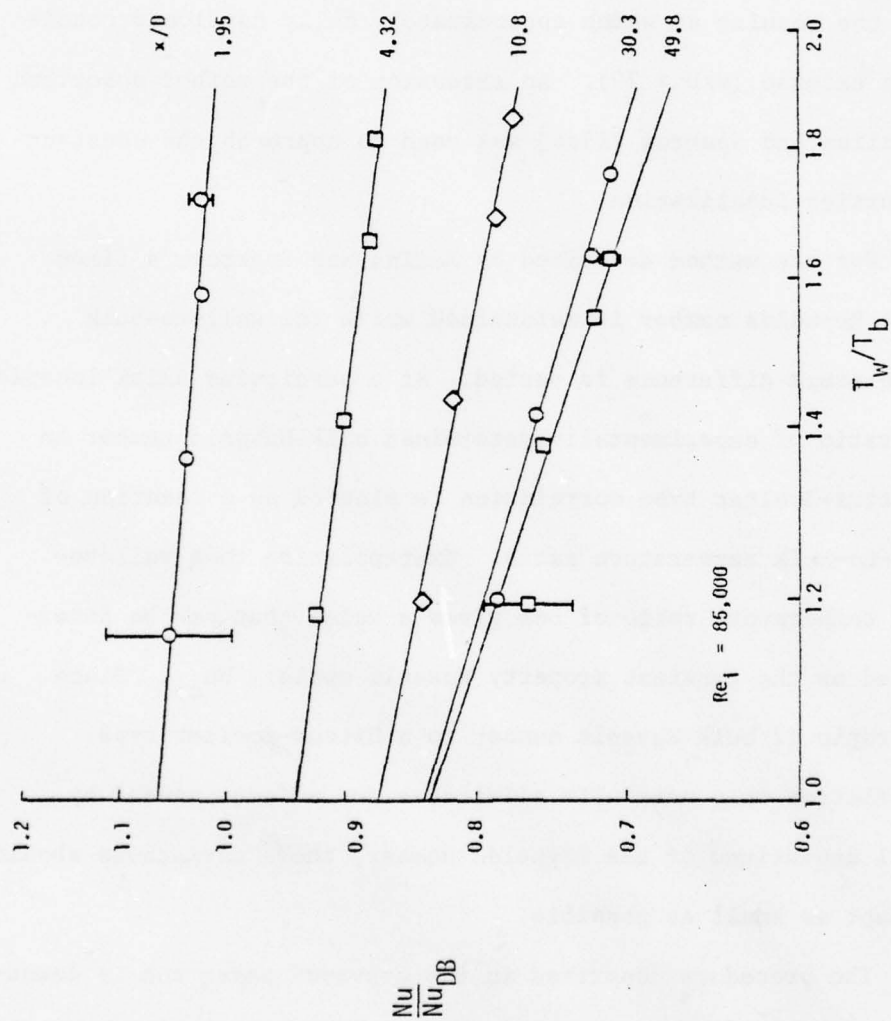


FIGURE 7. TECHNIQUE FOR DETERMINING CONSTANT PROPERTY NUSSELT NUMBER

axial locations are shown. For this investigation the Dittus-Boelter type correlation (equation 1) was used.

For the H_2 - CO_2 mixture at fully developed conditions, ($x/D \approx 50.0$), Fig. 7 shows the ratio Nu_{CP}/Nu_{DB} to be approximately 0.84. From these results, it was determined that the Dittus-Boelter type equation (equation 1) does not predict correct Nusselt numbers for a Prandtl number of 0.34. For fully developed conditions with air or helium as the experimental fluid, the ratio Nu_{CP}/Nu_{DB} varied from 0.96 to 1.11. Table 6 summarizes the Nu_{CP}/Nu_{DB} ratios found for the various experimental conditions. As shown in Table 6, the ratio Nu_{CP}/Nu_{DB} decreased at the higher Reynolds number for each of the individual gases.

The error bars on Fig. 7 indicate that a band of the experimental uncertainty of the data can be extrapolated to a T_w/T_b ratio of one to find the estimated uncertainty in the constant property Nusselt number. This technique was used by Reynolds, Swearingen, and McEligot [1969]. The uncertainty in Nu_{CP}/Nu_{DB} in this investigation varied from ± 0.08 at small x/D to ± 0.05 at large x/D . Appendix C describes the method used for calculating uncertainty in the measured Nusselt number and a discussion of the trends noted.

It remains to find a correlation to predict the correct constant property Nusselt number for the Prandtl number of the H_2 - CO_2 mixture. Pickett [1976] suggests a correlation of a form comparable to the Dittus-Boelter type correlation, but

Table 6
Ratio of Nu_{CP}/Nu_{DB} for Experimental Conditions

GAS	Re_i (Approx.)	Nu_{CP}/Nu_{DB} (At $x/D = 50.0$)
AIR	29000	1.11
AIR	84000	0.96
HELIUM	9000	1.07
HELIUM	27000	1.05
H ₂ -CO ₂	34000	0.90
H ₂ -CO ₂	85000	0.84

with the exponent of the Prandtl number changed to 0.55,

$$Nu_{CP} = 0.021 Re^{0.8} Pr^{0.55} \quad (21)$$

for the constant property Nusselt numbers of helium-argon mixtures ($0.42 < Pr < 0.49$). Equation (21) predicted the constant property Nusselt number of the helium-argon mixtures to within five percent for the range of Reynolds numbers between 31,200 and 102,000.

By using the value of 0.84 for the Nu_{CP}/Nu_{DB} ratio from the H_2 - CO_2 mixture ($Re_b = 85,000$), the value of the exponent on the Prandtl number of equation (1) would change from 0.4 to 0.56. Thus, the present experiment indicates that Pickett's correlation may now be valid for the Prandtl number range of 0.34 to 0.49. Figure 8 shows the constant property Nusselt number normalized by equation (21) plotted as a function of Prandtl number. The results at the higher Prandtl numbers ($0.42 < Pr < 0.49$) are from Pickett [1976]. Two trends were substantiated by the current experiment with a lowering of the Prandtl number to 0.34: (1) for a particular Prandtl number, the ratio of Nu_{CP} divided by equation (21) decreased as the Reynolds number increased, and (2) this effect became more pronounced as the Prandtl number decreased.

To account for the variation of properties and entrance effects in this investigation, the correction factors suggested by Magee [1964] were used:

$$\left[(T_w/T_b)^{-0.4} + 0.6 D/x \right] \quad (22)$$

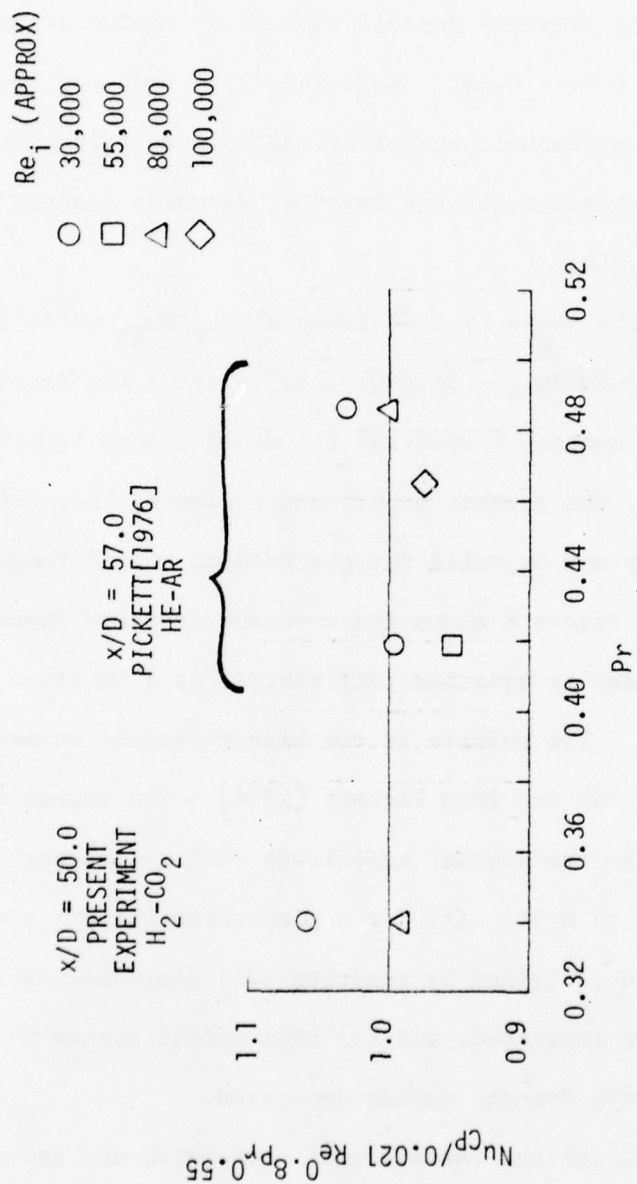


FIGURE 8. COMPARISON OF Nu_{cp} TO EMPIRICAL CORRELATION OF PICKETT (1976) FOR FULLY DEVELOPED CONDITIONS.

The term $(T_w/T_b)^{-0.4}$ accounts for the variation of properties, and the term $0.6 D/x$ accounts for the entrance effects. If these correction factors are applied to equation (1), the resulting equation is

$$Nu_b = 0.021 Re_b^{0.8} Pr_b^{0.4} [(T_w/T_b)^{-0.4} + 0.6 D/x] \quad (23)$$

For x/D between 1.4 and 49.8 this equation predicted all of the measured bulk Nusselt numbers for air and helium within ± 15 percent and 96 percent of the Nusselt numbers within ± 10 percent.

If the correction factors (relation 22) are applied to equation (21), the resulting relation is

$$Nu_b = 0.021 Re_b^{0.8} Pr_b^{0.55} [(T_w/T_b)^{-0.4} + 0.6 D/x] \quad (24)$$

This equation predicted the H_2 - CO_2 mixture Nusselt numbers in the fully developed region within ± 13 percent, but under-predicted the Nusselt numbers in the entrance region by as much as 18 percent. To have the same level of accuracy with the H_2 - CO_2 data that was obtained with the air and helium data, changes to the correlation were necessary.

As previously discussed, the transport properties of H_2 - CO_2 vary with temperature in approximately the same manner as those of air and helium. For this reason the term $(T_w/T_b)^{-0.4}$ was retained as a reasonably accurate correction factor for the variation of properties downstream. Kays [1966] discusses the effect of different Prandtl numbers in the thermal entrance region of circular tubes. He shows that as the Prandtl number

decreases, the effect of the entrance region on the Nusselt number is more pronounced. As a consequence of this observation, the coefficient in the term, $0.6 D/x$, of equation (24) was revised. Since H_2-CO_2 has a lower Prandtl number than air, one would expect the coefficient to have a larger value than 0.6. Pickett [1976] determined that a value of 0.85 worked best for the coefficient of the entrance effects term for helium-argon ($0.42 < Pr < 0.49$). A value of 0.85 was used for the coefficient in equation (24), and the result was compared to the experimentally determined bulk Nusselt numbers of H_2-CO_2 . The complete correlation, accounting for entrance effects and variation of properties becomes

$$Nu_b = 0.021 Re_b^{0.8} Pr_b^{0.55} [(T_w/T_b)^{-0.4} + 0.85 D/x.] \quad (25)$$

For x/D between 1.4 and 49.8 this equation predicted all of the measured bulk Nusselt numbers for H_2-CO_2 within ± 15 percent and 91 percent within ± 10 percent.

Measured bulk Nusselt numbers normalized by equation (25) are plotted on Fig. 9 as a function of x/D . For clarity, only results from four H_2-CO_2 experimental runs were plotted. The data plotted are from experimental runs that include the complete range of experimental variables for the H_2-CO_2 mixtures. The greatest difference between the experimental data and equation (25) occurred at high heating rates in the x/D range between 4.0 and 10.0. In this range equation (25) underpredicted the measured Nusselt numbers by 8 to 12 percent.

$Re_{b,i}$
 ○ 34300
 ● 33900
 □ 82600
 ■ 87100

$(T_w/T_b)_{MAX}$
 1.18
 1.85
 1.20
 1.85

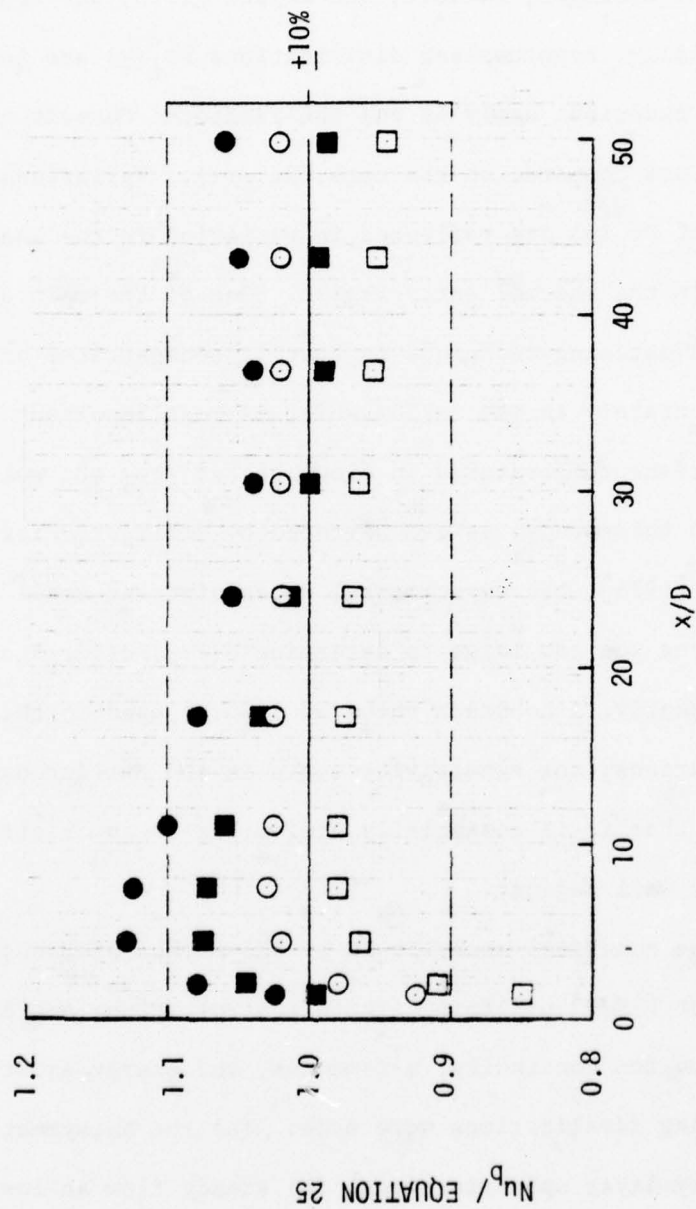


FIGURE 9. COMPARISON OF LOCAL BULK NUSSLETT NUMBERS TO EQUATION 25 FOR H_2-CO_2 MIXTURES

DETERMINATION OF TURBULENT PRANDTL NUMBER

Numerical Analysis

In order to deduce the turbulent Prandtl number, the technique of McEligot, Pickett, and Taylor [1976] was applied. Essentially, hypothesized distributions $Pr_t(y)$ are introduced in the numerical analysis and the predicted Nusselt numbers, $Nu(x)$, are compared to the data, $Nu_{CP}(x)$. Variations in the shape of $Pr_t(y)$ are reflected in variation in the shape of $Nu(x)$ in the thermal entry region. One of the main advantages of this matching technique is that it concentrates on determining Pr_t accurately in the region which is most important for predicting surface temperatures in flows heated from the wall.

In this study, as demonstrated by McEligot, Pickett, and Taylor [1976], the experimental uncertainty at small axial distances was too large to determine $d(Pr_t)/d(y/r_w)$ clearly. Consequently, a constant value of Pr_t was used in the present calculations; the sensitivity tests in the earlier paper also showed that it is essentially equivalent to an effective $Pr_{t,w}$ for the wall region.

The numerical analysis is by the method of Bankston and McEligot [1970] utilizing finite control volume approximations to solve the continuity, x-momentum, and energy equations. The following idealizations were made: (a) the axisymmetric boundary layer approximations, (b) steady flow at low velocities, (c) constant mixture concentration, and (d) negligible axial

conduction. Initial conditions are specified and boundary conditions are the no-slip, impermeable wall with the observed wall heat flux variation specified. The effective viscosity is predicted with a combination of the van Driest mixing length [1956] and Reichart middle law [1951],

$$\ell_{VD} = \kappa y \{1 - \exp(-y^+/y_\ell^+)\} \quad (26)$$

and

$$\epsilon_M = \epsilon_{VD} \cdot \left(2 - \frac{y}{r_w}\right) \cdot [1 + 2\left(\frac{r}{r_w}\right)^2]/6 \quad (27)$$

The wall temperature is used to evaluate properties in y^+ for variable properties. With $\kappa = 0.4$ and $y_\ell^+ = 26$, this representation yields adiabatic friction factors within about one percent of the Drew, Koo, and McAdams correlation [1932] over the range of Reynolds numbers used in this study.

The program uses implicit algebraic equations to represent the governing equations. These equations are iterated at each axial step to treat their coupling and the non-linear terms.

Prediction with Constant Properties

For predictions under the constant property idealizations, the mixture properties are independent of temperature. Then, as the inlet condition is a fully developed flow, only the energy equation is solved.

The inlet Reynolds number, inlet Prandtl number, constant properties condition (exponents in equations 10, 11 and 12 set

equal to zero), wall heat flux variation, and different values of Pr_t were used as input to the numerical procedure. For the first three diameters, the experimental axial wall heat flux variation resembled an exponential approach to a ramp with a positive slope but a negative second derivative. For the remaining length, the wall heat flux was constant within two percent. The same axial variation of wall heat flux was used for all of the constant property numerical calculations. The axial variation of wall heat flux was taken from an experimental run with the lowest heat flux. Due to the large uncertainty in the immediate thermal entry, only results for x/D greater than eight were used to determine $Pr_{t,w}$. For the numerical predictions, the Reynolds number was taken to be the inlet Reynolds number of the lowest heating rate in the four run series.

From the numerical analysis, the axial variation of $Nu(x)$ was calculated. By comparing graphs of the experimentally measured $Nu_{CP}(x)$ to the calculated $Nu(x)$, $Pr_{t,w}$ for the hydrogen-carbon dioxide mixture was determined. The variation of $Pr_{t,w}$ with respect to Reynolds number was examined by comparing Nu_{CP} at different Reynolds numbers, but the same Prandtl number.

Constant property predictions are shown in Figure 10 for two assumed values of Pr_t . The normalization at $Re_i = 85,000$ shows that the predicted values fall about twenty percent below the accepted Dittus-Boelter correlation (equation 1) in the downstream region. Since the measured heat flux variation served

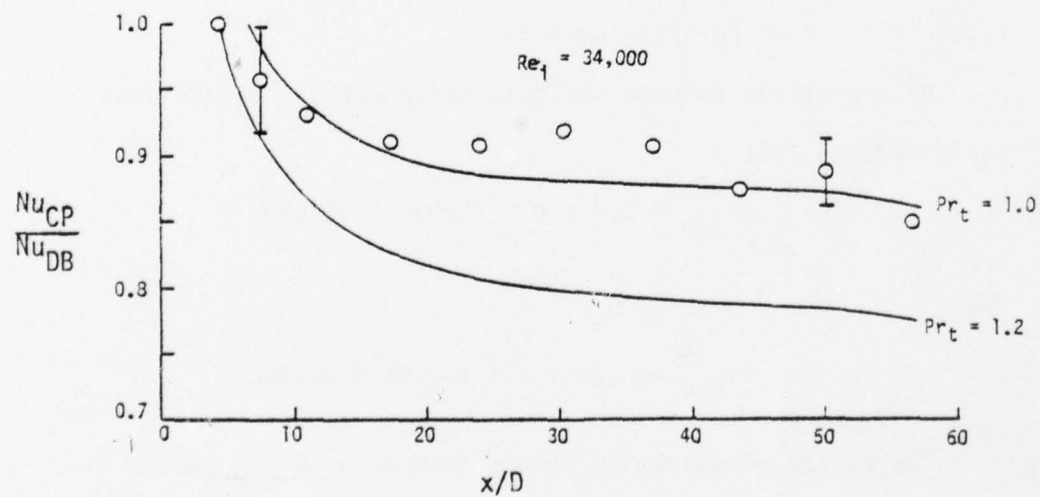
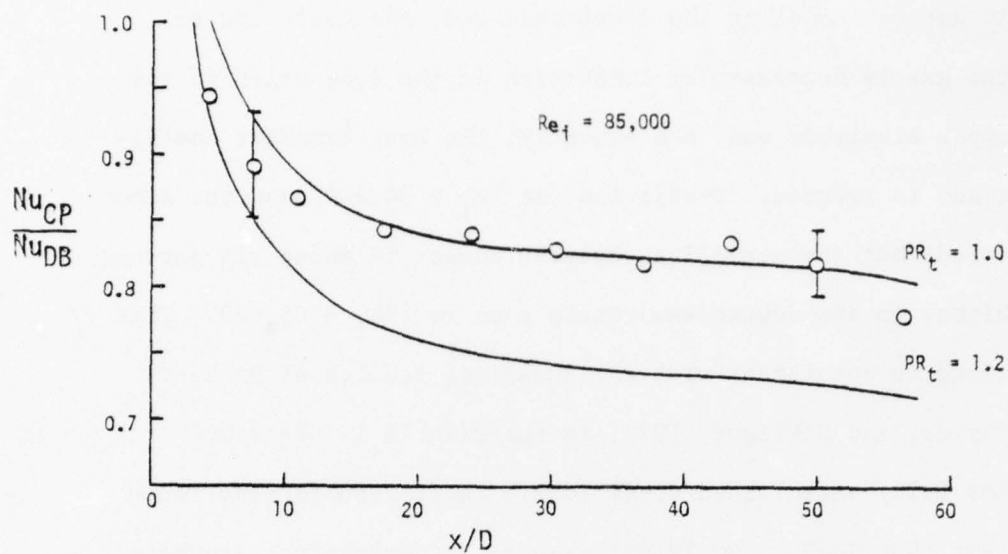


FIGURE 10. DETERMINATION OF $P_{t,w}$ FOR CONSTANT PROPERTIES DATA

as the thermal boundary condition, a constant Nusselt number is not achieved; at the downstream end, the heat flux to the gas is decreased by conduction in the tube walls to the upper electrode and, consequently, the heat transfer coefficient is reduced. Predictions at $Re_i = 34,000$ show the same trends but the normalized Nusselt number is about six percent higher in the downstream region than for $Re_i = 85,000$. This trend is consistent with the numerical results of Pickett, Taylor, and McEligot [1977] in the range $0.1 < Pr < 0.7$ for fully established conditions. Their results also forecast that Nu/Nu_{DB} would decrease as Pr decreases. Brackets indicating the experimental uncertainty of the measured $Nu_{CP}(x)$ are also included. This uncertainty was attained from extrapolations to constant properties taken from plots similar to Figure 7 for both Reynolds numbers.

By comparison between the data and numerical predictions, it is deduced that

$$Pr_{t,w} = 1.0 \pm 0.1 \text{ for } Re \approx 85,000$$

and

$$Pr_{t,w} = 0.95 \pm 0.1 \text{ for } Re \approx 34,000$$

The effect of molecular Prandtl number on $Pr_{t,w}$ can be examined using the results from similar plots of $Nu_{CP}(x)$ vs. axial location as summarized in Table 7. The deduced $Pr_{t,w}$ for the H_2-CO_2 mixture was compared with deduced $Pr_{t,w}$ values

Table 7

Variation of Turbulent Prandtl Number With Respect to Molecular
Prandtl Number

GAS	MOLECULAR WEIGHT	PRANDTL NUMBER	$Pr_{t,w}$	REYNOLDS NUMBER
H_2-CO_2	14.5	0.34	$\left\{ \begin{array}{l} 1.0 \pm 0.1 \\ 0.95 \pm 0.1 \end{array} \right.$	 85000 34000
HE-AR[Pickett, 1976]	15.30	0.42	1.1 ± 0.1	32000
	29.70	0.49	1.0 ± 0.1	31600
AIR[McEligot, Pickett, & Taylor, 1976]	28.97	0.72	0.9 ± 0.1	44500

for air and helium-argon mixtures from the study by Pickett [1976]. As shown, that while the earlier studies showed a potential trend ($Pr_{t,w}$ increasing as Pr is reduced), the present work does not extend it. Considering these data to date, one can best summarize the results as confirming Reynolds' analogy ($Pr_{t,w} = 1$) within ten percent over this range of Pr .

Prediction with Gas Property Variation

In order to increase power densities in closed Brayton cycle systems, high heating rates may be employed. Consequently, the temperature-dependence of the fluid transport properties causes significant variation in properties and coupling of the governing equations. The results and correlations based on the constant properties idealizations become less valid. In this section, the modifications accounting for property variation when applying the turbulent Prandtl number are tested. For both series of data the maximum wall temperature was about 810K (1000 F) leading to maximum T_w/T_i and T_w/T_b ratios of 2.8 and 1.8, respectively. Thus, the density varies by a factor of 2.8 and viscosity by 2.3 within the test section.

The numerical method of Bankston and McEligot [1970] was developed to account for property variation so predictions are straightforward once the functional dependences of the properties are entered as subroutines. For the highest heating rate of each of the two series of runs, the entering conditions and wall heat flux distribution were taken from the results of the data reduction program and were applied as boundary conditions in the numerical analysis.

There are two major assumptions concerning the simple turbulence model. First, the van-Driest mixing length is modified to account for higher heating rates by evaluating the properties in the damping function at the wall temperature,

as suggested by Bankston and McEligot [1970] from examination of data for pure gases. Secondly, the turbulent Prandtl numbers deduced from the constant properties comparisons were employed directly, i.e., 1.0 at the higher Reynolds number and 0.95 at the lower. In addition, it is implicitly assumed that no chemical reaction takes place between H_2 and CO_2 and there is no significant thermally induced diffusion separating the components. Further assumptions are the relations for variation of fluid properties as described earlier.

The numerical predictions are presented as solid lines in Figure 11 with constant property predictions at the same inlet Reynolds numbers dashed for comparison. The trends predicted are the same as observed for pure gases [McEligot, Magee, and Leppert, 1965] and for mixtures of argon and helium [Pickett, Taylor and McEligot, 1977]. The Nusselt number is reduced--or "deteriorates"--both from the reduction in local Reynolds number as the gas mixture is heated and from the property variation across the tube. At these heating rates, most of the reduction occurs in the first twenty diameters and then is more gradual downstream.

Comparison to the data confirms the numerical predictions. At the higher flow rate, agreement is within six percent and for the lower it is closer yet. For the former, a change to $Pr_{t,w} = 0.95$ would improve the agreement, but the experimental uncertainty does not warrant the additional precision this

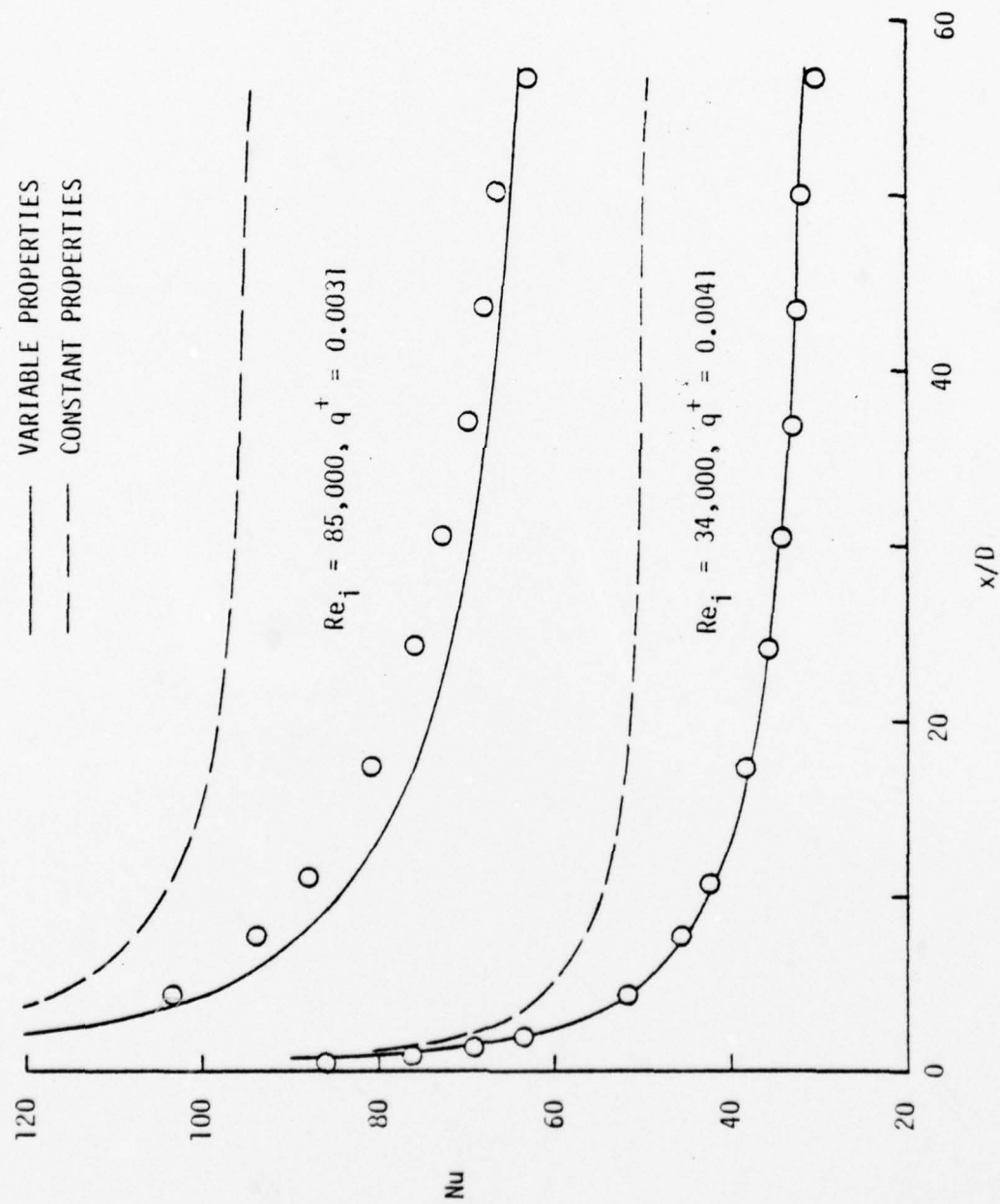


FIGURE 11, NUMERICAL PREDICTIONS COMPARED TO DATA FOR RUNS AT HIGHEST HEATING RATES. [EXPERIMENTAL UNCERTAINTY APPROXIMATELY PRESENTED BY SIZE OF SYMBOLS.]

revision would imply. This close comparison demonstrates that the assumptions mentioned previously are reasonable as a group and indicates that the numerical prediction method should be useful over the range of conditions encompassed by the present investigation.

CONCLUSIONS

The object of this investigation was to study the momentum and heat transfer characteristics for turbulent flow of a hydrogen-carbon dioxide mixture (molecular weight = 14.5) in tubes. This mixture has a molecular Prandtl number of 0.34 and tests with it serve to indicate how a proposed working fluid, helium-xenon, will perform in a closed Brayton cycle. The range of inlet Reynolds numbers in the heated experiments was between 34,000 and 88,000 and the T_w/T_b ratio was between 1.18 and 1.85. Experimental results were compared to existing empirical correlations, and to results from a numerical analysis. From this investigation, the following conclusions have been made:

1. The Drew, Koo and McAdams [1932] correlation

$$f_{DKM} = 0.0014 + 0.125 Re_b^{-0.32}$$

predicts the adiabatic friction factor for the H_2 - CO_2 mixture to within ± 5 percent in the Reynolds number range of 35,000 to 92,000.

2. A correlation suggested by Taylor [1967]

$$f = (0.0014 + 0.125 Re_w^{-0.32}) (T_w/T_b)^{-0.5}$$

for turbulent flow in tubes with heat addition underpredicted experimental results by as much as 11 percent for the H_2 - CO_2 mixture.

3. Dittus-Boelter [McAdams, 1954] type correlations developed

from pure gas data

$$Nu_{DB} = 0.021 Re^{0.8} Pr^{0.4}$$

overpredict hydrogen-carbon dioxide Nusselt numbers for constant property, fully developed conditions by about 15 percent. An equation of similar form,

$$Nu = 0.021 Re^{0.8} Pr^{0.55}$$

but with the exponent of the Prandtl number revised to 0.55 predicts constant property Nusselt numbers for the H_2 - CO_2 mixture to within ± 6 percent. This result can be combined with the results from Pickett [1976] for helium-argon mixtures ($0.42 < Pr < 0.49$) to predict constant property Nusselt numbers in the Prandtl number range of 0.34 to 0.49.

4. The entrance and property effects can be accounted by using the equation

$$Nu_b = 0.021 Re_b^{0.8} Pr_b^{0.55} [(T_w/T_b)^{-0.4} + 0.85 D/x].$$

This equation predicted the bulk Nusselt numbers of the H_2 - CO_2 mixture to within ± 15 percent for x/D between 1.4 and 49.8. This same result was found by Pickett [1976] for helium-argon mixtures ($0.42 < Pr < 0.49$).

5. The turbulent Prandtl number in the wall region, $Pr_{t,w}$ was determined to be

$$Pr_{t,w} = 1.0 \pm 0.1 \text{ for } Re = 85,000$$

$$Pr_{t,w} = 0.95 \pm 0.1 \text{ for } Re = 34,000.$$

Although earlier studies with air and helium-argon mixtures show a potential trend of $Pr_{t,w}$ increasing as Pr is reduced, the present study does not extend it. Thus, Reynolds' analogy ($Pr_{t,w} = 1$) is confirmed within 10 percent for a Pr of 0.34. Also, the effect of Reynolds number on $Pr_{t,w}$ is shown to be slight but inconclusive due to experimental uncertainty.

6. At maximum wall heating rates ($(T_w/T_b)_{MAX} = 1.85$), $Pr_{t,w}$ determined from constant property conditions can be used in a variable properties numerical analysis to predict $Nu_b(x)$. For the particular experimental runs studied ($Re_i = 34,000$ & $85,000$ and $Pr_i = 0.34$), the use of experimentally determined $Pr_{t,w}$ values provided calculated $Nu_b(x)$ which agreed with measured $Nu_b(x)$ within the accuracy of the experiment.

APPENDIX A.
Mixture Properties

Hydrogen-Carbon Dioxide
Molecular Weight = 14.50

Temperature	Property				
[F]	μ [$\frac{\text{lbm}}{\text{ft hr}}$]	k [$\frac{\text{Btu}}{\text{hr ft F}}$]	c_p [$\frac{\text{Btu}}{\text{lbm F}}$]	i [$\frac{\text{Btu}}{\text{lbm}}$]	c [$\frac{\text{ft}}{\text{sec}}$]
40.00	.03250	.05050	.51650	238.00	1530.00
70.00	.03420	.05250	.52050	253.56	1572.00
100.00	.03580	.05450	.52400	269.23	1613.00
130.00	.03730	.05650	.52800	285.01	1653.00
160.00	.03870	.05840	.53100	300.90	1692.00
190.00	.04020	.06030	.53450	316.88	1730.00
220.00	.04170	.06220	.53750	332.96	1768.00
250.00	.04320	.06410	.54050	349.13	1804.00
280.00	.04450	.06600	.54300	365.38	1840.00
310.00	.04590	.06800	.54600	381.72	1875.00
340.00	.04730	.07000	.54900	398.15	1909.00
370.00	.04880	.07200	.55200	414.67	1943.00
400.00	.05020	.07410	.55450	431.27	1976.00
430.00	.05160	.07580	.55750	447.95	2009.00
460.00	.05330	.07770	.56000	464.71	2041.00
490.00	.05470	.07960	.56250	481.55	2072.00
520.00	.05610	.08160	.56500	498.46	2103.00
550.00	.05750	.08360	.56750	515.45	2134.00
580.00	.05880	.08560	.56950	532.51	2164.00
610.00	.06020	.08760	.57200	549.63	2193.00
640.00	.06150	.08960	.57400	566.82	2223.00
670.00	.06280	.09140	.57600	584.07	2251.00
700.00	.06400	.09340	.57800	601.38	2280.00
730.00	.06520	.09540	.57950	618.74	2308.00
760.00	.06640	.09730	.58150	636.16	2335.00
790.00	.06760	.09930	.58300	653.63	2362.00
820.00	.06880	.10130	.58500	671.15	2390.00
850.00	.07010	.10330	.58650	688.72	2417.00
880.00	.07120	.10520	.58800	706.34	2443.00
910.00	.07240	.10720	.59000	724.01	2469.00
940.00	.07350	.10920	.59150	741.73	2495.00
970.00	.07470	.11120	.59300	759.50	2521.00
1000.00	.07580	.11320	.59450	777.31	2546.00
1030.00	.07700	.11520	.59600	795.17	2571.00
1060.00	.07800	.11720	.59750	813.12	2596.00
1090.00	.07900	.11910	.59900	831.07	2621.00
1120.00	.08000	.12100	.60050	849.06	2645.00
1150.00	.08100	.12300	.60200	867.10	2669.00
1180.00	.08190	.12490	.60350	885.18	2694.00
1210.00	.08290	.12690	.60500	903.31	2717.00
1240.00	.08400	.12890	.60650	921.48	2741.00
1270.00	.08500	.13090	.60800	939.70	2764.00
1300.00	.08590	.13280	.60950	957.96	2789.00
1330.00	.08680	.13480	.61050	976.26	2811.00
1360.00	.08760	.13680	.61200	994.60	2833.00

APPENDIX B. EXPERIMENT

Apparatus

A schematic diagram of the experiment is shown in Fig. B1.

Two regulators were used to reduce and stabilize the pressure from the gas supply. On the experiments with the H_2 - CO_2 mixture, four high pressure bottles were connected to a manifold to allow ample experimental run time. A sketch of the test section area displaying the location of thermocouples, pressure taps, and electrodes, is shown in Fig. B2. A sketch of the draft shield is shown in Fig. B3.

Mass flow rate was measured with three instruments. A Brooks rotometer was used to obtain a rough measurement of the flow rate. A Meriam laminar flow element as described by Pickett [1976] also served as a check on the mass flow rate. A tubular flowmeter that had the same inside diameter as the test section served as the primary mass flow rate instrument. This flowmeter has two pressure taps with a 58.38 cm (23.00 in) spacing and its theory of operation is described under a separate heading in this appendix.

Bourdon tube gages by Heise measured the static pressure just downstream of the rotometer and at inlet static pressures to the other mass flow rate instruments. Pressure drops in the test section and flow measuring instruments were measured with a MKS Baratron

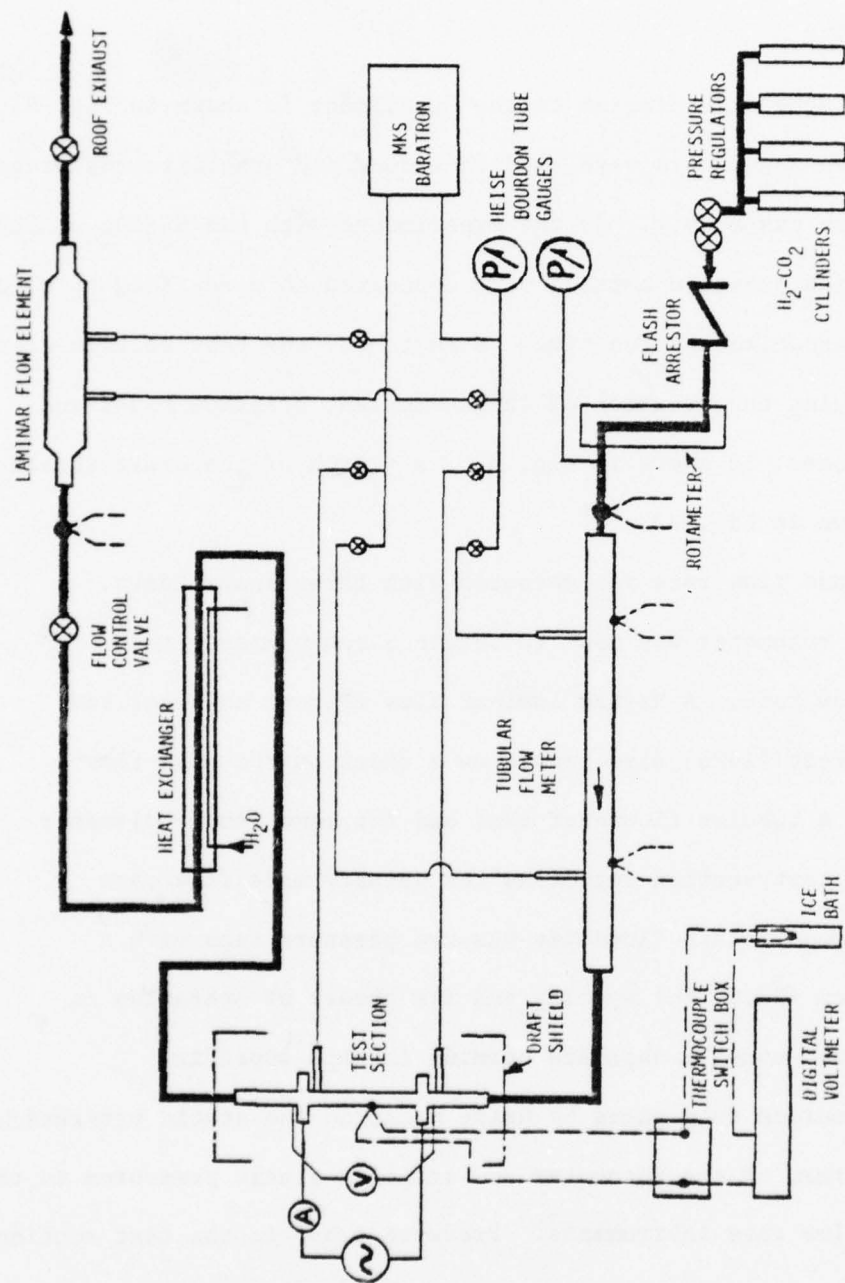


FIGURE B1. SCHEMATIC DIAGRAM OF EXPERIMENTAL APPARATUS

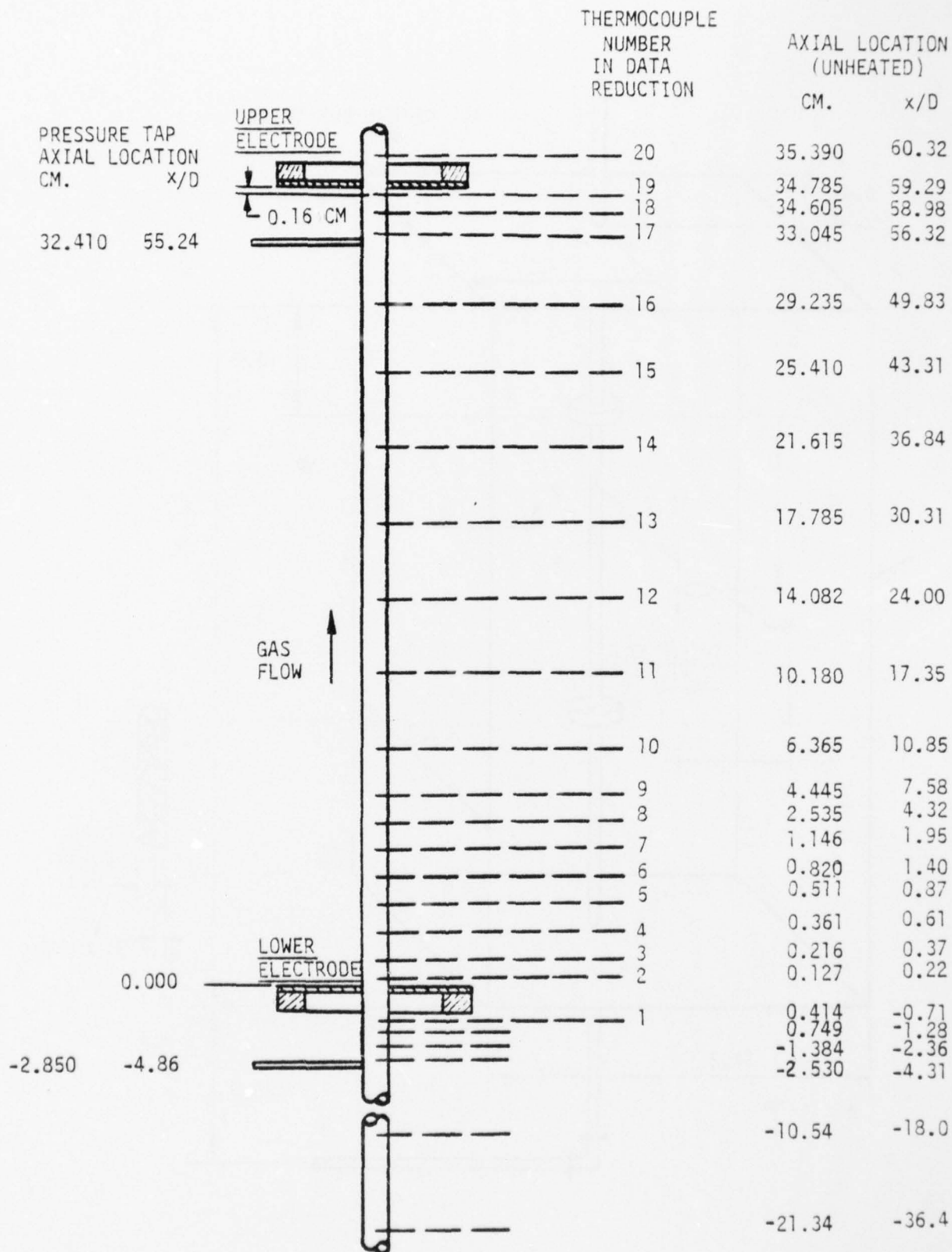


FIGURE B2. DIAGRAM OF TEST SECTION

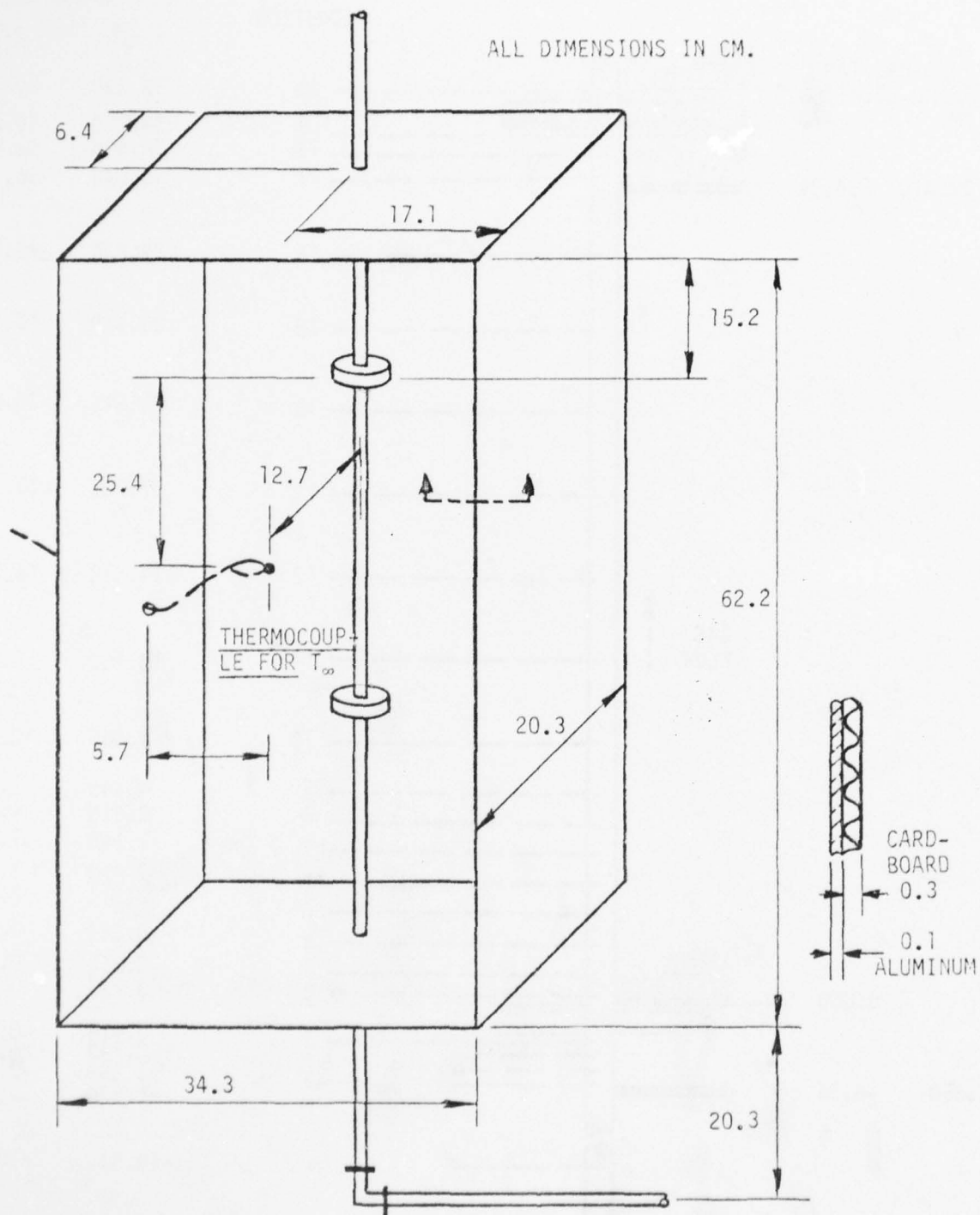


FIGURE B3. DETAIL OF DRAFT SHIELD

differential pressure meter.

Current was measured with a Weston Model 370 a.c. ammeter.

The power per unit length was then determined as

$$q'_{\text{GEN}} = I^2 R' \quad (\text{B1})$$

where R' is the resistance per unit length of the test section as discussed under a separate heading in this appendix.

A Fluke differential voltmeter measured the voltage across the test section to serve as a check on power measurements.

Gas temperature measurements were made at the tubular flowmeter inlet (rotometer outlet) and at the laminar flow element inlet by inserting thermocouples in the gas stream. Thermocouple output was measured with a Hewlett Packard Model 3450A digital voltmeter. An ice bath was used as a reference for all of the thermocouples. Thermocouples were selected for measurement using a manual switch. The numbered wall thermocouples on Fig. B2 were used in the computer program that reduced the experimental data for the heated runs. The unnumbered thermocouples were used to determine the amount of preheating of the gas before it entered the heated section. The position of each thermocouple after expansion due to heating was calculated in the same computer program. The expansion coefficient was obtained from tabulated data supplied by the International Nickel Company to Coon [1968]. The expansion coefficient was expressed as a linear function of temperature,

$$\alpha = (7.26 \times 10^{-6}) + [(0.0012 \times 10^{-6}) (T - 70)]$$

(T in degrees Fahrenheit, in/inF) (B2)

After the gas passed through the test section, it was cooled by a chilled water counterflow heat exchanger. The valve used to control the flow rate was located downstream of the heat exchanger. The uncertainties of the instruments used in this investigation are listed later in Table C1.

Procedure

Before any experimental runs with gas flow were performed, the test section was heated without flow in order that the heat lost to the environment and the resistance of the test section could be determined. These items are discussed in detail in later sections of this appendix.

To insure that test runs with only the experimental gas were being made, the system went through a purging cycle before each set of experimental runs. This cycle consisted of :

- 1) evacuating the system, 2) pressuring the system with an inert gas (argon) to approximately 0.7 MN/m^2 (100 PSIG) and blowing down to approximately 0.07 MN/m^2 (10 PSIG), 3) repeating step 2, 4) evacuating the system, 5) pressurizing and blowing down the system with the test gas in a similar manner to step 2, 6) pressurizing the system with the test gas to experimental run pressure level.

The desired inlet Reynolds number was established by adjusting the pressure level and mass flow rate. Without power being supplied to the test section, measurements were taken so that calculation of the adiabatic friction coefficient was possible. Adiabatic runs were generally made before and after a series of heated runs. The measured adiabatic friction coefficients were compared to the Drew, Koo, and McAdams [1932] correlation (equation 15), and agreement served as a partial check on mass flow rate measurement.

The test section was then heated to the desired level. After a short wait, so that a steady-state condition was established, the thermocouple readings, pressure drop, pressure level, voltage, and current measurements were manually recorded. The inlet Reynolds number was maintained approximately constant while the test section wall temperature was varied by varying the power input. Measurements were taken for a number of different power settings.

Appendix D shows a listing of the H_2 - CO_2 heated data obtained in this study.

Heat Loss Calibration

In order to calculate the heat transfer coefficient, the heat addition to the gas, q'_{gas} , must be determined. If an energy balance for a small element of the test section is performed as shown in Fig. B4, the result is

$$q'_{\text{gas}} = q'_{\text{gen}} - \left(\frac{\partial q_{\text{cond}}}{\partial x} + q'_{\text{loss}} \right). \quad (\text{B3})$$

The heat generated in the small section of the tube; q'_{gen} , is found from equation (B1). The current was measured, and the calculation of the resistance per unit length is discussed in the next section. The net axial heat loss due to conduction is

$$\frac{\partial q_{\text{cond}}}{\partial x} = -kA_{\text{cs}} d^2 T_w / dx^2. \quad (\text{B4})$$

The second derivative was determined using a numerical parabolic fit described by McEligot [1963]. The variation of thermal conductivity with temperature for Inconel 600 was determined from tabulated data supplied by the International Nickel Company to Coon [1968] and was expressed as a linear function of temperature

$$k = 7.91 + 0.0055T \text{ (Btu/hr-ft-F)} \quad (\text{B5})$$

(T in degrees Fahrenheit)

The heat loss term, q'_{loss} , is the total heat lost from the tube due to natural convection and radiation. The tube was first heated until thoroughly oxidized so that the heat loss calibration could be done without the emissivity of the test

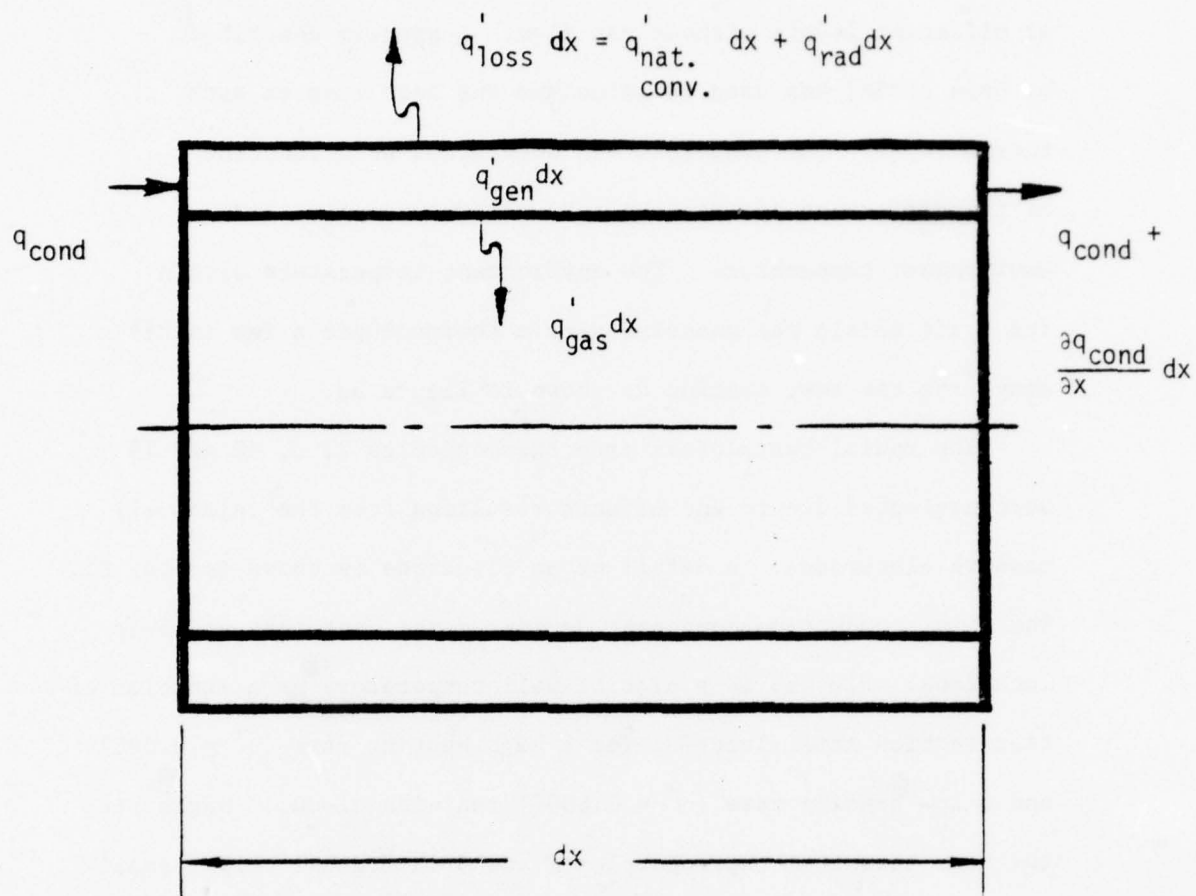


FIGURE B4. ENERGY FLOWS FROM ELEMENT OF TEST SECTION

section changing further.

To determine the heat loss, the test section was heated at different levels without gas flow. A program described by Coon [1968] was used to calculate the heat loss at each thermocouple. The heat loss was determined as a function of the difference between the tube wall temperature and environment temperature. The environment temperature within the draft shield was measured with a thermocouple a few inches away from the test section as shown in Figure B3.

The radial heat losses from thermocouples 2, 3, 18 and 19 were neglected due to end effects resulting from the relatively massive electrodes. A detail of an electrode is shown in Fig. B5. The axial conduction component dominated the heat loss at these locations. Fig. B6 is a plot of wall temperature as a function of test section axial location for a high heating rate ($q^+ = 0.0031$) and a low heating rate ($q^+ = 0.0007$) run with H_2-CO_2 . Neglecting the heat loss from thermocouples 2 and 3 introduces only a small error because these thermocouples are at relatively low temperatures. Heat losses from thermocouples at the highest temperatures are generally about 5 percent of the heat added to the gas during high heating rate runs with H_2-CO_2 . If the heat losses at thermocouples 2 and 3 are both estimated to be equal to heat loss from thermocouple 4, and if the heat losses at thermocouples 18 and 19 are both estimated to be equal to the heat loss from thermocouple 15, the change in the Nusselt numbers at these axial positions is

STAINLESS STEEL DIA.
0.11 CM. THK.
x4.76 CM. DIA.

FIGURE B5. DETAIL OF TEST SECTION UPPER ELECTRODE

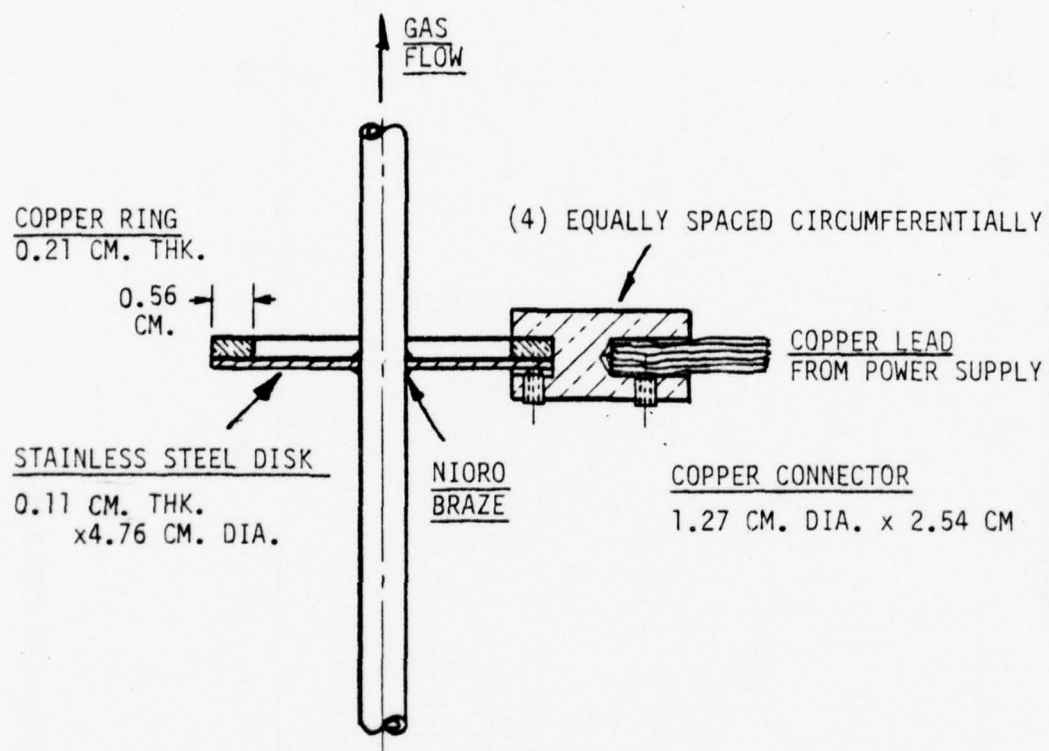


FIGURE B5. DETAIL OF TEST SECTION UPPER ELECTRODE

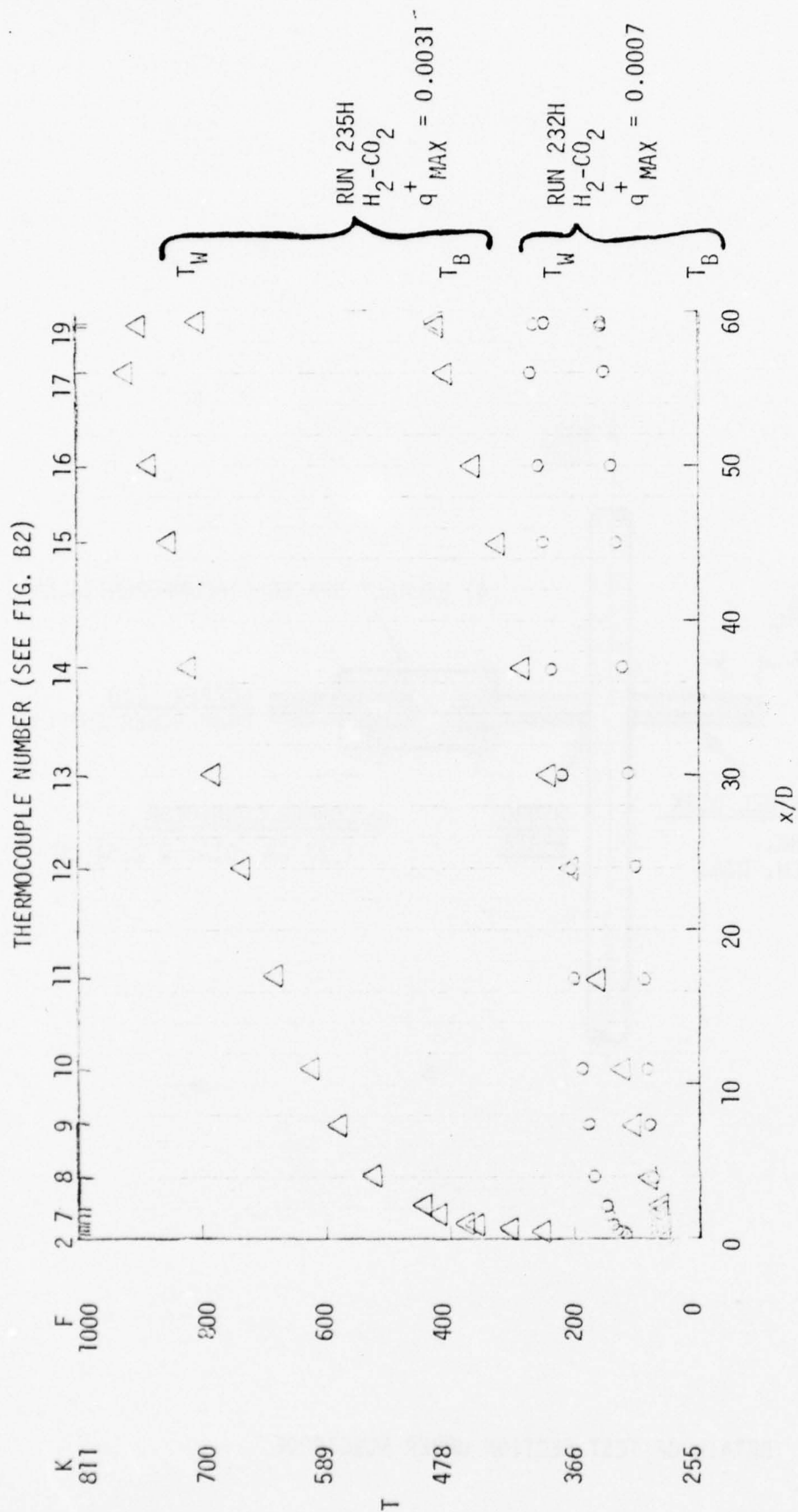


FIGURE B6. AXIAL WALL AND BULK TEMPERATURE PROFILES

less than 3% with no significant change in the Nusselt numbers at all other axial positions.

The data for the remaining thermocouples were fitted with an equation of the form:

$$q'_{\text{loss}} = C_1(T_w - T_\infty) + C_2(T_w - T_\infty)^2 + C_3(T_w - T_\infty)^3 \quad (\text{B6})$$

(BTU/hr-ft) ($T_w - T_\infty$ in degrees Fahrenheit)

The numerical values of C_1 , C_2 , and C_3 are listed in Table B1. Figure B7 shows the curves from the deduced values of C_1 , C_2 and C_3 in equation (B6) and the data points. The heat loss was essentially the same for thermocouples 7 through 10 and the data points and deduced curve for thermocouple 9 are shown. The same is true for thermocouples 11 through 16 and the data points and deduced curve for thermocouple 13 are shown. As shown, the curve fit for thermocouple 5 does not fit the data well at the higher temperature differences and could be improved with a better curve fitting procedure. The estimated uncertainty in equation (B6) is dominated by the uncertainty in the current measurement. A complete analysis of the uncertainty in the q'_{loss} term was not undertaken due to its relatively small contribution to the overall uncertainty in the Nusselt number. A heat loss calibration on a similar test section is reported in a more detailed report by Bingham [1977].

Table B1
Thermocouple Heat Loss Constants

Thermocouple	C_1 (BTU/hr ft °F)	C_2 (BTU/hr ft °F ²)	C_3 (BTU/hr ft °F ³)
4	-2.31×10^{-2}	1.07×10^{-3}	-2.74×10^{-6}
5	1.34×10^{-2}	4.65×10^{-3}	-1.09×10^{-5}
6	6.11×10^{-2}	-4.01×10^{-5}	4.09×10^{-7}
7	9.67×10^{-2}	4.49×10^{-4}	-3.56×10^{-7}
8	6.89×10^{-2}	5.00×10^{-4}	-2.52×10^{-7}
9	7.72×10^{-2}	3.72×10^{-4}	-1.12×10^{-7}
10	7.32×10^{-2}	3.22×10^{-4}	-6.07×10^{-8}
11	6.98×10^{-2}	2.67×10^{-4}	-5.52×10^{-9}
12	6.62×10^{-2}	2.38×10^{-4}	2.28×10^{-8}
13	6.40×10^{-2}	2.24×10^{-4}	3.41×10^{-8}
14	6.21×10^{-2}	2.09×10^{-4}	5.01×10^{-8}
15	6.14×10^{-2}	2.00×10^{-4}	6.17×10^{-8}
16	6.23×10^{-2}	2.08×10^{-4}	5.08×10^{-8}
17	1.56×10^{-1}	3.50×10^{-4}	-2.49×10^{-8}

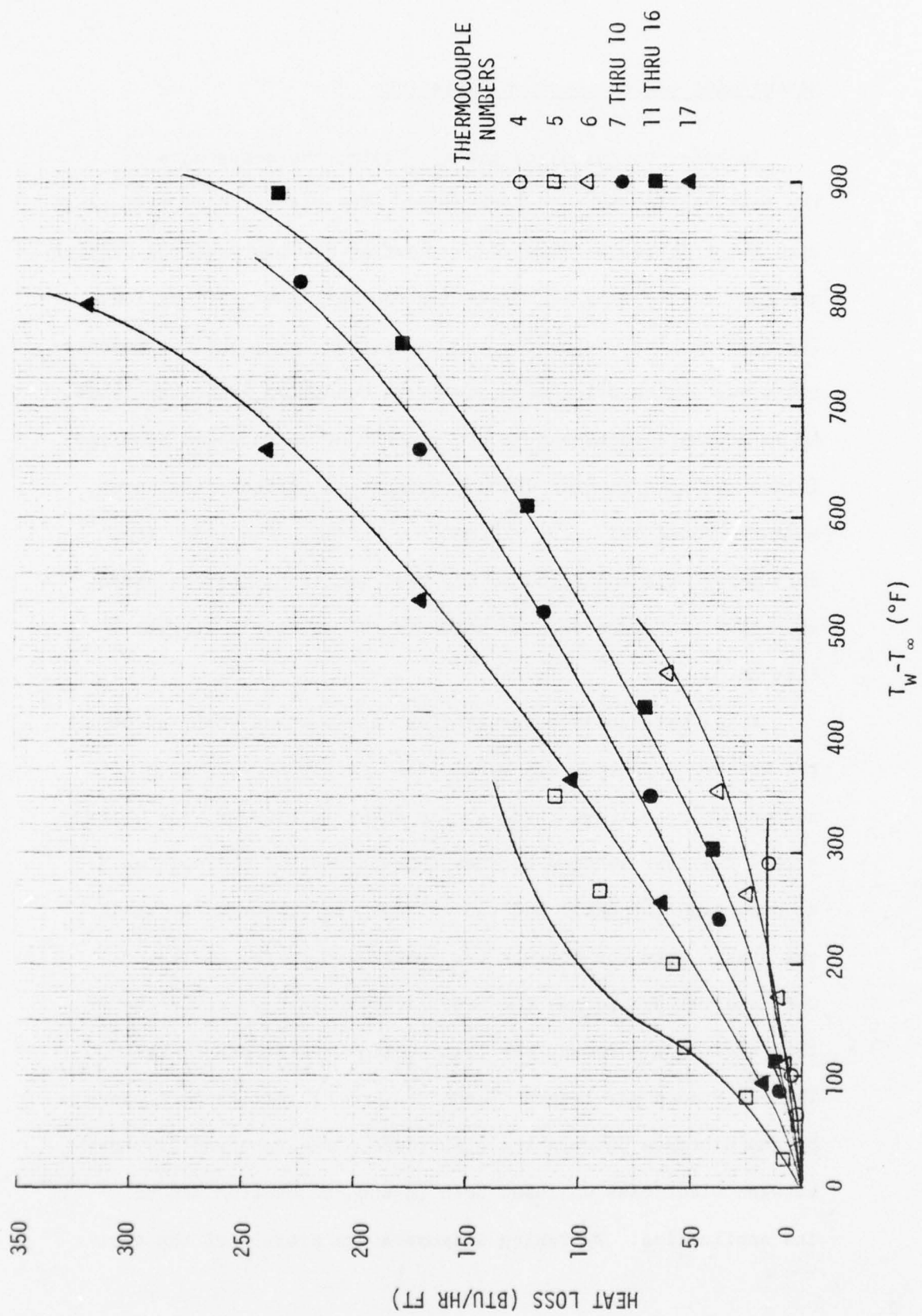


FIGURE B7. HEAT LOSS CALIBRATION

Measurement of Test Section Resistance

In order to calculate the q'_{gen} term, the resistance of the test section must be determined. The variation of resistance with temperature was measured by heating the test section without gas flow in the same manner as for the heat loss calibration. The test section was heated to the desired level and the measurements were taken after a steady-state condition was established. As an accurate root-mean-square reading of voltage was required (since the power source did not generate a perfect sine wave), a Weston Model 341 a.c. voltmeter was used. The leads from this meter were connected to the test section at points above and below the electrodes as shown in the schematic diagram Fig. B8.

For a particular power setting, the current going through the Weston voltmeter was known from its known resistance and resulting voltage reading. As shown in Fig. B8, the voltage across the test section becomes the addition of the voltage drop through the meter and the voltage drop through the small resistance from the voltage tap connection to the electrodes. Once the voltage across the test section and current in the test section are known, the test section resistance is known. The resistance per length is then the total resistance divided by the distance between the electrodes. The unheated distance between electrodes was used both in the calibration and in its application. By taking a temperature profile of the test

$$R_{TS} = \frac{E_{TS}}{i_{TS}}$$

$$E_{TS} = E_M + i_M (R_1 + R_2)$$

$$i_M = E_M / R_M$$

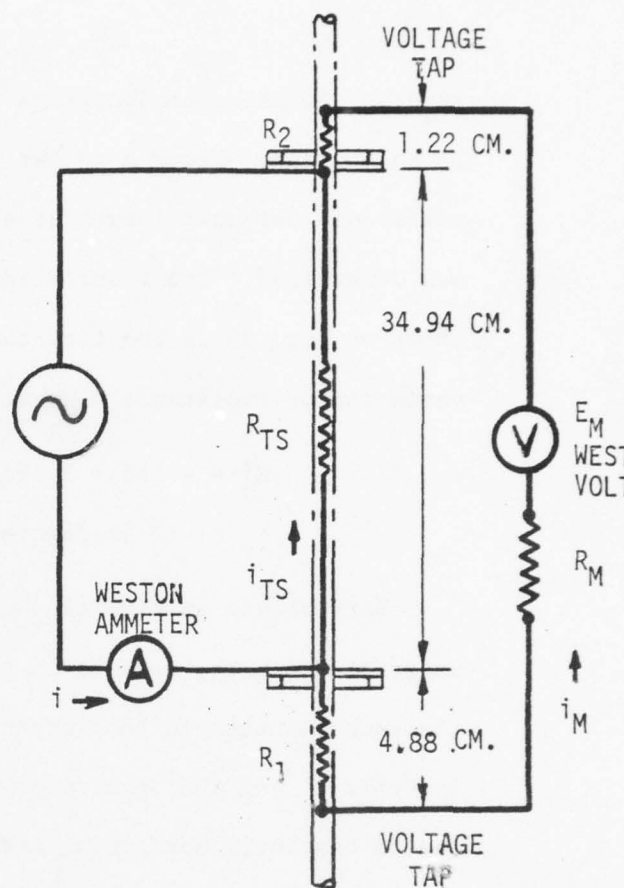
$$i_{TS} = i - i_M$$

$$R_M = 2.858 \, \Omega \text{ (1.5 VOLT RANGE)}$$

$$= 5.608 \, \Omega \text{ (3.0 VOLT RANGE)}$$

$$R_1 \approx (0.002 \, \Omega/\text{CM}) \times (4.88 \text{ CM})$$

$$R_2 \approx (0.002 \, \Omega/\text{CM}) \times (1.22 \text{ CM})$$



NOMENCLATURE

i	current through Weston ammeter
i_{TS}	current through test section
i_M	current through Weston voltmeter
R_{TS}	resistance of test section
R_M	resistance of Weston voltmeter
R_1	resistance of section from lower electrode to lower voltage tap
R_2	resistance of section from upper electrode to upper voltage tap
E_{TS}	voltage across test section
E_M	voltage read on Weston voltmeter

FIGURE B8. CIRCUIT FOR MEASUREMENT OF TEST SECTION RESISTANCE

section, an integrated average test section temperature can be calculated. After a number of power settings, a plot of resistance per unit length as a function of wall temperature was determined. The results are shown on Fig. B9. Also shown on Fig. B9 is the line that was used to approximate the variation of resistance with temperature,

$$R' = 4.553 + 3.898 \times 10^{-4} (T) \text{ (m}\Omega/\text{in)} \quad (B7)$$

(T in degrees Fahrenheit)

Bars placed on Fig. B9 show the estimated experimental uncertainty in the resistance per unit length. They include the uncertainties in the current and voltage readings as shown in Table C1 and the uncertainty in the test section length due to heating. Horizontal bars that show the estimated uncertainty in the average wall temperature were not included.

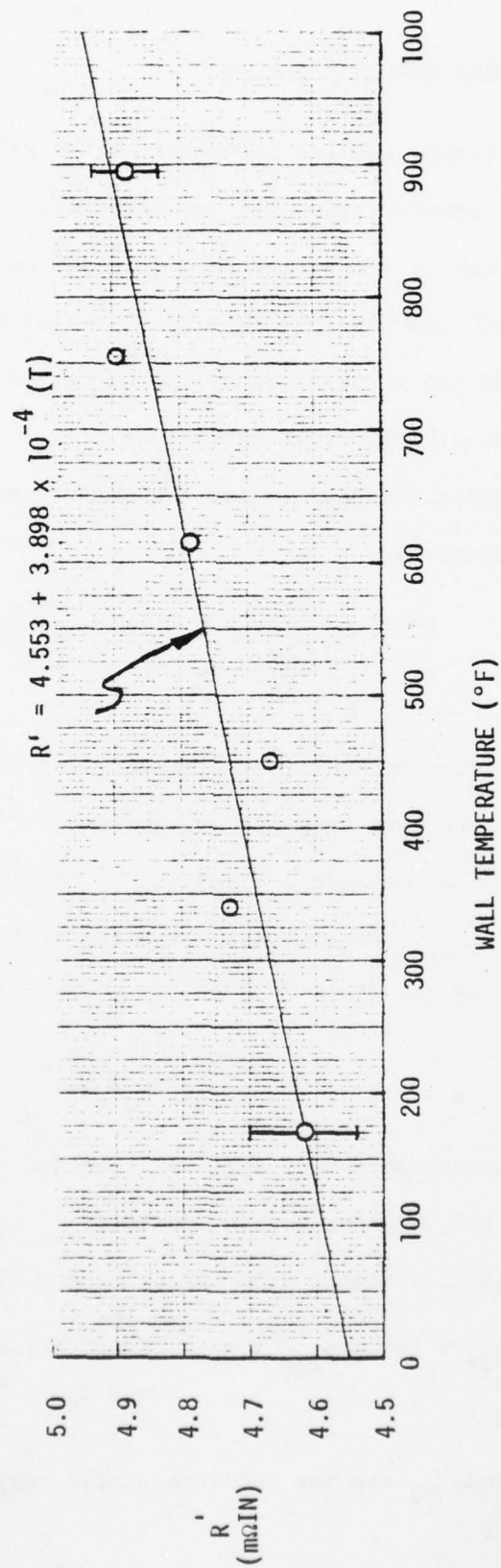


FIGURE B9. VARIATION OF TEST SECTION RESISTANCE WITH RESPECT TO TEMPERATURE

Mass Flow Rate Determination

A calibrated tubular flowmeter, which will be referred to as the flowmeter, was used for mass flow rate determination. This flowmeter is a circular tube of 0.588 cm (0.231 in) diameter with two pressure taps 58.42 cm (23.00 in) apart. The upstream tap is preceded by 100 diameters to approach fully developed conditions for turbulent flow.

The inside diameter of the flowmeter can be determined from the relation,

$$f = \frac{\Delta p_{fr}}{4 \frac{L}{D} \frac{\rho_{av}}{2g_c} V^2} = \frac{D^5 g_c \pi^2 \rho_{av} \Delta p_{fr}}{32 L \dot{m}^2} \quad (B8)$$

if the mass flow rate, friction factor, and the distance between the pressure taps (L) are known for a set of experimental runs that measure ρ_{av} and Δp_{fr} . In equation (B8), the density, ρ_{av} , was evaluated from the static pressure and temperature of the gas,

$$\rho_{av} = \frac{1}{RZ_{av}} \left(\frac{P_1 + P_2}{T_1 + T_2} \right) \quad (B9)$$

The friction pressure drop Δp_{fr} was obtained by subtracting the calculated momentum pressure drop Δp_{mom} from the total measured static-pressure drop Δp across the flowmeter,

$$\Delta p_{fr} = \Delta p - \Delta p_{mom} = \Delta p - \frac{16 \dot{m}^2 RZ_{av}}{\pi^2 D^4 g_c} \left(\frac{T_{b2}}{P_2} - \frac{T_{b1}}{P_1} \right) \quad (B10)$$

where T_{b1} and T_{b2} are the absolute static temperatures at the

first and second pressure taps, respectively, and p_1 and p_2 are the static pressures.

Choosing the experimental correlation of Drew, Koo, and McAdams [1932] between friction factor and mass flow rate, (equation (15) rearranged),

$$f_{DKM} = 0.0014 + 0.125 \left[\frac{4\dot{m}}{\pi D u} \right]^{-0.32} \quad (B11)$$

allows one to solve for the diameter of flowmeter (consistent with that choice). Our unknowns in equations (B8) and (B11) are the friction factor and the inside diameter of the flowmeter. The mass flow rate must be known from an instrument independent of the flowmeter. The remainder of the variables can be measured during experimental runs. Thus, calibration was essentially a determination of the diameter of the flowmeter based on the choice of equation (B11) as a reference.

To determine the mass flow rate, a Parkinson-Cowan Type D1 positive displacement flowmeter (PDFM) was located in series with the calibrated tubular flowmeter. The PDFM is specified to have an experimental uncertainty of 0.5 percent at ambient conditions. In addition, the PDFM was calibrated with a Collins 120 liter gasometer in the Exercise Physiology Laboratory. The inside diameter of the gasometer tank was measured at several axial locations. Its diameter was determined to be 41.37 cm (16.287 in) with an estimated uncertainty of ± 0.01 cm or 0.02 percent. The gasometer displaces a measured volume of air (determined by its inside

diameter and length of travel) into the PDFM. The PDFM directly measures total volume which flowed during a given time interval, and a comparison of the two volumes can be made. Several runs were made at two different flow rates. At a flow rate corresponding to a Reynolds number of approximately 13,000 through the flowmeter, 0.0555 m^3 (1.96 ft^3) of air was read on the PDFM for every 0.0566 m^3 (2.00 ft^3) through the gasometer. Similarly, at a Reynolds number of approximately 20,000, 0.0561 m^3 (1.98 ft^3) of air was read on the PDFM for every 0.0566 m^3 (2.00 ft^3) through the gasometer. All readings were within an experimental uncertainty of 0.5 percent. Thus, it was determined that the PDFM could be used to measure mass flow rate to within 0.5 percent.

The PDFM could then be used in series with the flowmeter to determine the inside diameter of the flowmeter. The PDFM has a limited capacity of $5.66 \text{ m}^3/\text{hr}$ ($200 \text{ ft}^3/\text{hr}$) and, therefore, could not be used during the adiabatic and heated test runs which were at higher Reynolds numbers. Several experimental runs with air were made to determine the inside diameter of the flowmeter at the upper capacity of the PDFM. To measure pressure drop, runs were made using either a Meriam 60 inch inclined water manometer with a 10 inch range or, a MKS Baratron differential pressure meter with a 1000 mm Hg range. Only runs in the higher ranges (lesser uncertainty) of these pressure drop instruments were used to determine the inside diameter of the flowmeter. A Heise Bourdon tube gage measured

the pressure at the upstream pressure tap. Inlet stagnation temperature was measured by a thermocouple in the gas stream just preceding the flowmeter. Thermocouples were also spot welded to the flowmeter wall near both pressure taps. These wall temperature readings were found to be essentially the same as the inlet stagnation temperature thermocouple for a given run. Therefore, the inlet stagnation temperature was used for both the inlet and exit of the flowmeter. Also, as the runs were all made at Mach numbers less than 0.1, the absolute static and stagnation temperatures of the gas stream were within 0.2 percent of each other.

A short computer program was written to solve equations (B8) and (B11) iteratively for the inside diameter of the flowmeter to within 0.00025 cm (0.0001 in) or about 0.04 percent. Equations (B8) and (B11) for the friction factor were set equal to each other to within 0.00001 (about 0.1 percent). Table B2 shows a summary of the experimental methods used to determine the inside diameter of the flowmeter. The diameter was determined to be 0.5878 cm (0.2314 in) with an uncertainty of ± 0.3 percent. The diameter determined from the MKS Baratron pressure drop was used as this instrument was used during the experimental runs for the measurement of pressure drop.

With the diameter determined within a small uncertainty, equations (B8) and (B11) can be used to measure mass flow rate for adiabatic and heated experimental runs. As shown in the mixture properties section of this report, the flowmeter

Table B2

Determination of Flow Meter Inside Diameter

Test	Method	ID (inches)	Uncertainty (inches)
1	Starret micrometer and small hole gage	0.2305	± 0.0005
2	Equations (B8) and (B11) solved simultaneously with pressure drop from MKS Baratron (average of four runs)	0.2314	± 0.0007
3	Equations (B8) and (B11) solved simultaneously with pressure drop from Meriam inclined manometer (average of six runs)	0.2311	± 0.0007

can also be used to verify gas mixture molecular weight if mass flow rate is known. The effect of the experimental uncertainty in the inside diameter of the flowmeter on mass flow rate is discussed in Appendix C. The total uncertainty on mass flow rate and its effect on Nusselt number are also discussed in Appendix C.

As stated earlier, a rotometer and laminar flow element were also used as a check on mass flow rate. Their readings only served as rough estimates of mass flow rates because they were not calibrated precisely at the conditions of this experiment.

Thermocouple Conduction Error

A thermocouple attached to the outside surface of a heated tube acts as a fin or extended surface which lowers the temperature at the point of attachment. Since this point also serves as the thermocouple junction, it measures a wall temperature lower than the value which would occur without its presence. The difference is known as "thermocouple conduction error" [Schneider, 1955]. Consequently, in an experiment such as the present study, the deduced Nusselt number is systematically increased unless corrected for this effect.

A subroutine was added to the program that reduced the heat transfer data to account for thermocouple conduction error. This subroutine is based upon extended surface analyses, and a copy of the subroutine is shown in Table B3. Details of the analysis are given in Pickett's report, Appendix E [1976]. The correction is of the order of 1 to 1½ percent of the tube wall temperature. The effect of a change in tube wall temperature on the Nusselt number is investigated in Appendix C. Table C4 shows that, for run number 235H at Reynolds number approximately 85,000 and x/D equals 56.3, a 2 degree change in wall temperature results in a change of Nusselt number of 0.21 (0.33 percent). However, the thermocouple conduction error was calculated to be about 15 °F. Thus, the effect on the Nusselt number in this case was about 2½ percent.

Table B3

Thermocouple Conduction Error Subroutine

The variables in the FORTRAN listing are defined as follows:

ACS	Cross-sectional area of thermocouple (ft^2)
ANUM	Numerator of THETA
AS	Equal to ACS
BETA	$1/\text{TFILM}$
BOLTZ	Stephan-Boltzmann constant ($\text{Btu/hr ft}^2 \text{ R}$)
CP	Specific heat at constant pressure of environment (Btu/lbm F)
DELTA	Wall thickness of test section (ft)
DEN	Density of environment (lbm/ft^3)
DENOM	Denominator of THETA
DT	TTC-TAMB
DTUBE	Test section outside diameter (ft)
EM	$\text{KTUBE} * \text{DELTA} / \text{HTCAS}$
EMIS	Emissivity of thermocouple wire
HI	Heat transfer coefficient on inside of test section ($\text{Btu/hr ft}^2 \text{ F}$)
HNC	Convective heat transfer coefficient of thermocouple ($\text{Btu/hr ft}^2 \text{ F}$)
HO	Heat transfer coefficient on outside of test section ($\text{Btu/hr ft}^2 \text{ F}$)
HR	Radiative heat transfer coefficient of thermocouple ($\text{Btu/hr ft}^2 \text{ F}$)
HTC	Total heat transfer coefficient of thermocouple ($\text{Btu/hr ft}^2 \text{ F}$)
HTCAS	$\text{SQRT}((\text{HR} + \text{HNC}) * \text{PER} * \text{KTC} * \text{ACS})$

IER	}	Error codes in subroutine BESK
JER		
KAIR		Thermal conductivity of environment (Btu/hr ft F)
KTC		Thermal conductivity of thermocouple wire (Btu/hr ft F)
KTUBE		Thermal conductivity of test section (Btu/hr ft F)
KO		Value of K_0 Bessel function
K1		Value of K_1 Bessel function
LAMBDA		Variable in argument of the K Bessel function
LAMRO		Argument of the K Bessel function
NU		Nusselt number
PAMB		Ambient pressure (psia)
PER		Perimeter of thermocouple (ft)
PI		π
RA		Rayleigh number
RO		Thermocouple diameter (ft)
TAMB		Ambient temperature (R)
TCDIA		Thermocouple diameter (ft)
TERR		TW-TTC
TFILM		Film temperature (R)
THAPX		$-0.5 * \text{ALOG}(\text{LAMRO}) / (\text{PI} * \text{EM})$
THETA		$(\text{TW} - \text{TTC}) / (\text{TW} - \text{TAMB})$
TTC		An array containing the values of uncorrected thermocouple temperatures (R)
TW		An array containing the values of corrected thermocouple temperatures (R)
VIS		Viscosity of environment (lbm/ft s)

FORTRAN listing of Thermocouple Conduction Error Subroutine

```

C          CONVERSION FROM MV TO DEG F BY INTERPOLATION IN TC TABLES
C          TABLES ENTERED IN DEG C, IF ICREF IS 1 ICE REFERENCE IS
C          USED, IF 2, TEMPERATURE CALLED TBOX IS USED AS
C          REFERENCE
C          TBOX ENTERED IN DEGREES F
C          SUBROUTINE TCERR(TTC, TAMB, HI, HO, TW)
C          REAL LAMBDA,KTUBE,KO,K1,NU,KAIR,KTC,LAMRO
C          PI=3.1416
C          BOLTZ=.1714E-8
C          TEST SECTION PARAMETERS
C          DTUBE=.0211
C          DELTA = 0.011
C          DELTA = DELTA / 12.
C          KTUBE=7.9+.0055*(TTC-460.)
C          TCDIA=.0004167
C          KTC=.00722*TTC+9.25
C          EMIS=.87
C          PER=PI*TCDIA
C          ACS=PI*TCDIA*TCDIA/4.
C          AS=ACS
C          RO=TCDIA/2.
C          ENVIRONMENTAL PROPERTIES
C          PAMB=13.2
C          TFILM=((TTC+TAMB)/2)
C          DEN=PAMB*.08072*491.7/(14.7*TFILM)
C          CP=.2402*(TFILM/491.7)**.095
C          KAIR=.01395*(TFILM/491.7)**.805
C          VIS=.1153E-4*(TFILM/491.7)**.67
C          BETA=1./TFILM
C          CALCULATIONS
C          DT=TTC-TAMB
C          RA=3600.*CP*DEN*DEN*32.2*BETA*DT*TCDIA**3/(VIS*KAIR)
C          NU=.315+.8*RA**.18
C          HNC=NU*KAIR/TCDIA
C          HR=EMIS*BOLTZ*(TTC**4-TAMB**4)/(TTC-TAMB)
C          HTCAS=SQRT((HR+HNC)*PER*KTC*ACS)
C          HTC=HTCAS/AS
C          IF((HO+HI).LE.0.0) GO TO 51
C          LAMBDA=SQRT((HO+HI)/(KTUBE*DELTA))
C          LAMRO=LAMBDA*RO
C          EM = KTUBE * DELTA / HTCAS
C          THAPX = (-0.5) * ALOG (LAMRO) / (PI * EM)
C          CALL BESK(LAMRO,0,KO,IER)
C          CALL BESK(LAMRO,1,K1,JER)
C          IF(IER.NE.0)GOTO 60
C          IF(JER.NE.0)GOTO 60
C          ANUM=1.-HO/HTC
C          DENOM=(HI+HO)/HTC+2.*KTUBE*DELTA*LAMRO*K1/(HTC*RO*RO*KO)
C          THETA=ANUM/DENOM
C          TW=(TTC-THETA*TAMB)/(1.-THETA)
C          TERR = TW - TTC
150      WRITE(6,150) TTC, TW, HO, HI, THETA, TERR
C          FORMAT(1H0, 6E17.6)
C          WRITE(6,150) LAMRO, EM, THAPX
C          GO TO 50
51      TW=TTC
50      RETURN
60      PRINT 160, IER, JER
160      FORMAT(1H0, I2, 2X, I2, 17H BESSEL FN ERROR )
C          STOP
C          END

```

.....

SUBROUTINE BESK

COMPUTE THE K BESSEL FUNCTION FOR A GIVEN ARGUMENT AND ORDER

USAGE

CALL BESK(X,N,BK,IER)

DESCRIPTION OF PARAMETERS

X - THE ARGUMENT OF THE K BESSEL FUNCTION DESIRED

N - THE ORDER OF THE K BESSEL FUNCTION DESIRED

BK - THE RESULTANT K BESSEL FUNCTION

IER - RESULTANT ERROR CODE WHERE

IER=0 NO ERROR

IER=1 N IS NEGATIVE

IER=2 X IS ZERO OR NEGATIVE

IER=3 X .GT. 170, MACHINE RANGE EXCEEDED

IER=4 BK .GT. 10**70

REMARKS

N MUST BE GREATER THAN OR EQUAL TO ZERO

SUBROUTINES AND FUNCTION SUBPROGRAMS REQUIRED

NONE

METHOD

COMPUTES ZERO ORDER AND FIRST ORDER BESSEL FUNCTIONS USING
SERIES APPROXIMATIONS AND THEN COMPUTES N TH ORDER FUNCTION
USING RECURRENCE RELATION.

RECURRENCE RELATION AND POLYNOMIAL APPROXIMATION TECHNIQUE
AS DESCRIBED BY A.J.M. HITCHCOCK, "POLYNOMIAL APPROXIMATIONS

TO BESSEL FUNCTIONS OF ORDER ZERO AND ONE AND TO RELATED
FUNCTIONS", M.T.A.C., V.11, 1957, PP. 86-88, AND G.N. WATSON,

"A TREATISE ON THE THEORY OF BESSEL FUNCTIONS", CAMBRIDGE
UNIVERSITY PRESS, 1958, P. 62

.....

AD-A062 442

ARIZONA UNIV TUCSON ENGINEERING EXPERIMENT STATION
CONVECTIVE HEAT TRANSFER FOR SHIP PROPULSION.(U)

F/6 20/13

UNCLASSIFIED

APR 78 A W SERKSNIS, D M MCELIGOT, M F TAYLOR N00014-75-C-0694
1248-6

NL

2 OF 2

AD
A062442



END

DATE
FILMED

3-79

DDC

A Note on Safety

As the hydrogen in the H_2 - CO_2 mixture has a wide range of flammability limits in air (4 to 75 percent of the total volume), some method of expending the gas must be considered. Burning the mixture with a flame source at some remote point is one solution. However, for convenience it was decided to exhaust the gas mixture directly to the atmosphere at a safe location.

From the outlet of the laminar flow element, tubing with as few joints as possible was directed out of the laboratory. The exhaust tubing extended above the building and away from any gas intakes in the roof vicinity. The experimental apparatus was tested to insure that leaks (preferential to hydrogen) were minimized.

As shown in the experimental procedure, an inert gas was used in the purging cycle to further reduce the chances of oxygen remaining in the gas lines.

A model 6103 flash arrestor was purchased from Matheson. It was installed just after the pressure regulators and gas bottle manifold to prevent backflow and to prevent flashbacks to the gas cylinders.

APPENDIX C
Uncertainty Analysis

To determine the validity of the deduced results it is necessary to determine their estimated experimental uncertainties. An analysis has been conducted in accordance with recognized procedures to estimate the percent uncertainty in the important heat transfer and friction characteristics along the test section. Doebelin [1966] considers the problem of computing a quantity N , where N is a known function of the n independent variables, $u_1, u_2, u_3, \dots, u_n$. That is,

$$N = \text{fn}(u_1, u_2, u_3, \dots, u_n) \quad (C1)$$

The u 's are the measured quantities (instrument or component outputs) and are uncertain by $\pm\Delta u_1, \pm\Delta u_2, \pm\Delta u_3, \dots, \pm\Delta u_n$, respectively. These uncertainties will cause an uncertainty ΔN in the computed result N . We are concerned with experimental uncertainties here rather than systematic errors, like the thermocouple conduction error which can be corrected. The u 's may be considered as absolute limits on the uncertainties, as statistical bounds such as 3σ limits, or as uncertainties on which we are willing to give certain odds as including the actual error. However, the method of computing ΔN and the interpretation of its meaning are different for the first case as compared with the second and third. After calculating the limits on the uncertainty in N , then $N \pm \Delta N$ and the percentage uncertainty is known. In all cases, systematic

errors (bias) were removed by calibration where they were known to exist.

If the individual errors are thought of as $\pm 3\sigma$ limits, then, as shown by Kline and McClintock [1953], the general equation used is

$$\Delta N = E_{\text{arss}} = \sqrt{(\Delta u_1 \frac{\partial f}{\partial u_1})^2 + (\Delta u_2 \frac{\partial f}{\partial u_2})^2 + \dots + (\Delta u_n \frac{\partial f}{\partial u_n})^2} \quad (C2)$$

where E_{arss} represents a $\pm 3\sigma$ limit on N and 99.7 percent of the values of N can be expected to fall within these limits (arss = absolute root-sum square).

An analysis was performed to determine the uncertainty of

- 1) calibrated tubular flowmeter inside diameter, D
- 2) mass flow rate, \dot{m}
- 3) local bulk Nusselt number, Nu

as calculated from the measured experimental data. Table C1 lists the uncertainties of the instruments (Δu 's) used in this investigation. The uncertainties of the directly measured quantities were determined from manufactures' specifications and experience. The uncertainty of the gas properties was not included.

For the determination of the uncertainty of the inside diameter of the calibrated tubular flowmeter, D , equation (B8) shows that

$$D = \text{fn}(\dot{m}, L, \rho_{\text{av}}, \Delta p_{\text{fr}}) \quad (C3)$$

Table C1

Uncertainties of Measured Values

Measured Quantity	Instrument	Uncertainty (Based on Manufacturer's specification unless otherwise stated)	Notes
Current	Weston Ammeter Model 370 No. 13605	0.0 to 2.0 amp range, $\pm 0.17\%$ of full scale 2.0 to 5.0 amp range, $\pm 0.25\%$ of full scale	
Voltage	Weston Voltmeter Model 341 No 23502	$\pm 0.5\%$ of full scale (1.5 volt full scale = 0.0075 volt 3.0 volt full scale = 0.0150 volt)	Voltmeter used to determine test section resistance (see Appendix B)
	Fluke Voltmeter Model 883AB	$\pm 0.1\%$ of input	Voltmeter used as a check on test section voltage
Wall and inlet bulk temperature	Hewlett-Packard Model 3450A Multi-Function Digital Voltmeter	$\pm 0.008\%$ of reading $\pm 0.01\%$ of range (100mV range = 0.01 mV)	
	Premium grade Chromel - Alumel thermocouples	± 2 F, 3/8% of reading above 553 K (535 F)	For relative measurements, uncertainty can be considered better as same spool of wire was used
Thermocouple location Pressure tap location	Gaertner Cathetometer	$\pm 0.1\%$ of distance from datum (see Figure B2)	(estimate of uncertainty)

Table C1 (cont.)

Measured Quantity	Instrument	Uncertainty (Based on Manufacturers' specification unless otherwise stated)	Notes
Test section I.D. and O.D.	Starret micrometer and small hole gage	± 0.001 inch	Uncertainty based on calibrated tubular flow meter uncertainty
Calibrated tubular flowmeter I.D.	see Table B2		Tubing for test section and flowmeter from same manufacturer shipment
Static pressure	Heise bourdon tube gage	± 0.15 psia	
Atmospheric pressure	Welch mercury manometer	± 0.05 psia (± 0.03 in Hg)	(estimate of uncertainty)
Pressure drop	MKS Baratron pressure meter	Accuracy of $\pm 0.02\%$ of full range plus 0.15% of dial reading. Repeatability of ± 0.005 to 0.02% of full range (full range = 1000 mmHg)	

The dominant uncertainty was determined to be in the measurement of mass flow rate. As the positive displacement flowmeter was used to measure mass flow rate, an experimental uncertainty of 0.5 percent in the mass flow rate was used. The partial derivative, $\partial D / \partial \dot{m}$ was evaluated by substituting data from a representative experimental run made to determine the diameter. The uncertainty was determined to be ± 0.0007 inch (0.3 percent) and is shown in Table B2.

For the determination of the uncertainty in the mass flow rate, \dot{m} , equation (B8) shows that

$$\dot{m} = \text{fn}(D, L, \rho_{av}, \Delta p_{fr}) \quad (C4)$$

when the calibrated tubular flowmeter is used to measure mass flow rate. Table C2 shows the change in the calculated mass flow rate for a change in variable for two representative test runs. The resulting uncertainties are summarized in Table C3. As shown in Table C3, the dominant uncertainty is in the diameter of the flowmeter, and the percentage uncertainty is relatively constant for the range of mass flow rates.

The uncertainty in the experimental Nusselt number which results from the uncertainty in a measured variable is shown in Table C4. The measured variables included mass flow rate, current, inlet bulk temperature of the gas, wall temperature, inlet static pressure, and the resistance per unit length of the test section. Uncertainties, Δu , in these measurements

Table C2

Change in Calculated Mass Flow Rate For a Change in Variable

u	Run No.	Δu	$\partial f / \partial u$
Static pressure at upstream tap	226H 232H	0.15 psi 0.15 psi	$0.13 \left[\frac{\text{lbm/hr}}{\text{lbf/in}^2} \right]$
Bulk temperature at upstream tap	226H 232H	2.0 °F 2.0 °F	$0.02 \left[\frac{\text{lbm/hr}}{^\circ\text{F}} \right]$ $0.04 \left[\frac{\text{lbm/hr}}{^\circ\text{F}} \right]$
Pressure drop across taps	226H 232H	0.0047 psi 0.0060 psi	$0.08 \left[\frac{\text{lbm/hr}}{\text{lbf/in}^2} \right]$ $0.06 \left[\frac{\text{lbm/hr}}{\text{lbf/in}^2} \right]$
Flowmeter inside diameter	226H 232H	0.0007 in 0.0007 in	$213.0 \left[\frac{\text{lbm/hr}}{\text{in}} \right]$ $505.0 \left[\frac{\text{lbm/hr}}{\text{in}} \right]$

Table C3

Percentage Uncertainties in the Measured Mass Flow Rate

Run No.	Gas	Re_i (approx)	\dot{m} (#m/hr)	E_{arss} (#m/hr)	Percentage Uncertainty
226H	H ₂ -CO ₂	34,000	17.51	0.16	0.9
232H	H ₂ -CO ₂	83,000	42.17	0.37	0.9

were assigned from Table C1 and their values are shown in Table C4. An uncertainty in mass flow rate of 1.5 percent was used in Table C4. The values of $\partial \text{Nu} / \partial u$ in Table C4 were attained by changing the variable by an amount equal to its estimated uncertainty and rerunning the data reduction program at the experimental conditions. It was found that a change of 0.2 psia to the inlet static pressure did not change the experimental Nusselt number. Also, an uncertainty of 0.00008 Ω/in on the resistance per unit length measurement had an insignificant effect on the percentage uncertainty in the experimental Nusselt number.

Three types of comparisons can be made from Table C4. A comparison between the two runs shows that the percentage uncertainty for a relatively low heating rate run to be much higher than a high heating rate run at about the same Reynolds number. The result is due to the relatively high percentage uncertainties in the inlet bulk and wall temperatures being much more dominant in the lower heating rate case. Secondly, the change in the percentage uncertainty along the axial length of the test section can be examined. The dominant uncertainty in the Nusselt number is due to uncertainty in the wall-to-bulk temperature difference. This difference is small in the entrance region, thus causing a large uncertainty in the Nusselt number. At large x/D , the temperature profile is fully developed and wall-to-bulk temperature difference is relatively

Table C4
Percentage Uncertainties in the Measured Bulk Nusselt Number

	x/D	VARIABLE, u								E _{area}	PERCENT UNCER- TAINTY
		h		I		T _b , t		T _w			
		$\frac{\partial Nu}{\partial u}$	Δu	$\frac{\partial Nu}{\partial u}$	Δu	$\frac{\partial Nu}{\partial u}$	Δu	$\frac{\partial Nu}{\partial u}$	Δu		
RUN # 232H GAS H ₂ -CO ₂ Re ₁ = 82,600 T _w T _b MAX -1.20	1.4	0.06		1.43		2.62		2.75		7.63	5.95
	2.0	0.07		1.37		2.37		2.53		6.97	5.68
	4.3	0.10	0.63 ftm/hr	1.23	0.5 amp	1.78	2°F	1.94	2°F	5.30	4.94
	10.8	0.19		1.18		1.44		1.58		4.32	4.47
	24.0	0.37		1.23		1.26		1.40		3.82	4.25
RUN # 235H GAS H ₂ -CO ₂ Re ₁ = 87,100 T _w = 1.85 T _b MAX	49.8	0.67		1.40		1.13		1.29		3.53	4.25
	56.3	0.71		1.40		1.05		1.22		3.32	4.18
	1.4	0.03		0.68		0.36		0.65		1.52	1.17
	2.0	0.03		0.64		0.30		0.58		1.34	1.10
	4.3	0.04		0.55		0.19		0.42		0.96	0.93
GAS H ₂ -CO ₂ Re ₁ = 87,100 T _w = 1.85 T _b MAX	10.8	0.07	0.66 ftm/hr	0.48	0.5 amp	0.13	2°F	0.31	2°F	0.72	0.82
	24.0	0.14		0.45		0.12		0.24		0.59	0.78
	49.8	0.29		0.46		0.12		0.21		0.57	0.86
	56.3	0.38		0.47		0.12		0.21		0.59	0.94

constant. The uncertainty in the Nusselt number becomes a minimum, and then increases with increasing x/D due to greater uncertainty in the bulk temperature. Thirdly, the individual variables can be compared to each other. For example, the uncertainty in mass flow rate becomes increasingly significant at higher heating rate and fully developed conditions.

APPENDIX D

HYDROGEN-CARBON DIOXIDE HEATED EXPERIMENTAL DATA

The headings and their definitions used in the listing of the heated flow data are below.

<u>Heading</u>	<u>Definition</u>
TIN	Inlet mixer temperature
TOUT	Calculated outlet temperature
I	Alternating current
E	Voltage drop between voltage taps
PR, IN	Inlet Prandtl number
GR/RESQ	Ratio of Grashof number to the square of the Reynolds number
MACH(2)	Mach number at thermocouple 2
MACH(16)	Mach number at thermocouple 16
T, SURR	Temperature of surroundings, T_{∞} (see Fig. B3)
TC	Thermocouple number
X/D	Axial position, corresponds to x/D in text
TW	Inside tube wall temperature, °F
TW/TB	Wall-to-bulk temperature ratio
HL/QGAS	Ratio of heat flux lost to QGAS
QGAS	Heat flux to gas
Q^+	Non-dimensional turbulent heat flux parameter. Corresponds to q^+ in text
PT	Pressure tap: 1-inlet, 2-outlet
TB	Bulk static temperature
PRESS DEFECT	Corresponds to \bar{p} in text

RUN 226H, DATE 05/12/77, GAS H2-CO2, MOLECULAR WT. = 14.50
 TOUT = 162.3 F, MASS FLOW RATE = 17.5 LB/HR, I = 66.0 AMPS, E = 4.078 VOLTS
 PR,IN = .338, GR/RESQ = .287E-03, MACH(2) = .090, MACH(16) = .098, I, SURR = 79.1 F

TC	X/D	TW (F)	TW/TB	BULK REYNOLDS	HL/OGAS	BULK NUSSELT	BTU/HRFT2	Q+
2	.4	100.9	1.071	34213.	-.077	147.31	14671.6	.000897
3	.4	110.3	1.090	34196.	.240	86.48	10926.8	.000668
4	.6	120.3	1.108	34173.	.078	83.37	12582.3	.000769
5	.6	136.5	1.136	34147.	.050	75.84	12915.4	.000790
6	.4	142.1	1.145	34095.	.026	69.07	13228.9	.000809
7	.3	153.1	1.168	34039.	.013	65.28	13397.4	.000819
8	.3	170.6	1.177	33807.	.013	55.84	13431.6	.000821
9	.3	179.5	1.181	33514.	.013	52.05	13441.9	.000822
10	.4	193.2	1.182	33224.	.014	49.93	13446.4	.000822
11	.4	206.2	1.181	32664.	.015	48.03	13447.8	.000822
12	.3	217.2	1.178	32124.	.016	46.59	13447.3	.000822
13	.3	229.3	1.175	31650.	.017	45.88	13445.3	.000822
14	.3	239.4	1.172	31174.	.018	45.22	13442.5	.000822
15	.4	250.8	1.169	30321.	.020	44.67	13435.9	.000821
16	.4	262.3	1.160	29923.	.052	44.05	13418.7	.000797
17	.4	255.3	1.150	29800.	.920	41.34	13028.7	.000436
18	.3	225.1	1.101	29789.	-.162	25.50	17133.1	.000997
19	.3					86.50	16303.5	

PT	X/D	STATIC PRESS. (PSIA)	TW/TB	TR (F)	PRESS DEFECT
1	.0	46.0	1.06	63.3	.206E-06
2	.55.3	45.5	1.17	156.7	.914E+00

AVERAGE BULK REYNOLDS 32105.
 AVERAGE PARAMETERS BETWEEN PRESSURE TAPS
 AVERAGE WALL REYNOLDS 26805.
 AVERAGE FRICTION FACTOR .00601

RUN 227H, DATE 05/12/77, GAS H2-CO2, MOLECULAR WT. = 14.50
 T_{IN} = 62.1 F, T_{OUT} = 285.7 F, MASS FLOW RATE = 17.5 LB/HR, I = 99.2 AMPS, E = 6.308 VOLTS
 PR_{IN} = .338, GR/RESQ = .743E-03, MACH(2) = .087, MACH(16) = .103, I_{SURR} = .84.1 F

TC	X/D	TW (F)	TW/TB	BULK REYNOLDS	HL/OGAS	BULK NUSSELT	OGAS BTU/HRFT2	O+
2	2	143.6	1.155	341149.	-.081	153.28	33383.0	.002054
3	4	168.7	1.198	341112.	-.263	87.56	33336.6	.001497
4	5	187.7	1.236	34059.	-.094	87.33	28400.4	.001747
5	9	194.7	1.247	34001.	-.012	89.18	31181.6	.001919
6	1	224.0	1.299	33876.	.041	69.90	29634.6	.001826
7	3	239.9	1.321	33753.	.018	65.62	30346.3	.001873
8	3	277.9	1.371	33262.	.019	55.21	30437.8	.001876
9	4	304.3	1.383	32619.	.019	48.71	30495.4	.001878
10	7	325.9	1.392	32010.	.021	45.39	30528.4	.001880
11	10	359.6	1.381	30946.	.023	43.58	30560.2	.001880
12	17	384.6	1.387	29038.	.025	42.40	30559.0	.001880
13	30	413.2	1.350	28147.	.026	41.55	30557.8	.001879
14	44	457.7	1.333	27320.	.028	41.18	30541.3	.001879
15	56	479.9	1.318	26551.	.032	40.58	30493.3	.001811
16	56	503.0	1.306	25923.	.071	38.44	29436.3	.001811
17	59	483.2	1.306	25731.	.935	23.99	16262.3	.001001
18	59	417.9	1.267	25717.	-.146	81.35	36684.4	.002257

PT 1 X/D 55.4 STATIC PRESS. (PSIA) 47.4 TW/TB 1.12 TB (F) 62.3
 2 55.4 46.8 1.31 273.2
 PRESS. DEFECT .553E-06
 .124E+01
 AVERAGE BULK REYNOLDS 30096.
 AVERAGE PARAMETERS BETWEEN PRESSURE TAPS
 WALL REYNOLDS AVERAGE FRICTION FACTOR
 21845. .00618

RUN 228H, DATE 05/12/77, GAS H2-CO2, MOLECULAR WT. = 14.50
 TTN = 62.0 F, TOUT = 412.4 F, MASS FLOW RATE = 17.4 LB/HR, I = 123.6 AMPS, E = 8.056 VOLTS
 PR,IN = .338, GR/RESQ = .111E-02, MACH(2) = .084, MACH(16) = .108, T, SUPP = .92.4 F

TC	X/D	TW (F)	TW/TB	REYNOLDS BULK	HL/QGAS	NUSSELT BULK	BTU/HRFT2 QGAS	Q+
2	.2	191.4	1.245	34003.	-.090	152.37	52528.7	.003242
3	.4	227.5	1.312	33944.	.272	85.71	37698.9	.002327
4	.6	261.5	1.373	33862.	.086	85.61	37698.9	.002731
5	.9	286.2	1.417	33773.	.081	75.09	44252.2	.002750
6	.4	321.7	1.475	33589.	.028	68.75	44549.8	.002900
7	1.0	345.1	1.510	33408.	.023	63.84	46983.6	.002919
8	.3	409.8	1.588	32662.	.024	53.08	47299.6	.002928
9	.6	456.1	1.618	31719.	.025	48.02	47435.6	.002936
10	.9	490.9	1.602	30861.	.026	45.08	47569.3	.002940
11	.4	543.5	1.574	29375.	.029	41.64	47692.6	.002943
12	.1	589.3	1.542	27935.	.032	39.37	47709.5	.002945
13	.0	626.9	1.510	26701.	.035	38.00	47706.5	.002944
14	.5	661.8	1.475	25662.	.038	36.89	47682.9	.002943
15	.8	691.0	1.441	24674.	.041	36.29	47638.2	.002940
16	.5	720.1	1.416	23728.	.045	35.91	47559.3	.002935
17	.2	752.0	1.352	22887.	.090	33.81	45699.4	.002820
18	.5	717.2	1.327	22590.	.134	37.20	43817.8	.002704
19	.5	610.5	1.227	22571.	-.129	74.42	56624.5	.003495

PT 1 2
 X/D 55.5
 STATIC PRESS. (PSIA) 48.5 47.7
 TW/TB 1.19 1.42
 TB (F) 62.8 389.9
 PRESS DEFECT .953E-06
 .156E+01
 AVERAGE BULK REYNOLDS 28525.
 AVERAGE PARAMETERS BETWEEN PRESSURE TAPS
 WALL REYNOLDS 18544.
 AVERAGE FRICTION FACTOR .00642

RUN 229H, DATE 05/12/77, GAS H2-CU2, MOLECULAR WT. = 14.50
 TIN = 62.4 F, TOUT = 552.1 F, MASS FLOW RATE = 17.3 LB/HR, I = 145.8 AMPS, E = 9.655 VOLTS
 PR,IN = .338, GR/RESQ = .165E-02, MACH(2) = .082, MACH(16) = .112, I, SURR = 100.0 F

TC	X/D	TW (F)	TW/TB	BULK REYNOLDS	HL/QGAS	BULK NUSSELT	BTU/HR FT ²	Q+
2	.2	242.9	1.340	33746.	-.095	153.45	73835.5	.004577
3	.4	242.2	1.431	33664.	.089	85.96	52579.0	.003259
4	.9	339.1	1.515	33549.	.076	84.05	61781.3	.003830
5	.1	372.7	1.573	33425.	.028	78.22	62693.7	.003886
6	.8	422.8	1.654	33184.	.026	69.52	65851.0	.004082
7	.0	458.0	1.704	32933.	.030	63.75	66114.8	.004098
8	.3	555.0	1.816	31911.	.032	51.85	66352.8	.004113
9	.6	626.6	1.852	30694.	.034	45.85	66582.5	.004127
10	.9	678.8	1.857	29634.	.038	42.48	66952.2	.004134
11	.1	756.7	1.817	27645.	.047	38.46	66761.7	.004137
12	.5	821.1	1.766	25937.	.043	35.80	66748.7	.004135
13	.7	871.1	1.711	24579.	.052	33.19	66713.3	.004130
14	.2	915.6	1.653	23257.	.056	33.06	66633.2	.004124
15	.5	950.3	1.594	22135.	.061	32.60	66524.0	.004115
16	.3	989.3	1.546	20999.	.110	32.04	66383.8	.004115
17	.1	1023.9	1.501	20109.	.041	30.45	63617.3	.003943
18	.3	967.6	1.414	19777.	-.092	37.69	67584.3	.004190
19	.6	806.1	1.251	19765.		70.24	76591.7	.004748

PT 1 2 X/D .0 55.6 STATIC PRESS. (PSIA) 49.7 48.8 TB (F) 63.8 520.0 PRESS DEFECT .140E-05 .191E+01

AVERAGE BULK REYNOLDS 27018. AVERAGE PARAMETERS BETWEEN PRESSURE TAPS AVERAGE FRICTION FACTOR .00658

RUN 231H, DATE 05/18/77, GAS H2-CD2, MOLECULAR WT. = 14.50
 TOUT = 254.0 F, MASS FLOW RATE = 42.6 LB/HR, I = 142.0 AMPS, E = 9.165 VOLTS
 PR.IN = .342, GR/RESO = .863E-03, MACH(2) = .111, MACH(16) = .130, I, SURR = 83.2 F

TC	X/D	TW	TW/TB	BULK REYNOLDS	HL7QGAS	BULK NUSSELT	BUTU/HRFI2	QGAS	O+
2	.2	162.4	1.186	83060.	-.046	232.54	66034.7	001636	
3	.4	189.6	1.237	82977.	.148	164.56	54973.5	001362	
4	.6	212.7	1.279	82860.	.046	153.12	60453.8	001498	
5	.9	228.3	1.306	82739.	.041	139.70	60819.9	001507	
6	1.1	249.1	1.342	82493.	.014	128.07	62527.5	001549	
7	2.0	261.6	1.360	82244.	.010	121.27	62846.2	001557	
8	4.3	298.6	1.410	81244.	.010	104.31	62970.8	001560	
9	7.6	322.9	1.434	79920.	.010	97.12	63099.5	001563	
10	10.9	342.1	1.434	78633.	.010	92.63	63177.7	001565	
11	17.4	371.6	1.432	76354.	.011	87.48	63278.6	001568	
12	24.0	398.3	1.425	74243.	.012	83.77	63355.8	001570	
13	30.4	421.0	1.415	72387.	.012	81.32	63411.4	001571	
14	36.9	443.3	1.403	70461.	.013	79.26	63461.2	001572	
15	43.4	462.4	1.388	68658.	.014	78.14	63495.3	001573	
16	49.9	483.0	1.376	66935.	.016	76.61	63496.9	001573	
17	56.5	504.8	1.366	65320.	.033	73.57	62507.0	001549	
18	59.1	495.9	1.341	64834.	.553	51.78	41552.8	001030	
19	59.4	443.7	1.266	64805.	-.051	108.09	67752.7	001679	

PT	X/D	STATIC PRESS. (PSIA)	TW/TB	TB (F)	PRESS DIFFERENTIAL
1	0	90.0	1.14	64.7	.576E-06
2	55.4	88.5	1.37	242.8	.988E+00

AVERAGE BULK REYNOLDS 74340.
 AVERAGE WALL REYNOLDS 51217.
 AVERAGE PARAMETERS BETWEEN PRESSURE TAPS
 AVERAGE FRICTION FACTOR .00485

RUN 232H, DATE 05/18/77, GAS H2-CO2, MOLECULAR WT. = 14.50
 TIN = 63.5 F, TOUT = 148.7 F, MASS FLOW RATE = 42.2 LB/HR, I = 95.0 AMPS, E = 5.986 VOLTS
 PR.IN = .341, GR/RESQ = .364E-03, NACH(2) = .116, MACH(16) = .126, T, SUPP = 83.0 F

TC	X/D	TW	TW/TB	REYNOLDS	HL/QGAS	BULK	NUSSELT	BTU/HRFT2	QGAS	O+
2	2	113.7	1.097	82480.	-.038	216.56	216.56	29182.2	29182.2	000734
3	4	113.7	1.116	82444.	.110	156.59	156.59	25314.2	25314.2	000636
4	6	132.4	1.132	82392.	.040	146.82	146.82	27029.6	27029.6	000679
5	9	137.9	1.142	82338.	.022	138.83	138.83	27518.6	27518.6	000692
6	1	145.6	1.155	82228.	.011	128.25	128.25	27647.6	27647.6	000700
7	4	150.4	1.162	82113.	.006	107.29	107.29	27985.2	27985.2	000703
8	3	165.6	1.183	81630.	.006	100.45	100.45	28019.4	28019.4	000704
9	7	176.4	1.193	81009.	.006	96.69	96.69	28039.2	28039.2	000705
10	10	184.6	1.198	80406.	.006	92.59	92.59	28071.2	28071.2	000706
11	17	197.7	1.201	79236.	.007	89.65	89.65	28085.3	28085.3	000706
12	30	209.5	1.200	77052.	.008	87.88	87.88	28094.2	28094.2	000706
13	36	220.7	1.199	76047.	.008	86.00	86.00	28108.8	28108.8	000707
14	33	240.7	1.196	75074.	.009	84.71	84.71	28108.8	28108.8	000707
15	49	251.2	1.195	74155.	.010	83.08	83.08	28104.5	28104.5	000697
16	56	263.2	1.196	73296.	.024	79.38	79.38	27743.5	27743.5	000649
17	59	260.0	1.184	72968.	.099	78.19	78.19	25622.9	25622.9	000649
18	59	239.0	1.148	72941.	-.030	109.64	109.64	29214.9	29214.9	000734

PT	X/D	STATIC PRESS. (PSIA)	TW/TE	TB (F)	PRESS. DEFECT
1	0	85.1	1.08	62.6	.247E-06
2	55.3	83.9	1.20	143.0	.751E+00

AVERAGE DULK REYNOLDS = 77968.
 AVERAGE WALL REYNOLDS = 62727.
 AVERAGE PARAMETERS BETWEEN PRESSURE TAPS
 AVERAGE FRICTION FACTOR = .00485

RUN 234H, DATE 05/27/77, GAS H2-CO2, MOLECULAR WT. = 14.50
 TIN = 54.7 F, TOUT = 349.8 F, MASS FLOW RATE = 44.2 LB/HR, I = 179.2 AMPS, E = 11.820 VOLTS
 PK.IN = .340, GR/RESQ = .164E-02, MACH(2) = .104, MACH(16) = .131, J, SURR = 92.6 F

TC	X/D	TW	TW/TB	BULK REYNOLDS	HL/OGAS	BULK NUSSELT	BTU/HRFT2	OGAS	O+
2	.2	211.8	1.304	87378.	-.048	254.11	105794.1	.02587	.02587
3	.4	254.4	1.385	87241.	.150	166.27	87850.3	.02148	.02148
4	.6	289.3	1.449	87048.	.044	156.51	96973.4	.02371	.02371
5	.9	313.4	1.492	86848.	.041	142.90	97418.5	.02382	.02382
6	1.4	346.4	1.548	86442.	.014	131.08	100333.6	.02453	.02453
7	2.0	367.0	1.579	86022.	.011	123.49	100757.3	.02464	.02464
8	4.3	427.7	1.657	84335.	.012	105.12	101044.9	.02471	.02471
9	7.6	470.4	1.685	82206.	.013	96.15	101351.4	.02478	.02478
10	10.9	502.8	1.692	80246.	.013	90.65	101547.1	.02483	.02483
11	17.4	552.2	1.682	76813.	.014	83.99	101796.6	.02489	.02489
12	24.1	594.4	1.660	73642.	.015	79.50	101980.6	.02493	.02493
13	30.4	629.4	1.633	70779.	.016	76.43	102114.0	.02497	.02497
14	37.0	663.6	1.606	68054.	.018	73.80	102221.6	.02501	.02501
15	43.5	689.9	1.571	65784.	.019	72.60	102290.5	.02502	.02502
16	50.0	719.6	1.544	63633.	.021	70.81	102318.7	.02507	.02507
17	56.6	753.3	1.524	61614.	.041	67.25	100609.7	.02460	.02460
18	59.2	732.3	1.475	60849.	.133	66.28	92303.1	.02257	.02257
19	59.5	654.4	1.376	60794.	-.052	99.18	109651.0	.02681	.02681

PT	X/D	STATIC PRESS. (PSIA)	TW/TB	TB (F)	PRESS DEFECT
1	.0	98.0	1.23	54.9	.840E-06
2	55.5	96.2	1.53	330.7	.123E+01

AVERAGE BULK REYNOLDS 74691.
 AVERAGE WALL REYNOLDS 44305.
 AVERAGE PARAMETERS BETWEEN PRESSURE TAPS
 AVERAGE FRICTION FACTOR .00484

RUN 235H, DATE 05/27/77, GAS H2-CO2, MOLECULAR WT. = 14.50
 TIN = 54.7 F, TOUT = 422.6 F, MASS FLOW RATE = 43.8 LB/HR, I = 198.8 AMPS, E = 13.200 VOLTS
 PR.IN = .340, GR/RESQ = .216E-02, MACH(2) = .101, MACH(16) = .132, T, SURR = 106.5 F

TC	X/D	TW (F)	TW/TD	BULK REYNOLDS	HL/OGAS	BULK NUSSELT	OGAS BIU/HRFT2	O+
2	.2	252.5	1.388	86649.	-.049	245.21	130759.0	.032220
3	.4	304.1	1.480	86442.	.139	165.01	109530.1	.002698
4	.6	346.1	1.556	86244.	.042	156.01	120067.6	.002958
5	.9	375.3	1.608	85997.	.038	142.20	120801.4	.002975
6	1.4	417.6	1.678	85495.	.014	130.20	124048.2	.003055
7	2.0	443.6	1.717	84979.	.012	122.15	124612.1	.003069
8	4.3	522.1	1.814	82949.	.014	103.15	125036.6	.003080
9	7.6	577.3	1.846	80386.	.015	87.83	125500.8	.003091
10	10.9	679.8	1.851	78108.	.016	80.85	126156.7	.003098
11	17.4	734.8	1.795	70341.	.018	75.66	126420.9	.003114
12	24.4	777.8	1.756	67085.	.020	72.37	126608.2	.003118
13	30.0	817.7	1.714	64350.	.021	69.78	126749.2	.003122
14	37.5	852.5	1.671	61755.	.025	67.76	126827.6	.003125
15	43.5	885.9	1.630	59250.	.025	66.22	126878.6	.003125
16	50.1	922.0	1.599	57055.	.046	63.04	124707.3	.003171
17	59.3	899.4	1.543	56249.	.067	62.58	121950.4	.003304
18	59.6	804.4	1.433	56197.	.054	92.55	136752.2	.003368

PT	X/D	STATIC PRESS. (PSIA)	TW/TE	TB (F)	PRESS T
1	.0	100.6	1.30	55.3	.114E-05
2	55.5	98.6	1.60	39.8.4	.140E+01

AVERAGE BULK REYNOLDS 72068.
 AVERAGE PARAMETERS BETWEEN PRESSURE TAPS
 AVERAGE WALL REYNOLDS 39342.
 AVERAGE FRICTION FACTOR .00491

APPENDIX E. POSSIBILITY OF INTERACTION
BETWEEN CARBON DIOXIDE AND HYDROGEN

by

Professor H. C. Perkins, Jr.

Reactions between CO₂ and H₂

The reaction to consider initially is the water-gas shift reaction given by



This reaction has been used in industry as



to produce hydrogen. For example, Wilson and Newell [1966] note that at 500°C (932°F) CO will reduce steam to produce H₂ when passed over an iron-chromium and cobalt oxide catalyst.

The equilibrium constant for the reaction (2) is known and is given by

$$K_p = \frac{x_{\text{CO}_2} x_{\text{H}_2}}{x_{\text{CO}} x_{\text{H}_2\text{O}}} \quad (\text{E3})$$

where x represents the mole fraction. Values of K_p are given in Benson [1977] and an abstracted table is given here.

Equilibrium Constant

T °K	T °F	K _p
500	440	135.2
1000	1340	1.386
1500	2240	0.371

Since the equilibrium constant decreases with increasing temperature, higher temperatures result in more CO and H₂O and less H₂ and CO₂. Results are given below for some equilibrium calculations for reaction (2) with equal concentrations of H₂ and CO₂, $x_{\text{CO}_2} = x_{\text{H}_2} = 0.5$, initially.

Equilibrium mole fractions [*]						
T	T	K _p	X	X	X	X
°K	°F		H ₂	CO ₂	CO	H ₂ O
2000	3140	0.214	0.159	0.159	0.341	0.341
1800	2780	0.265	0.170	0.170	0.330	0.330
1500	2240	0.371	0.192	0.192	0.308	0.308
1000	1340	1.386	0.27	0.27	0.23	0.23
500	440	135.2	0.46	0.46	0.04	0.04

* 1 mole CO₂, 1 mole H₂ initially

From these results we see that at relatively low temperatures one can produce substantial amounts of CO and H₂O if the reaction can go to equilibrium. In order to determine the end point of the reaction, one must investigate the chemical kinetics - that is, how fast does the reaction take place.

Kinetics

In their book, "New Energy Technology," Hottel and Howard [1971] indicate that the water gas reaction is important in coal gasification

schemes. They then comment that "excess steam increases the H_2/CO ratio through the water-gas shift reaction which maintains itself in substantial equilibrium at coal gasification temperatures." A reading of the subsequent chapter indicates that coal gasification temperatures can be taken as around 1800°F (1255K). No information on times at these temperatures is given, but since gasification generally involves flow through a fluidized bed or other form of reactor which is several feet long we might expect times at least on the order of 0.1 to 1 sec (i.e., 10 feet at 10-100 ft/sec).

Fortunately, we can do better than this single piece of information. Graven and Long [1954] have measured the kinetics of both the forward and backward reactions for the water-gas reaction and we can use their results to determine the change, if any, in CO_2 and H_2 as these flow through a heated tube.

The kinetic data are presented in terms of the reaction rate constant K_1 defined, for example, by the rate equation

$$\frac{dH_2O}{dt} = K_1 (H_2)^{1/2} (CO_2)$$

where the concentrations are in moles/liter. Their experiment was done in a quartz vessel at temperatures from 875°C to 1050°C (1600°F - 1925°F), at a pressure of about 1 atmosphere. For the initial case of CO_2 and H_2 each at 1/2 atm. partial pressure, they found

$$K_1 = 9.5 \times 10^{10} \exp (-57000/RT) \quad (E4)$$

where K has units of (liters)^{1/2}/(mole)^{1/2}(s).

The data were determined for the case H_2 and CO_2 proceeding only to 2% of completion or less while flowing for about 0.5 sec at the given temperature.

The reverse reaction $CO + H_2O \rightarrow CO_2 + H_2$ was also studied. Both the forward and reverse reaction rates were determined only for the specific case involving the initial stages of these reactions, i.e., no CO and H_2O initially present for the $CO_2 + H_2$ reaction.

The proposed mechanism for the forward reaction is:



Thus, while the reaction is in process one can expect to have as species: H_2 , H, CO_2 , CO, OH, H_2O . Graven and Long also indicate that small quantities of O_2 (about 1%) accelerate the reaction by as much as a factor of 100.

Given an initial concentration of 1 mole H_2 and 1 mole CO_2 at one atmosphere total pressure, we have for [redacted] of 0.01 sec (1 foot/100 ft/sec), i.e., at the end of [redacted] test section:

T °K	T °F	K_1	H_2O moles/liter	H_2O/CO_2
1000	1340	0.0324	1.53×10^{-7}	2.5×10^{-5}
1264	1816	13.0	-	0.01
1400	2060	118	5.5×10^{-4}	0.09

Thus, we see that at temperatures below 1800°F for times ≤ 0.01 sec, the molal concentration of H_2O and CO will each be less than 1%. At temperatures above 1800 F concentrations of H_2O and CO can become significant for times > 0.01 sec.

Effect of Pressure on Equilibrium

Given

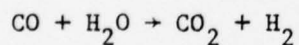


the equilibrium constant as given in equation (E3) may be generalized to the form

$$K_P = \frac{x_C^{v_3} x_D^{v_4}}{x_A^{v_1} x_B^{v_2}} \left(\frac{P}{P_0} \right)^{v_3 + v_4 - v_1 - v_2} \quad (E7)$$

where x = mole fraction.

Since the reaction considered here has all v 's = 1, i.e.,



equation (E7) reduces to equation (E3)

$$K_P = \frac{x_{CO_2} x_{H_2}}{x_{CO} x_{H_2O}}$$

and pressure has no effect on the final concentrations at equilibrium for this reaction.

Effect of Pressure on Kinetics

Again we have



with

$$K_1 = 9.5 \times 10^{-10} \exp [-57000/RT]$$

for

$$\frac{d(\text{H}_2\text{O})}{dt} = K_1 (\text{H}_2)^{1/2} (\text{CO}_2)$$

Changing the pressure changes the concentration (moles/liter) of H_2 and CO_2 but does not change K_1 .

As an example, using $P_{\text{total}} = 5 \text{ atm}$ at $x_{\text{H}_2} = 0.5 = x_{\text{CO}_2}$, we have partial pressures of 2.5 atm each for H_2 and CO_2 and the concentrations are 5 times greater than before. After $\Delta t = 0.01 \text{ sec}$ at 1000K, we find, $(\text{H}_2\text{O})/(\text{CO}_2) = 5.5 \times 10^{-5}$. At 1000K at $P = 1 \text{ atm}$, we previously found $(\text{H}_2\text{O})/(\text{CO}_2) = 2.5 \times 10^{-5}$.

At 1400K and both partial pressures equal to 2.5 atm, we find $(\text{H}_2\text{O})/(\text{CO}_2) = 0.203$ versus 0.091 with $P_{\text{total}} = 1 \text{ atm}$.

Roughly speaking, increasing pressure by a factor of 5 doubles the ratios of $\text{H}_2\text{O}/\text{CO}_2$ and CO/CO_2 produced. Increasing pressure by a factor of 10 increases $\text{H}_2\text{O}/\text{CO}_2$ and CO/CO_2 by factors of about 3.

Summary

We can conclude that the H_2/CO_2 data of Serksnis are not significantly affected by reactions between CO_2 and H_2 . The effect of any residual O_2 and of possible catalytic action by the tube walls

could give cause for concern as temperatures rise above perhaps 1300°F.

References cited

Benson, R. S., 1977. Advanced Engineering Thermodynamics, 2nd Ed. Pergamon.

Graven, W. M. and F. J. Long, 1954. Kinetics and Mechanisms of the Two Opposing Reactions of the Equilibrium $\text{CO} + \text{H}_2\text{O} = \text{CO}_2 + \text{H}_2$. J. Amer. Chem. Soc., 76, p 2602-2607.

Hottel, H. C. and J. B. Howard, 1971. New Energy Technology, MIT Press.

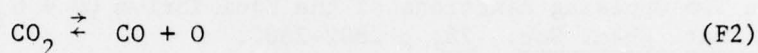
Wilson, J. G. and A. B. Newall, 1966. General and Inorganic Chemistry. Cambridge: Cambridge U. P.

APPENDIX F. CONSIDERATION OF DISSOCIATING GASES

by

Professor H. C. Perkins, Jr.

At sufficiently high temperatures many gases are known to dissociate. For example:

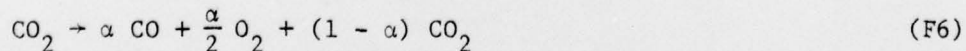


Assuming thermal equilibrium, one can calculate the gas concentrations as a function of temperature for the above reactions. For example, for equation (F1) we have for the equilibrium constant

$$K_p(T) = \frac{x_{\text{CO}} x_{\text{O}_2}^{1/2}}{x_{\text{CO}_2}} \left(\frac{P}{P_o} \right)^{1 + \frac{1}{2} - 1} \quad (\text{F5})$$

This information together with the relationship that $\sum x_i = 1$ and a known initial concentration enables one to determine the equilibrium composition as a function of temperature.

Common practice is to define a "degree of dissociation" called α . The equilibrium constant can then be related to α . We have here



If $\alpha = 0$, no dissociation has taken place; if $\alpha = 1$, then the CO_2 has completely dissociated. Since the mole fraction is equal to the ratio

of partial pressure to total pressure, we have

$$x_{\text{CO}} = \frac{2\alpha}{2+\alpha} = P_{\text{CO}}/P_{\text{total}} \quad (\text{F7})$$

$$x_{\text{O}_2} = \frac{\alpha}{2+\alpha} = P_{\text{O}_2}/P_{\text{total}} \quad (\text{F8})$$

$$x_{\text{CO}_2} = \frac{2(1-\alpha)}{2+\alpha} = P_{\text{CO}_2}/P_{\text{total}} \quad (\text{F9})$$

Substituting into the K_p expression yields

$$K_p(T) = \sqrt{\frac{\alpha}{2+\alpha}} \frac{\alpha}{1-\alpha} \cdot \left(P/P_o \right)^{1/2} \quad (\text{F10})$$

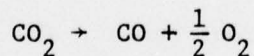
and at $P_o = 1$ atm the expression reduces to

$$K_p(T) = \sqrt{\frac{\alpha}{2+\alpha}} \frac{\alpha}{1-\alpha} P^{1/2} \quad (\text{F11})$$

If the final pressure is known and temperature is known, the degree of dissociation at equilibrium can be determined.

Some results for reaction (F1) at a pressure of 1 atm follow:

Dissociation of carbon dioxide.



T	T	α	K_p
$^{\circ}\text{K}$	$^{\circ}\text{F}$		
2000	3140	0.015	0.00137
2400	3860	0.099	0.0218
3000	4940	0.444	0.340

The effect of increased pressure is to reduce the degree of dissociation,

(i.e., reduce the number of molecules) and to maintain higher concentrations of CO_2 .

For the reaction $\text{H}_2 \rightarrow 2\text{H}$ we have

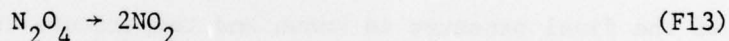
$$K_p = \frac{4\alpha^2}{(1-\alpha^2)} \left(\frac{P}{P_o} \right) \quad (\text{F12})$$

at $P = 1 \text{ atm}$:

Dissociation of hydrogen.

T	T	K_p	α	x_{H}	x_{H_2}
K	$^{\circ}\text{F}$				
2000	3140	2.63×10^{-6}	0.020	0.039	0.960
3550	5930	0.4367	0.314	0.477	0.522

Both of the above cases involve very high temperatures. One reaction of interest because it shows significant dissociation at low (i.e., room) temperatures is the reaction



The heat transfer to N_2O_4 undergoing dissociation has been studied by Presler [1966], Callaghan and Mason [1964] and Furgason and Smith [1962].

Thus we see that dissociation reaction can occur over a wide range of temperatures for different gases. Why are we interested in dissociation? McKisson [1954] noted an interest in order to utilize the reversible endothermic nature of the dissociation reaction to increase the energy absorbing capacity of gaseous coolants. In his study he noted five requirements for this application:

1. that the mean temperature of a reaction be low enough that material properties are not limiting,
2. that the products of dissociation be chemically compatible with the materials used in system components,

3. that the reactant-product equilibrium occur over a minimum temperature range,
4. that the rates of both the forward and reverse reactions be rapid,
5. and that the heat of reaction be large.

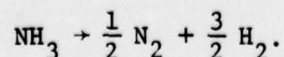
In his study he considered only items 3 and 5. Based on these criteria, he concludes that the suitable gases for use below 3000°F are limited to the halogen gases (F_2 , Cl_2 , Br_2 , I_2) and hydrogen iodide (HI). Unfortunately, neither the halogen gases nor their dissociation products are desirable fluids in the environment due to a combination of their health hazard and corrosive nature.

Why dissociation?

There appear to be two possible reasons to consider dissociation as a means to improve Brayton cycle system performance.

First, for a given maximum temperature at the turbine inlet more energy can be stored in the working fluid if dissociation occurs since the ΔH_{disc} is required to accomplish the dissociation. If this energy can be recovered in the turbine, then expanding across the same pressure difference (as for the nondissociating case) will result in a greater work output.

Second, the effect of dissociation is to increase the volume flow rate through the turbine. Again assuming the same ΔP and ΔT across the turbine as with no dissociation, we can double the number of moles (for a diatomic dissociation) and hence the volume flow through the turbine. Gasparovic [1970] notes that "at higher temperature, ammonia dissociates exothermally according to the reaction



This occurrence is favourable because, due to the greater number of moles in the turbine compared with that in the compressor, work is increased, albeit at the cost of the heat supplied." He also points out a problem with dissociation for this reaction since the reverse reaction is not possible without catalysts; the working fluid of the cycle would soon become a mixture of NH_3 , N_2 and H_2 and no further dissociation would take place. The components would have to be sized for this mixture.

Naturally, if recombination occurs in the turbine so that advantage (1) is fully realized, then advantage (2) cannot be fully realized.

Kinetics

An important aspect to using dissociation as a means to improving performance is the kinetics of the recombination reaction. The residence time in a combustion can or a heat exchanger might range from a few milliseconds to a second. But the time to pass through the turbine is more like 0.5 ms. Thus, to recover the energy of dissociation in the turbine the recombination rate must be high. Bray [1959] has discussed these ideas as applied to a hypersonic nozzle flow. If the expansion is very rapid, "frozen" flow results and the recombination rate becomes too low for significant recombination to occur, hence equilibrium is not maintained. Interestingly, Bray notes that the shape of the nozzle exercises an influence on whether the flow is in the equilibrium or frozen regime.

Where to from here?

Lighthill [1957] has developed a model, now called the Lighthill Ideal Dissociating Gas, which is applicable to diatomic gases from 1000K to 7000K. Bray [1959] and Benson [1977] have used this model to analyze flow where kinetics is important so that α (the degree of dissociation) can be determined as a function of position through a nozzle. It is possible that this model could be extended (modified) to be used for flow through a turbine-regenerator system. The model is based on homogeneous gas reaction and the effect of the walls though not critical in a nozzle, could be important here.

Information on the kinetics is of critical importance. For the $\text{N}_2\text{O}_4 \rightarrow 2\text{NO}_2$ system the reaction is so fast that Pressler assumes complete equilibrium at any temperature. This situation is clearly not the case with all reactions. Kinetics information for elementary reactions is in the Leeds reports [Baluch et al., 1968-1969].

I consider the idea worthy of further study in which the kinetics could be included to determine where in the cycle the recombination occurs. Since one is dealing with a variable mixture, analysis of the temperature (enthalpy) change through the turbine will require some thought. Other problems include

- (1) what gases, if any, are suitable candidates as the working fluid considering that desired peak temperatures

- are about 2500°F,
- (2) what is the effect of surfaces on the recombination, and
 - (3) how much larger (heavier) must the heater be to provide the required additional energy?

References

- Benson, R. S., 1977. Advanced Engineering Thermodynamics, 2nd ed., Pergamon.
- Bray, K. N. C., 1959. Atomic Recombination in a Hypersonic Wind Tunnel Nozzle. J. Fluid Mech., 6, 1.
- Callaghan, M. J. and Mason, D. M., 1964. Momentum and Heat Transfer Correlations for a Reacting Gas in Turbulent Pipe Flow. AIChE J., 10, 52-55.
- Gasparović, N., 1970. Working Fluids and Cycles for Thermal Power Plants with Large Unit Outputs. Tech. Rpt. WTHD Nr. 19, Mech. Engr., Delft. (Also Gasparović, N., 1969. Fluide und Kreisprozesse für Wärmekraftanlagen mit grossen Einheiten leistung. Brennstoff-Wärme-kraft, 21, 347-359.)
- Lighthill, M. J., 1957. Dynamics of a Dissociating Gas. J. Fluid Mech., 2, 1.
- McKisson, R. L., 1954. Dissociation - Cooling: A Discussion. Tech. Rpt. LRL-86, Livermore Research Lab., Calif.
- Presler, A. F., 1966. An Experimental Investigation of Heat Transfer to Turbulent Flow in Smooth Tubes for the Reacting N_2O_4 - NO_2 System. NASA TN D-3230.

REFERENCES

- Bammert, K. and Klein, R., 1974. The Influence of He-Ne, He-N₂ and He-CO₂ Gas Mixtures on Closed Cycle Gas Turbines. ASME Paper 74-GT-124.
- Bammert, K., Rurik, J., and Griepentrog, H., 1974. Highlights and Future Developments of Closed-cycle Gas Turbines. ASME Paper 74-GT-7.
- Bankston, C. A. and McEligot, D. M., 1970. Turbulent and Laminar Heat Transfer to Gases With Varying Properties in the Entry Region of Circular Ducts. Int. J. Heat Mass Transfer, 13, 319-344.
- Bingham, B., 1977. Heat Loss Calibration of a Smooth Circular Tube. Tech-memo, Aero. Mech. Engr. Dept., Univ. of Arizona.
- Campbell, D. A. and Perkins, H. C., 1968. Variable Property Turbulent Heat and Momentum Transfer for Air in a Vertical Rounded Corner Triangular Duct. Int. J. Heat Mass Transfer, 11, 1003-1012.
- Coon, C. W. Jr., 1968. The Transition From the Turbulent to the Laminar Regime for Internal Convective Flow with Large Property Variations Ph.D. dissertation, Univ. of Arizona.
- DiPippo, R. and Kestin, J., 1969. The Viscosity of Seven Gases up to 500°C and Its Statistical Interpretation. Fourth Symposium on Thermal Physical Properties, 304-313.
- Doebelin, E. O., 1966. Measurement Systems: Application and Design, New York: McGraw-Hill.
- Drew, T. B., Koo, E. C. and McAdams, W. M., 1932. The Friction Factor in Clean, Round Pipes. Trans. Am. Inst. Chem. Engrs., 28, 56-72.
- Hess, W. G., 1965. Thermocouple Conduction Error with Radiation Heat Loss. M.S.E. Thesis, University of Arizona.
- Hilsenrath, J. C., Beckett, W., Benedict, W. S., Fano, L., Hoge, H. J., Masi, J. F., Nuttall, R. L., Touloukian, Y. S. and Wooley, H. W. 1955. Table of Thermal Properties of Gases. NBS Circular 564.
- Hirschfelder, J. O., Curtiss, C. F. and Bird, R. B., 1964. Molecular Theory of Gases and Liquids, New York: Wiley.
- Humble, L. V., Lowdermilk, W. H., and Desmon, L. G., 1951. Measurements of Average Heat-transfer and Friction Coefficients for Subsonic Flow of Air in Smooth Tubes at High Surface and Fluid Temperatures. NACA Report 1020.

- Kays, W. M., 1966. Convective Heat and Mass Transfer, New York: McGraw-Hill.
- Kline, S. J. and McClintock, F. A., 1953. The Description of Uncertainties in Single Sample Experiments. Mech. Engng., 75, 38.
- Liepmann, H. W., and Roshko, A., 1957. Elements of Gas Dynamics, New York: Wiley.
- Magee, P. M., 1964. The Effect of Large Temperature Gradients on Turbulent Flow of Gases in the Thermal Entrance Region of Tubes. TR 247-4, Mechanical Engineering Dept., Stanford University.
- Malina, J. A. and Sparrow, E. M., 1964. Variable-property, Constant-property, and Entrance-region Heat Transfer Results for Turbulent Flow of Water and Oil in a Circular Tube. Chem Eng. Sci., 19, 953-961.
- McAdams, W. H., 1954. Heat Transmission, 3rd Ed., New York: McGraw-Hill.
- McEligot, D. M., 1963. Effect of Large Temperature Gradients on Turbulent Flow of Gases in the Downstream Region of Tubes. TR 247-5, Mechanical Engineering Dept., Stanford University.
- McEligot, D. M., Magee, P. M., and Leppert, G., 1965. Effect of Large Temperature Gradients on Convective Heat Transfer: The Downstream Region. J. Heat Transfer, 87, 67-76.
- McEligot, D. M., Pickett, P. E. and Taylor, M. F., 1976. Measurements of Wall Region Turbulent Prandtl Numbers in Small Tubes. Int. J. Heat Mass Transfer, 19, 799-803.
- Mock, E. A., 1970. Closed Brayton Cycle System Optimization for Undersea, Terrestrial, and Space Applications. von Karman Institute for Fluid Dynamics, Brussels, Belgium
- Moen, W. K., 1960. Surface Temperature Measurement. Inst. Control Syst., 33, 70-73.
- Perkins, K. R., Schade, K. W., and McEligot, D. M., 1973. Heated Laminarizing Gas Flow in a Square Duct. Int. J. Heat Mass Transfer, 16, 897-916.

- Pickett, P. E., 1976. Heat and Momentum Transfer to Internal, Turbulent Flow of Helium-Argon Mixtures in Circular Tubes. M.S.E. Report, Aerospace and Mechanical Engineering Department, University of Arizona.
- Pickett, P. E., Taylor, M. F., and McEligot, D. M., 1977. Heat-ed Turbulent Flow of Helium-Argon Mixtures in Tubes, Int. J. Heat Mass Transfer, in process.
- Reichardt, H., 1951. Complete Representation of Turbulent Velocity Distribution in Smooth Pipes. Z. Angew. Math Mech., 31, 208.
- Reynolds, A. J., 1975. The Prediction of Turbulent Prandtl and Schmidt Numbers. Int. J. Heat Mass Transfer, 18, 1055-1069.
- Reynolds, H. C., Swearingen, T. B., and McEligot, 1969. Thermal Entry for Low Reynolds Number Turbulent Flow. J. Basic Eng., 91, 87-94.
- Reynolds, W. C. and Perkins, H. C., 1970. Engineering Thermodynamics, New York: McGraw-Hill.
- Schneider, P. J., 1955. Conduction Heat Transfer, Reading, Mass: Addison-Wesley.
- Shapiro, A. H., 1953. The Dynamics and Thermodynamics of Compressible Fluid Flow, Vol. 1, New York: Ronald Press.
- Svehla, R. A., and McBride, B. J. Fortran IV Computer Program for Calculations of Thermodynamic and Transport Properties of Complex Chemical Systems. NASA TN D-7056.
- Taylor, M. F., 1967. Correlation of Friction Coefficients for Coefficients With Large Variations in Fluid Properties. NASA TM X-2145.
- Taylor, M. F., 1970. Prediction of Friction and Heat Transfer Coefficients With Large Variations in Fluid Properties. NASA TM X-2145.
- Touloukian, Y. S. and Ho, C. Y., 1970. Thermophysical Properties of Matter, Longon: Plenum Press.
- van Driest, E. R., 1956. On Turbulent Flow Near a Wall. J. Aeronaut. Sci., 23, 1007-1001 and 1036.
- van Wylen, G. J. and Sonntag, R. E., 1973. Fundamentals of Classical Thermodynamics, 2nd Ed., New York: Wiley.

DISTRIBUTION LIST

<u>Recipient</u>	<u>Number of Copies</u>
Office of Naval Research 800 North Quincy Street Arlington, Virginia 22217 Attn: Mr. Keith Ellingsworth, Code 473	3
Defense Documentation Center Building 5 Cameron Station Alexandria, Virginia 22314	12
Naval Research Laboratory 4555 Overlook Avenue Washington, D. C. 20390 Attn: Technical Information Division	
Code 2627	6
Code 2629	6
Engineering Materials Division	1
U. S. Naval Postgraduate School Monterey, California 93940 Attn: Prof. P. F. Pucci, Mechanical Engineering	1
U. S. Naval Academy Annapolis, Maryland 21402 Attn: Department of Mechanical Engineering	1
Naval Sea Systems Command Crystal City, National Center #3 Washington, D. C. 20360 Attn: NSEA 033	1
NSEA 035	1
Naval Ships Engineering Center Century Building 4 Washington, D. C. 20362 Attn: NSEC 6147	1
NSEC 6146	1
Naval Ship R & D Center Annapolis, Maryland 21402 Attn: Mr. Sid Cox	1

National Science Foundation 1800 G Street, N. W. Washington, D. C. 20550	1
NASA Lewis Research Center 21000 Brookpark Road Cleveland, Ohio 44135 Attn: Dr. Bert Probst	1
Defense Advanced Research Projects Agency 1400 Wilson Boulevard Arlington, Virginia 22209 Attn: Dr. George Donahue	1
Maritime Administration 14th & E Streets. N. W. Washington, D. C. 20230 Attn: Mr. Frank Critelli	1
Electric Power Research Institute P. O. Box 10412 Palo Alto, California 94303 Attn: Dr. Arthur Cohn	1
Mr. G. Max Irving Office of Naval Research Resident Representative University of New Mexico Bandolier Hall West - Room 204 Albuquerque, NM 87131	1
Assistant Chief for Technology Office of Naval Research, Code 200 Arlington, Virginia 22217	1
Dr. Rudolph J. Marcus Office of Naval Research Pasadena Branch Office 1030 East Green Street Pasadena, California 91106	1
AiResearch Manufacturing Company of Arizona 402 S. 36th Street P. O. Box 5217 Phoenix, Arizona 85010 Attn: Mr. Ray A. Rackley	2
Mr. Keith M. Johansen	1

AiResearch Manufacturing Company
2525 West 190th Street
Torrance, California 90509
Attn: Mr. Murray Coombs

1

Dr. W. H. Theilbahr
Naval Weapons Center (Code 3161)
China Lake, California 93555

1

Office of Naval Research, Code 438
800 North Quincy Street
Arlington, Virginia 22217
Attn: Mr. Robert Mindak

1

U.S. Department of Energy
Division of Fossil Fuel Utilization
Washington, D. C. 20545
Attn: Mr. J. W. Fairbanks

1